UNIVERSIDADE FEDERAL DO RIO GRANDE DO SUL
FACULDADE DE FARMÁCIA
PROGRAMA DE PÓS-GRADUAÇÃO EM CIÊNCIAS FARMACÊUTICAS

NANOPARTÍCULAS LIPÍDICAS INOVADORAS CONTENDO FUCOXANTINA: DESENVOLVIMENTO TECNOLÓGICO, CONTROLE DE QUALIDADE E AVALIAÇÃO TOXICOLÓGICA

Letícia Malgarim Cordenonsi

Porto Alegre
2018

UNIVERSIDADE FEDERAL DO RIO GRANDE DO SUL
FACULDADE DE FARMÁCIA
PROGRAMA DE PÓS-GRADUAÇÃO EM CIÊNCIAS FARMACÊUTICAS

NANOPARTÍCULAS LIPÍDICAS INOVADORAS CONTENDO FUCOXANTINA: DESENVOLVIMENTO TECNOLÓGICO, CONTROLE DE QUALIDADE E AVALIAÇÃO TOXICOLÓGICA

Tese apresentada por **LETÍCIA MALGARIM CORDENONSI** para obtenção do TÍTULO DE DOUTOR em Ciências Farmacêuticas**.**

Orientador (a): Prof.ª Dr. Elfrides Eva Scherman Schapoval
Coorientador (a): Prof.ª Dr. Renata Platcheck Raffin

Porto Alegre
2018

Tese apresentada ao Programa Pós-Graduação em Ciências Farmacêuticas, em nível de Doutorado da Faculdade de Farmácia da Universidade Federal do Rio Grande do Sul e aprovada em 14 de dezembro de 2018, pela Banca Examinadora constituída por:

Prof. Dr. Diogo Miron
Universidade Federal do Rio Grande do Sul – UFRGS

Prof. Dr. Nathalie Ribeiro Wingert
Universidade Federal do Rio Grande do Sul – UFRGS

Prof. Dr. Sabrina Nunes Nascimento
Universidade Federal do Rio Grande do Sul – UFRGS

CIP - Catalogação na Publicação

Malgarim Cordenonsi, Leticia
NANOPARTÍCULAS LIPÍDICAS INOVADORAS CONTENDO FUCOXANTINA: DESENVOLVIMENTO TECNOLÓGICO, CONTROLE DE QUALIDADE E AVALIAÇÃO TOXICOLÓGICA / Leticia Malgarim Cordenonsi. -- 2018.
237 f.
Orientadora: Elfrides Eva Scherman Schapoval.

Coorientadora: Renata Platcheck Raffin.

Tese (Doutorado) -- Universidade Federal do Rio Grande do Sul, Faculdade de Farmácia, Programa de Pós-Graduação em Ciências Farmacêuticas, Porto Alegre, BR-RS, 2018.

1. fucoxantina. 2. cancer. 3. nanoparticulas lipidicas. 4. validação. 5. avaliação toxicológica. I. Scherman Schapoval, Elfrides Eva, orient. II. Platcheck Raffin, Renata, coorient. III. Título.

Elaborada pelo Sistema de Geração Automática de Ficha Catalográfica da UFRGS com os dados fornecidos pelo(a) autor(a).

Este trabalho foi realizado nas dependências do Laboratório de Controle de Qualidade Farmacêutico Elfrides Schapoval, na Faculdade de Farmácia da Universidade Federal do Rio Grande do Sul, com bolsa de estudos CAPES e *no Dipartimento di Scienze del Farmaco* da *Università degli Studi di Pavia* (Pavia/Itália), através do Programa PDSE/CAPES.

Aos meus pais
que me apoiaram em
todos momentos e me
incentivaram a aceitar desafios.

AGRADECIMENTOS

Primeiramente agradeço aos meus pais, Paulo Cezar e Maria Izabel, e a meu irmão Carlos, por me mostrarem a importância do estudo, pelo amor incondicional e por sempre acreditarem em mim.

Agradeço, de forma especial, à minha orientadora Prof[a]. Elfrides Schapoval, por ter acreditado em mim, pelo incentivo à pesquisa e pela oportunidade que me concedeu de realizar o mestrado e doutorado e, acima de tudo pelo exemplo de profissional e pessoal. Agradeço também à minha coorientadora Prof[a]. Renata Raffin pelos ensinamentos transmitidos e aos demais professores do grupo.

Agradeço à Prof[a]. Giuseppina Sandri pela acolhida e pela oportunidade de trabalho junto ao seu grupo de pesquisa na *Università Degli Studi di Pavia* e também aos colegas de laboratório pelo acolhimento e amizade.

Aos meus colegas do Laboratório 402, em especial à Rafaela, Julia, Joanna, Lívia e Mariana. Obrigada pelo convívio, auxílio e pela amizade.

Ao Prof. Helder Teixeira e o LATOX pela parceria científica.

Aos membros da banca examinadora, pela disponibilidade em avaliar e contribuir com este trabalho.

A todos que mesmo não citados, contribuíram para este trabalho e participaram desta etapa na minha vida. Muito obrigada!

APRESENTAÇÃO

De acordo com as normas vigentes no Regimento do Programa de Pós-Graduação em Ciências Farmacêuticas, da Universidade Federal do Rio Grande do Sul, a presente Tese foi redigida na forma de capítulos, com encarte de publicações, para uma melhor compreensão e discussão dos resultados obtidos. Assim, este exemplar encontra-se dividido da seguinte forma:

- Introdução contendo a apresentação do tema;
- Objetivo geral e objetivos específicos do trabalho;
- Revisão bibliográfica;
- Capítulo I: Caracterização da fucoxantina e do seu isômero e o desenvolvimento de método analítico indicativo de estabilidade por CLAE;
- Capítulo II: Desenvolvimento de nanopartículas lipídicas inovadoras contendo uma combinação de manteiga de bacuri e óleo de tucumã;
- Capítulo III: Desenvolvimento e caracterização de hidrogel contendo nanopartículas lipídicas inovadoras de fucoxantina para aplicação cutânea;
- Capítulo IV: Avaliação toxicológica *in vitro* de nanopartículas lipídicas contendo fucoxantina e seus isômeros;
- Capítulo V: O papel da quitosana como revestimento de nanopartículas lipídicas na liberação de fucoxantina na pele;
- Discussão geral: proporcionar uma compreensão geral dos resultados obtidos;
- Conclusões;
- Referências.

RESUMO

A fucoxantina (FUCO) tem apresentado efeitos promissores no tratamento do câncer, como promotor da apoptose, indutor da interrupção do ciclo celular, supressor de metástases e ação cutânea na melanogênese induzida por raios UVB. As nanopartículas lipídicas (NL) apresentam destaque frente a outros sistemas e novas matérias-primas vêm sendo utilizadas para sua preparação, destacando-se as matérias-primas provenientes da Amazônia brasileira. No entanto, a FUCO é uma molécula instável, o que limita seu uso. Diante do exposto, o presente trabalho visa o desenvolvimento de NL inovadoras contendo uma combinação de manteiga de bacuri e óleo de tucumã para a incorporação da FUCO (NL-FUCO). O **Capítulo I** apresenta a caracterização por espectrometria de massas e de ressonância magnética nuclear da FUCO matéria-prima, que foi adquirida em duas apresentações, incorporada em um óleo e em pó. As duas matérias-primas da FUCO foram identificadas como total-*trans* e 9'-*cis* FUCO, respectivamente. Na etapa seguinte, foi desenvolvido um método analítico indicativo de estabilidade por Cromatografia Líquida de Alta Eficiência (CLAE) para a quantificação e controle de qualidade da FUCO e do seu isômero. Para isto, foi utilizada uma coluna C18, fase móvel isocrática composta por acetonitrila e água pH 7,0 (9,5:0,5 *v/v*) e detecção em 450 nm. Os resultados demonstraram que o método é linear na faixa de concentração estudada, preciso e exato. A robustez do método foi avaliada por desenho experimental Box-Behnken, demonstrando que as modificações nos fatores estudados não interferiram na quantificação da FUCO. No **Capítulo II**, as NL inovadoras foram desenvolvidas com o preparo de seis formulações, variando as proporções da manteiga de bacuri e do óleo de tucumã, pelo método homogeneização de alto cisalhamento. Na etapa seguinte, estas formulações foram caracterizadas e os resultados indicaram que o diâmetro médio das NL foram inferiores a 255 nm, com baixo índice de polidispersão (pdI) e potencial zeta entre -11 mV e -24 mV. A avaliação da morfologia por microscopia eletrônica de transmissão (MET) demonstrou partículas esféricas, homogêneas e com dimensões nanométricas. No estudo de estabilidade, todas as formulações mantiveram-se estáveis por dois meses à temperatura ambiente, porém a formulação com 5% de manteiga de bacuri e 4% de óleo de tucumã apresentou melhores resultados. No **Capítulo III,** está descrita a incorporação da FUCO na formulação de NL inovadoras

anteriormente selecionada. As NL-FUCO apresentaram diâmetro médio de 243 nm, baixo pdI, alta taxa de encapsulação e teor adequado. O método por CLAE para quantificação da FUCO nas NL demonstrou ser linear, preciso e exato. Na segunda etapa, as NL-FUCO foram incorporadas em um hidrogel e apresentaram pH adequado para aplicação cutânea, mantendo sua dimensão nanométrica, com baixo pdI e teor próximo a 100%. No estudo de fotoestabilidade com luz UVA, as NL protegeram a FUCO. No estudo de estabilidade, as NL-FUCO mostraram-se estáveis durante 45 dias armazenadas em 6 ºC, 25 ºC e 40 ºC. O estudo de dissolução indicou uma liberação sustentada da FUCO a partir das NL, quando comparada à FUCO livre. Através dos estudos de permeação cutânea *in vitro,* foi possível quantificar a FUCO na epiderme e na derme e comprovou-se a capacidade das NL em modificar a permeação da FUCO. Quando o estrato córneo foi removido, as concentrações da FUCO aumentaram na epiderme e na derme. Em conclusão, os resultados obtidos demonstram que as NL-FUCO são um sistema promissor para aplicação cutânea. O **Capítulo IV** apresenta a avaliação toxicológica *in vitro* da FUCO e das NL-FUCO, através dos ensaios de citotoxicidade por MTT, vermelho neutro e o método de exclusão com azul de Tripan. Concomitantemente, foram avaliadas as espécies reativas de oxigênio e nitrogênio e o potencial de membrana mitocondrial. A partir dos resultados obtidos, NL-FUCO se mostrou biocompatível com células 3T3 até a concentração de 80 µg/mL. Houve aumento de espécies reativas de oxigênio e nitrogênio e do potencial de membrana mitocondrial, sugerindo que a FUCO possui capacidade pró-oxidante e impulsiona a síntese de adenosina trifosfato (ATP). Porém, são necessários estudos para a investigação da toxicidade *in vivo* das NL-FUCO. No **Capítulo V,** descreve-se o papel da quitosana no revestimento das NL-FUCO. O revestimento com quitosana aumentou o tamanho das NL, entretanto os valores se mostraram adequados para sistemas nanométricos. Com a análise do potencial zeta e a da MET pode-se confirmar a presença do revestimento com quitosana. O estudo de bioadesão *in vitro* foi realizado com membrana de casca de ovo e confirmou que revestimento de quitosana aumentou significativamente a bioadesão das NL. O estudo de proliferação *in vitro* evidenciou que as LN-FUCO mantiveram as propriedades de proliferação da quitosana.

Palavras-chave: Fucoxantina, câncer, nanopartículas lipídicas, validação, estudo de estabilidade, avaliação toxicológica.

ABSTRACT

Fucoxanthin (FUCO) has shown promising effects in the cancer treatment, such as apoptosis promoter, cell cycle arrest, inhibition of metastasis and cutaneous action in UVB induced melanogenesis. Lipid nanoparticles (LN) are prominent compared to other systems and new raw materials are being used for the preparation, highlighting the raw materials coming from the Brazilian Amazon. However, FUCO is an unstable molecule, which limits its use. Therefore, the present work aims to develop of innovative LN containing a combination of bacuri butter and tucumã oil for the incorporation of FUCO (LN-FUCO). **Chapter I** presents the characterization by mass spectrometry and nuclear magnetic resonance of FUCO raw material, which was acquired in two presentations, incorporated in an oil and powder. The two FUCO raw materials were identified as total-*trans* and 9'-*cis* FUCO. In the next step, an analytical method was developed for the quantification and quality control of FUCO and its isomer by High Performance Liquid Chromatography (HPLC). For this, a C18 column, isocratic mobile phase composed of acetonitrile and water pH 7.0 (9.5:0.5 *v/v*) and detection at 450 nm were used. The results demonstrated that the method is linear in the concentration range studied, accurate and precise. The robustness of the method was evaluated by the Box-Behnken experimental design, demonstrating that the modifications in the factors studied did not interfere in the quantification of FUCO. **In Chapter II**, the innovative LN were developed, six formulations were prepared, varying the proportion of the butter of bacuri and of the oil of tucumã, by high shear homogenization method. In the next step, these formulations were characterized and the results indicated that the mean diameter of LN were lower than 255 nm, polydispersion index (pdI) lower and zeta-potential between -11 mV and -24 mV. The assessment of morphology by transmission electron microscopy showed spherical homogeneous and with nanometric dimensions particles. In the stability study, all formulations were stable for two months at room temperature; however, the formulation with 5% bacuri butter and 4% tucumã oil presented the best result. **Chapter III** describes the incorporation of FUCO in the innovative LN. The LN-FUCO presented a mean diameter of 243 nm, pdI lower, high entrapment efficiency and adequate drug loading. The HPLC method for quantification of FUCO in LN was shown to be linear, precise and accurate. In the second step, the LN-FUCO were incorporated in a hydrogel and presented a suitable pH for cutaneous application,

maintaining its nanometric dimension, with pdI lower and close to 100% drug loading. In the study of photostability with UVA light, LN protected FUCO. In the stability study, LN-FUCO were stable for 45 days stored at 6 °C, 25 °C and 40 °C. The dissolution studies indicated a sustained release of FUCO from LN as compared to FUCO free. Through *in vitro* skin permeation studies, it was possible to quantify the FUCO in the epidermis and dermis and to demonstrate the ability of LN to modify the FUCO permeation. When the stratum corneum was removed, FUCO concentrations increased in the epidermis and in the dermis. In conclusion, the results obtained demonstrate that LN-FUCO is a promising system for cutaneous application. **Chapter IV** presents the *in vitro* toxicological evaluation of FUCO and LN-FUCO through MTT assay, neutral red, and trypan blue dye exclusion test. Concomitantly, the reactive oxygen and nitrogen species and the mitochondrial membrane potential were evaluated. From the results, LN-FUCO is biocompatible with 3T3 cells up to the concentration of 80 µg/mL. There were increased reactive species and mitochondrial membrane potential, suggesting that FUCO possesses pro-antioxidant capacity and boosts the synthesis of adenosine triphosphate (ATP). However, studies are needed to investigate the *in vivo* toxicity of LN-FUCO. In **Chapter V** describes the role of chitosan in the coating of LN-FUCO. The chitosan coating increased the size of the LN; however the values were shown to be adequate for nanometric systems. The presence of chitosan can be confirmed by the analysis of the zeta-potential and MET. *In vitro* bioadhesion study was performed with egg shell membrane and confirmed that chitosan coating significantly increased the bioadhesion of LN. *In vitro* study showed that the LN-FUCO maintained the proliferation properties of chitosan.

Keywords: Fucoxanthin, cancer, lipid nanoparticles, validation, stability studies, toxicological evaluation.

LISTA DE FIGURAS

Figura 1. As principais camadas da pele, a epiderme, a derme e a hipoderme e seus vários anexos 33
Figura 2. Rotas para atravessar o estrato córneo: (A): via transepidérmica: via intercelular e transcelular e (B) via transapêndices 35
Figura 3. Níveis de invasão do câncer de pele: (I): é limitado à epiderme; (II): invade parcialmente a derme papilar; (III): preenche completamente a derme papilar; (IV): estende-se até a derme reticular; (V): estende-se para a hipoderme 37
Figura 4. Alga *Laminaria japonica* e em destaque a região da alga que é utilizada para extrair a fucoxantina. 39
Figura 5. Estrutura da (a) total-*trans* fucoxantina, (b) 9'-*cis* fucoxantina (c) 13-*cis* fucoxantina e (d) 13'-*cis* fucoxantina. 40
Figura 6. Fatores (moléculas e mecanismos) que são regulados pela fucoxantina, resultando em efeitos anticarcinogênicos 45

LISTA DE ABREVIATURAS

ANOVA	Análise de variância
ATP	Adenosina trifosfato
Bcl-2	Célula-B do linfoma 2
CG	Cromatografia gasosa
CLAE	Cromatografia líquida de alta eficiência
COSY	*Homonuclear correlation spectroscopy*/Ressonância magnética nuclear bidimensional
COX-2	Ciclooxigenase 2
CYP3A4	Citocromo P450 3A4
DAD	Detector de arranjo de diodos
DLS	*Dynamic light scattering*/ Espalhamento de luz dinâmico
DNA	Ácido desoxirribonucléico
DPR	Desvio padrão relativo
DSC	*Differential scanning calorimetry*/ Calorimetria exploratória diferencial;
EM	Espectrometria de massas
FUCO	Fucoxantina
GIJC	*Gap junctional intercellular communication*/Junção da comunicação intracelular
ICH	*International Council for Harmonization*
INCA	Instituto Nacional do Câncer
I-κB	Proteína inibitória κB
m/z	Relação massa/carga
MAPK	Proteínas quinases ativadas por mitógenos
MC1R	Receptor de melanocortina 1
MET	Microscopia eletrônica de transmissão
MMP-9	Metaloproteína de matris-9
MTT	3-(4,5-dimetiltiazol-2-il)-2,5-difenil-2H tetrazolato de bromo
NF-Kb	Fator nuclear κB
NR	*Neutral red/* Vermelho neutro
NL	Nanopartículas lipídicas
NL-FUCO	Nanopartículas lipídicas contendo fucoxantina

pdI	Índice de polidispersão
PRB	Proteína de susceptibilidade ao retinoblastoma
R	Coeficiente de correlação
RMN ^{1}H	Ressonância magnética nuclear de hidrogênio
ROS	*Reactive Oxygen Species*/ Espécies reativas do oxigênio
RNS	*Reactive Nitrogen Species*/ Espécies reativas de nitrogênio
USP	*The United States Pharmacopeia/* Farmacopeia Americana
UVA	Raios ultravioletas A
UVB	Raios ultravioletas B
UVC	Raios ultravioletas C

SUMÁRIO

1. INTRODUÇÃO 23
2. OBJETIVOS 27
3. REVISÃO BIBLIOGRÁFICA 31
3.1 Pele 33
3.2 Câncer de pele 36
3.3 Carotenoides 37
3.4 Fucoxantina (FUCO) 38
3.4.1 Estabilidade 41
3.4.2 Atividades farmacológicas 42
3.4.3 Tratamento e prevenção do câncer 45
3.5 Matérias-primas de origem vegetal da Amazônia 46
4. CAPÍTULO I - Caracterização da fucoxantina e do seu isômero e o desenvolvimento de método analítico indicativo de estabilidade por CLAE 49
4.2 Artigo científico 53
5. CAPÍTULO II - Desenvolvimento de nanopartículas lipídicas inovadoras contendo uma combinação de manteiga de bacuri e óleo de tucumã 83
5.1 Introdução 85
5.2 Artigo científico 87
6. CAPÍTULO III - Desenvolvimento e caracterização de hidrogel contendo nanopartículas lipídicas inovadoras de fucoxantina para aplicação cutânea . 111
6.1 Introdução 113
6.2 Artigo científico 115
7. CAPÍTULO IV - Avaliação toxicológica *in vitro* de nanopartículas lipídicas contendo fucoxantina e seus isômeros 143
7.1 Introdução 145
7.2 Artigo científico 147
8. CAPÍTULO V – O papel da quitosana como revestimento de nanopartículas lipídicas na liberação de fucoxantina na pele 171
8.1 Introdução 173
8.2 Artigo científico 175
9. DISCUSSÃO GERAL 195

10. CONCLUSÕES..... 211
11. REFERÊNCIAS 215

1. INTRODUÇÃO

Em todo o mundo, mais de oito milhões de pessoas morrem anualmente em decorrência de câncer. No Brasil, o câncer de pele não melanoma é o que apresenta maior incidência, correspondendo a 29% de todos os tumores malignos registrados no país. O Instituto Nacional do Câncer (INCA) estima que, entre 2018-2019, irão surgir aproximadamente 600 mil novos casos de câncer, dentre estes 170 mil são de pele (WHO, 2012; BRASIL, 2017).

No tratamento do câncer, o uso de quimioterápicos produz efeitos colaterais graves, há resistência intrínseca à quimioterapia e o tratamento com radiação é tóxico, eliminando não apenas células tumorais, mas também células saudáveis. Na busca de novos medicamentos, há um crescente interesse em produtos naturais a partir de fontes marinhas, e especialmente produtos provenientes de algas (MOLASSIOTIS et al., 2005; MUTHUIRULAPPAN e FRANCIS, 2013). O carotenoide fucoxantina (FUCO) é um pigmento laranja presente em algas marinhas, que tem apresentado efeitos promissores no tratamento do câncer, como promotor da apoptose, indutor da interrupção do ciclo celular, supressor de metástases e ação cutânea na melanogênese induzida por raios ultravioletas B (UVB) (SHIMODA et al., 2010; KUMAR, MASASHI e KAZUO, 2013).

As nanopartículas estão sendo empregadas com sucesso na área farmacêutica por aumentarem a eficiência em sistema na entrega de substâncias ativas lipofílicas, aumentarem a seletividade e a eficiência, protegerem contra degradação e reduzirem os efeitos colaterais (BONIFÁCIO et al., 2014). A aplicação cutânea de carreadores coloidais tem como objetivo a liberação sustentada da substância ativa encapsulada, podendo suprir a pele por um período de tempo prolongado, proporcionando índices terapêuticos mais adequados, além de reduzir os efeitos adversos em sítios não específicos e a irritação no local de administração (BARRATT, 2003). Diante do exposto, as nanopartículas lipídicas (NL) apresentam destaque frente a outros sistemas nanoestruturados, pois possibilitam a incorporação de ativos lipofílicos. Além disso, os seus componentes possuem baixa citotoxicidade e a possibilidade de produção por método simples, sem o uso de solventes orgânicos (ALMEIDA e SOUTO, 2007; SHAH et al., 2007).

Novas matérias-primas vêm sendo utilizadas para a preparação de NL, destacando-se as matérias-primas provenientes da Amazônia brasileira. O presente trabalho propõe o uso inédito da combinação da manteiga de bacuri e o óleo de

tucumã para a produção de NL inovadoras para aplicação cutânea. Estas matérias-primas são emolientes e também podem ser utilizadas como um agente hidratante. Como novos ativos, bacuri tem alto nível de tripalmitina e ácido palmitoleico graxo, além disso, representa uma rica fonte de xantonas e benzofenonas poli-isopreniladas. O tucumã é rico em ômega 3, 6 e 9, carotenoides e também é uma importante fonte de vitamina B2 (DE ROSSO e MERCADANTE, 2007; ACUNA, JANCOVSKI e KENNELLY, 2009; MORAIS e GUTJAHR, 2009; LUSTOSA et al., 2016).

Diante do exposto, a FUCO tem ação promissora no tratamento tópico do câncer de pele, entretanto a molécula é extremamente instável, o que limita seu uso. Assim, o presente trabalho visa o desenvolvimento de NL inovadoras contendo uma combinação de manteiga de bacuri e óleo de tucumã para a incorporação da FUCO (NL-FUCO) para aplicação cutânea, bem como, a avaliação toxicológica *in vitro* da FUCO e das NL-FUCO.

2. OBJETIVOS

2.1 Objetivo Geral

Desenvolver e caracterizar nanopartículas lipídicas inovadoras contendo uma combinação de manteiga de bacuri e óleo de tucumã para a incorporação da fucoxantina, bem como, conduzir estudos para validação de metodologia analítica por cromatografia líquida de alta eficiência para o controle de qualidade.

2.2 Objetivos Específicos

- Caracterizar por meio das técnicas de espectrometria de massas e de ressonância magnética nuclear a FUCO matéria-prima, que foi adquirida em duas apresentações, incorporada em um óleo e em pó;
- Desenvolver e validar metodologia analítica para determinação da FUCO por cromatografia líquida de alta eficiência;
- Desenvolver e caracterizar as nanopartículas lipídicas inovadoras contendo matérias-primas da Amazônia brasileira pelo método de homogeneização de alto cisalhamento;
- Incorporar a FUCO nas nanopartículas lipídicas inovadoras anteriormente preparadas e realizar a caracterização físico-química;
- Incorporar a suspensão de nanopartículas lipídicas inovadoras contendo FUCO em um gel e realizar a caracterização físico-química;
- Realizar estudo de dissolução e permeação cutânea *in vitro*;
- Realizar estudos toxicológicos *in vitro*;
- Revestir as nanopartículas lipídicas contendo FUCO com quitosana.

3. REVISÃO BIBLIOGRÁFICA

3.1 Pele

A pele é o maior órgão do corpo humano e representa a principal comunicação com o meio externo. Diversas funções são desempenhadas pela pele, como a regulação da temperatura corporal, função sensorial, proteção física e contra radiação ultravioleta. A pele possui pH levemente ácido, variando entre 4,60-5,80, decorrente da presença de aminoácidos e de ácido lático (DEGIM, 2006; BOLZINGER et al., 2012).

Apesar de sua espessura variar de acordo com as diferentes partes do corpo, a estrutura fundamental da pele é basicamente a mesma, conforme demonstrado na Figura 1. É composta de três camadas principais, a epiderme estratificada e vascularizada, a derme e a hipoderme, possuindo ainda vários anexos como folículos pilosos e glândulas sudoríparas e sebáceas. A epiderme, que constitui a camada mais externa, é a que merece mais atenção nos estudos de permeação cutânea. Esta camada é subdividida em cinco estratos, que são denominados, da parte inferior para superior, em germinativo ou basal, espinhoso, granuloso, lúcido e estrato córneo. A maior parte da epiderme é constituída por um epitélio escamoso, que é formado principalmente pelos queratinócitos (JUNQUEIRA E CARNEIRO, 2004; LACHMAN, LIEBERMAN e LINKKANIG, 2010; BENSON e WATKINSON, 2012).

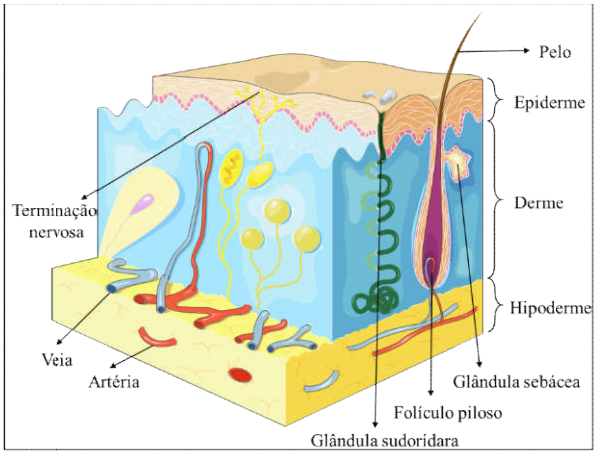


Figura 1. As principais camadas da pele: a epiderme, a derme e a hipoderme e seus vários anexos (Figura produzida pelos elementos da Servier Medical Art: www.servier.fr/servier-medical-art).

O estrato córneo, com apenas 10 a 15 μm de espessura, regula a perda de água e previne a entrada de substâncias prejudiciais e de microrganismos na superfície da pele. Estruturalmente, o estrato córneo é uma camada heterogênea, composta por queratinócitos localizados em uma matriz lipídica organizada em bicamadas lamelares. Esta camada é constituída por aproximadamente 15 a 20% de água, sendo esta quantidade importante para manter a elasticidade e integridade da pele (KULKARNI, 2010; BENSON e WATKINSON, 2012).

Abaixo da epiderme está localizada a derme, que é constituída por fibras proteicas de colágeno, elastina e matriz extracelular. Essa camada de tecido conjuntivo tem a função de dar suporte, elasticidade e flexibilidade aos tecidos. Serve de barreira à permeação de fármacos muito lipofílicos, diminuindo assim a permeação destes para as camadas mais profundas. Na epiderme estão localizados os capilares, glândulas sebáceas e sudoríparas, folículos pilosos, nervos e terminações nervosas, vasos sanguíneos e linfáticos (JUNQUEIRA E CARNEIRO, 2004; DEGIM, 2006; LACHMAN, LIEBERMAN e LINKKANIG, 2011).

A camada mais interna é a hipoderme ou tecido celular subcutâneo, que não faz parte da pele propriamente dita, apenas a une aos órgãos subjacentes. É uma camada de reserva energética, sendo composta por adipócitos, proporcionando ação isolante contra o frio (JUNQUEIRA E CARNEIRO, 2004; LACHMAN, LIEBERMAN e KANIG, 2010; BOLZINGER et al., 2012).

Conforme apresentado na Figura 2, existem duas maneiras para a substância ativa atravessar o estrato córneo intacto, via transepidérmica ou via transapêndices.

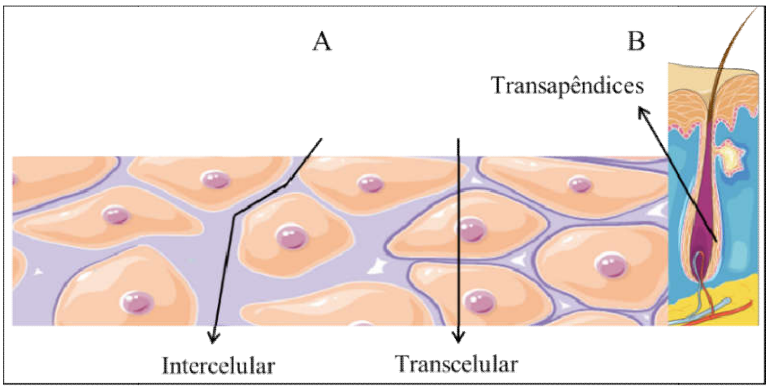


Figura 2. Rotas para atravessar o estrato córneo: (A): via transepidérmica: via intercelular e transcelular e (B) via transapêndices (Figura produzida pelos elementos da Servier Medical Art: www.servier.fr/servier-medical-art).

Pela via transepidérmica, a substância ativa pode percorrer dois caminhos, a via intercelular e transcelular. Na via intercelular, que é o caminho mais comum, a permeação ocorre entre os corneócitos e a substância ativa passa pela matriz extracelular, de características hidrofílicas. Na via transcelular, a permeação ocorre através dos corneócitos e da matriz lipídica, encontrando estruturas lipofílicas e hidrofílicas, o que lhe dificulta a permeação. Na via transapêndices, a permeação ocorre através dos anexos da pele, como os pêlos e as glândulas. Esta última, não é considerada como uma rota significativa para a permeação de fármacos, porque os anexos cutâneos ocupam somente 0,1% da área total da superfície da pele. No entanto, a entrega da substância ativa por esta via pode ser importante para a permeação de compostos que se difundem lentamente e de substâncias com elevado peso molecular, tais como as nanopartículas (TROMMER e NEUBERT, 2006; LADEMANN et al., 2011; LANE 2013).

Desta forma, a pele é uma barreira natural para a penetração de substâncias. Portanto, dificilmente uma substância ativa administrada topicamente, sem uma formulação adequada, atingirá as camadas mais profundas da pele, em concentrações suficientes para o tratamento de tumores cutâneos. Dentre os métodos utilizados para melhorar a penetração cutânea de fármacos, pode-se citar os sistemas de liberação modificados como os lipossomas e as nanopartículas (MOSER et al., 2001; WELSS, BASKETTER e SCHRÖDER, 2004). Entretanto, não existe regra para predizer como ocorre a permeação de sistemas nanoestruturados,

pois vai depender das características físico-químicas de cada sistema, como o diâmetro de partícula e a hidrofobicidade (ALVAREZ-ROMÁN et al., 2004). O efeito oclusivo, devido à dimensão nanométrica das partículas, é um fator que deve ser considerado, pois afeta a penetração de substâncias ativas, podendo ocasionar um controle maior da penetração dos sistemas nanoestruturados (JAIN et al., 2014).

Além da barreira natural que a pele representa, há evidências que demonstram que a maioria das células cancerosas possui resistência à apoptose ou apresentam mecanismos de apoptose defeituosos, permitindo assim o desenvolvimento incontrolável de células. O processo de apoptose, portanto, é o principal alvo de agentes quimioterápicos (OKADA e MAK, 2004; CHINEMBIRI et al., 2014).

3.2 Câncer de pele

O câncer de pele é a neoplasia mais frequentemente diagnosticada em caucasianos em todo o mundo e a incidência continua aumentando devido ao aumento da exposição à luz ultravioleta. Além disso, existem outros agentes causadores, dos quais incluem-se vírus, predisposição genética, agentes mutagênicos presentes em alimentos e em produtos químicos (ERB et al., 2005).

A doença é caracterizada pelo crescimento anormal e descontrolado das células que compõem as diferentes camadas da pele. Define-se os diferentes tipos de câncer de pele de acordo com a camada da pele que é afetada (Figura 3). O mais frequente é o câncer de pele não melanogênico, também chamado de carcinoma basocelular, que é responsável por 70% dos casos e surge nas células basais, que se encontram na camada mais profunda da epiderme. O carcinoma epidermóide é responsável por 25% dos casos e afeta as células espinhosas. O mais agressivo e raro, detectado em 4% dos pacientes, é o melanoma, que tem origem nos melanócitos (CHINEMBIRI et al., 2014; BRASIL, 2015).

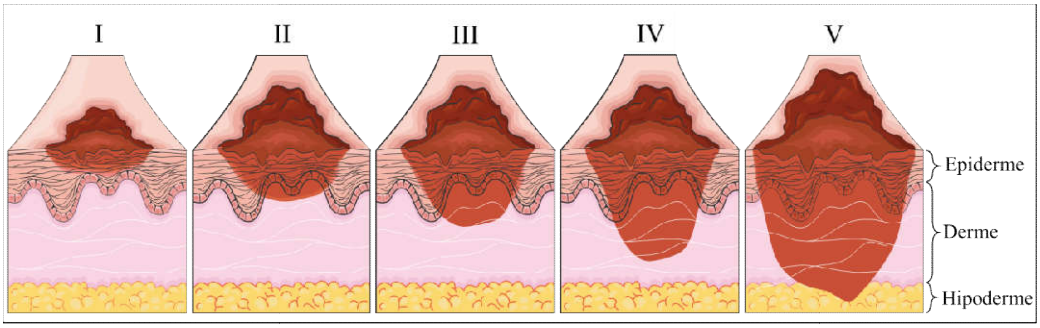


Figura 3. Níveis de invasão do câncer de pele: (I): é limitado à epiderme; (II): invade parcialmente a derme papilar; (III): preenche completamente a derme papilar; (IV): estende-se até a derme reticular; (V): estende-se para a hipoderme (Figura produzida pelos elementos da Servier Medical Art: www.servier.fr/servier-medical-art).

No tratamento tópico do câncer de pele, a substância ativa necessita atravessar o estrato córneo para atingir as camadas mais profundas da pele, onde está localizado o tumor. Entretanto, o estrato córneo forma a principal barreira contra a penetração de substâncias na pele, devido as suas bicamadas lipídicas e os queratinócitos (TROMMER e NEUBERT, 2006; LADEMANN et al., 2011; LANE 2013).

3.3 Carotenoides

Os carotenoides são amplamente difundidos na natureza, estando presentes em algas, plantas superiores, fungos e bactérias, sendo responsáveis pela coloração amarela, laranja ou vermelha destes (MCNULTY, JACOB e MASON, 2008; GAMMONE, RICCIONI e D'ORAZIO, 2015). Estruturalmente, os carotenoides são tetraterpenoides que contêm oito unidades de isopreno, formando assim uma estrutura básica de 40 carbonos. Esta estrutura básica pode ser modificada através de reações de ciclização, hidrogenação e desidrogenação; introdução de grupos contendo moléculas de oxigênio; rearranjos, encurtamento da cadeia ou combinações dessas modificações, resultando em diversas estruturas (YAHIA e ORNELAS, 2010).

A classificação dos carotenoides pode ser dada de acordo com sua origem, em marinhos ou terrestres e de acordo com sua estrutura química, em carotenos ou

xantofilas. Os carotenos não possuem oxigênio em sua estrutura química, apresentando características hidrofóbicas, como o β-caroteno e o licopeno. As xantofilas são pigmentos amarelos e possuem oxigênio na estrutura química, apresentando-se quimicamente menos hidrofóbicas e mais polares que os carotenos. O oxigênio pode estar ligado à molécula como uma hidroxila ou como pares de átomos de hidrogênio que são substituídos por átomos de oxigênio atuando como uma ponte (grupamento epóxido). O grupo das xantofilas inclui a FUCO, luteína, zeaxantina, neoxantina, entre outros compostos (MCNULTY, JACOB e MASON, 2008; GAMMONE, RICCIONI e D'ORAZIO, 2015).

Os efeitos benéficos dos carotenoides contra o câncer e doenças cardiovasculares foram reconhecidos e estimulam intensas investigações sobre o papel desses compostos como antioxidantes e como reguladores de resposta do sistema imune. Apesar de muitas hipóteses comprovadas, suas funções não estão completamente elucidadas *in vivo* (UENOJO, MARÓSTICA JUNIOR e PASTORE, 2007).

3.4 Fucoxantina (FUCO)

A FUCO é considerada o mais abundante de todos os carotenoides com pigmentação alaranjada que não são convertidos em vitamina A (não pró-vitamina A). Este carotenoide é encontrado em cloroblastos de numerosas classes de macroalgas e microalgas marinhas, como *Undaria pinnatifia* (Wakame), *Laminaria japonica* (Ma-Kombu), *Phaeodactylum tricornutum* e *Cylindrotheca closterium.* Essas algas crescem ao longo da costa do Pacífico e sua colheita ocorre entre os meses de junho e julho. Logo após a colheita, a alga é seca e a FUCO é extraída. O seu rendimento médio é de 20 mg por 100 g de alga seca, porém, a quantidade extraída pode diferir significativamente dependendo da espécie da alga (Figura 4) (SHIMODA et al., 2010; KIM et al., 2012; GAGEZ et al., 2012).

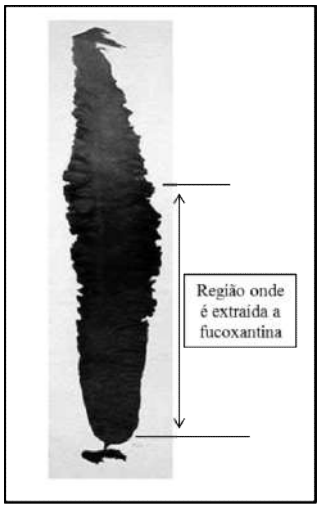


Figura 4. Alga Laminaria japonica e em destaque a região da alga que é utilizada para extrair a fucoxantina (Adaptado de KANAZAWA et al., 2008).

A estrutura completa da FUCO, incluindo a sua quiralidade, foi elucidada por Englert e colaboradores (1990). A molécula da FUCO apresenta massa molecular de 658,92 g/mol e fórmula molecular $C_{42}H_{58}O_6$. É considerada uma estrutura molecular única devido ao grupo alênico (Figura 5), além de grupos funcionais incluindo hidroxilas, epóxido, carbonilas e carboxilas que estão presentes em sua cadeia de polieno (SHO, 2001; SHIMODA et al., 2010; ZHANG et al., 2015).

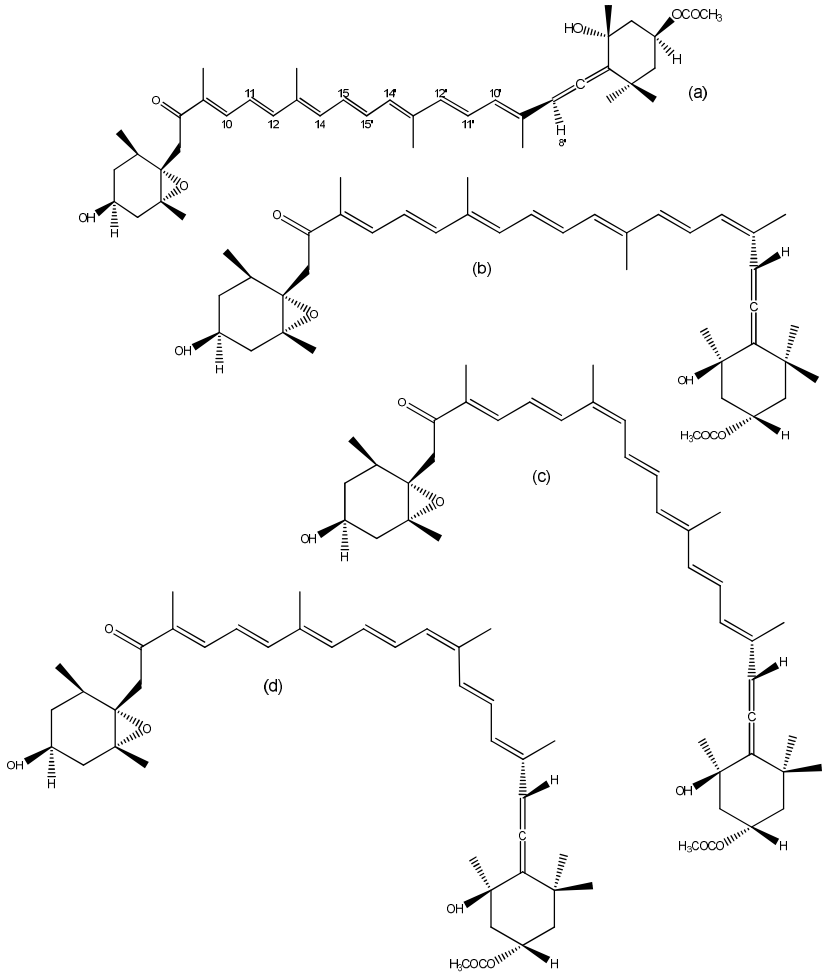


Figura 5. Estrutura da (a) total-*trans* fucoxantina, (b) 9'-*cis* fucoxantina (c) 13-*cis* fucoxantina e (d) 13'-*cis* fucoxantina.

Os carotenoides, em geral, são encontrados em várias formas isoméricas devido à configuração do comprimento da sua cadeia e o conjugado de duplas ligações característicos deste grupo (BOON et al., 2010). Na cadeia de polieno da FUCO, cada ligação dupla pode ter duas configurações, designadas como *cis* ou *trans,* dependendo da disposição dos grupos substituintes. A forma total-*trans* da FUCO é o principal isômero encontrado na natureza. A presença de uma ligação dupla *cis* cria maior impedimento estérico entre os átomos de hidrogênio e / ou grupos metílicos, de modo que os isômeros *cis* são geralmente menos estáveis termodinamicamente do que a forma total-*trans*. Em algas marrons (*Undaria pinnatifida*), total-*trans* FUCO foi o principal isômero encontrado (88%), seguido de uma pequena quantidade de 13-*cis* e 13'-*cis* FUCO (9%) (NAKAZAWA et al*.,* 2009;

ZHANG et al., 2015). Nakazawa e colaboradores (2009) relatam que, embora existam trabalhos sobre os efeitos dos isômeros total-*trans*, pouco se sabe sobre os efeitos biológicos dos isômeros *cis* e a comparação entre eles.

3.4.1 Estabilidade

Como ocorre com outros carotenoides, a FUCO sofre degradação durante o armazenamento, com exposição ao calor, luz, oxigênio, enzimas, lipídios insaturados e outras moléculas pró-oxidantes (AMAN, SCHIEBER e CARLE, 2005; SANGEETHA, BHASKAR, BASKARAN, 2009).

Existem poucos estudos que avaliaram a estabilidade da FUCO. O primeiro foi publicado em 2010, por Hii e colaboradores (2010), no qual foi avaliada a estabilidade da FUCO, por espectrofotometria, quando extraída da alga *Sargassum binderi*. Foram testados diferentes valores de pH, o uso de antioxidante ácido ascórbico 1,0%, a exposição à luz e sob condições escuras no período de 4 semanas. Os resultados revelaram que a FUCO apresentou maior estabilidade quando armazenada em condições sob abrigo da luz e em pH alcalino, em comparação à condição neutra e ácida. Ao abrigo da luz, a adição de ácido ascórbico retarda a degradação da FUCO. Em conclusão, a FUCO é sensível à exposição à luz e às condições de pH ácido, podendo ser estabilizada com a adição de ácido ascórbico.

Em outro estudo, a FUCO foi extraída de algas marrons (*Sargassum binderi*) e submetida a um estudo de estabilidade com diferentes valores de pH, exposição à luz (escuro e claro) e a diferentes temperaturas de armazenamento (4 ºC, 25 ºC e 50 ºC). Os testes de estabilidade demonstraram que a FUCO é mais estável entre os valores de pH 5,0 e 7,0, armazenada ao abrigo da luz e à temperatura entre 4 ºC e 25 ºC (YIP et al., 2014).

Do mesmo modo, Zhao e colaboradores (2014) investigaram os efeitos do aquecimento, exposição ao oxigênio e luz sobre a estabilidade da FUCO (*Costaria costata*) quando vinculada em óleo de canola. Os resultados demonstraram que o aquecimento promoveu a degradação da FUCO a partir de 25 ºC até 100 ºC, na ausência de luz e de oxigênio, ressaltando que com o aumento gradativo da temperatura houve a formação de isômeros *cis*, 13-*cis*, 13'-*cis* e 9'-*cis* da FUCO. A exposição ao oxigênio promoveu a degradação oxidativa a 25 ºC, enquanto que a

luz fluorescente gerou a degradação dos isômeros 13-*cis* e 13'-*cis*, além da formação considerável do isômero 9'-*cis*.

3.4.2 Atividades farmacológicas

Estudos demonstram que a FUCO possui várias atividades biológicas, atuando no tratamento da dislipidemia (WOO et al., 2010), na prevenção da obesidade (MAEDA et al., 2009), como antidiabético (MAEDA et al., 2007), antioxidante (HEO e JEON, 2009) e no tratamento e prevenção do câncer (MIYASHITA et al., 2011).

Enfatizando nos estudos sobre farmacologia do tratamento e prevenção do câncer, existem linhas de pesquisas com diferentes linhagens celulares e *in vivo*, evidenciando que a FUCO exerce efeitos anticarcinogênicos que envolvem diferentes moléculas e vias, como está esquematizado na Figura 6.

A supressão da formação de tumores de pele foi relatada por Nishino (1995), quando a FUCO foi administrada oralmente em animais. Além da diminuição na percentagem de ratos com tumores, o número médio de tumores por rato também diminuiu significativamente. Da mesma forma, a FUCO também suprimiu o crescimento de melanoma em ratos (KIM, et al*.,* 2013).

O efeito pró-oxidante da FUCO sobre as células cancerosas está sendo relacionado com a produção de radicais livres, propondo que este seja um dos mecanismos pelos quais a FUCO protege contra as células cancerosas (KOTAKE-NARA et al., 2001; SANGEETHA, BHASKAR, BASKARAN, 2009). A inibição do crescimento em linhagens celulares de leucemia pela FUCO foi estudada por Kim e colaboradores (2010) e este efeito foi atribuído à geração de espécies reativas do oxigênio (*Reactive Oxygen Species* - ROS), que leva à apoptose, pela parada do ciclo celular na fase da interfase G1. Entretanto, na literatura também está relatado que a atividade antioxidante da FUCO é devida ao grupo epóxido e às hidroxilas presentes na molécula, consideradas como fortes antioxidantes (BERTRAM e VINE, 2005; D'ORAZIO et al.,2012).

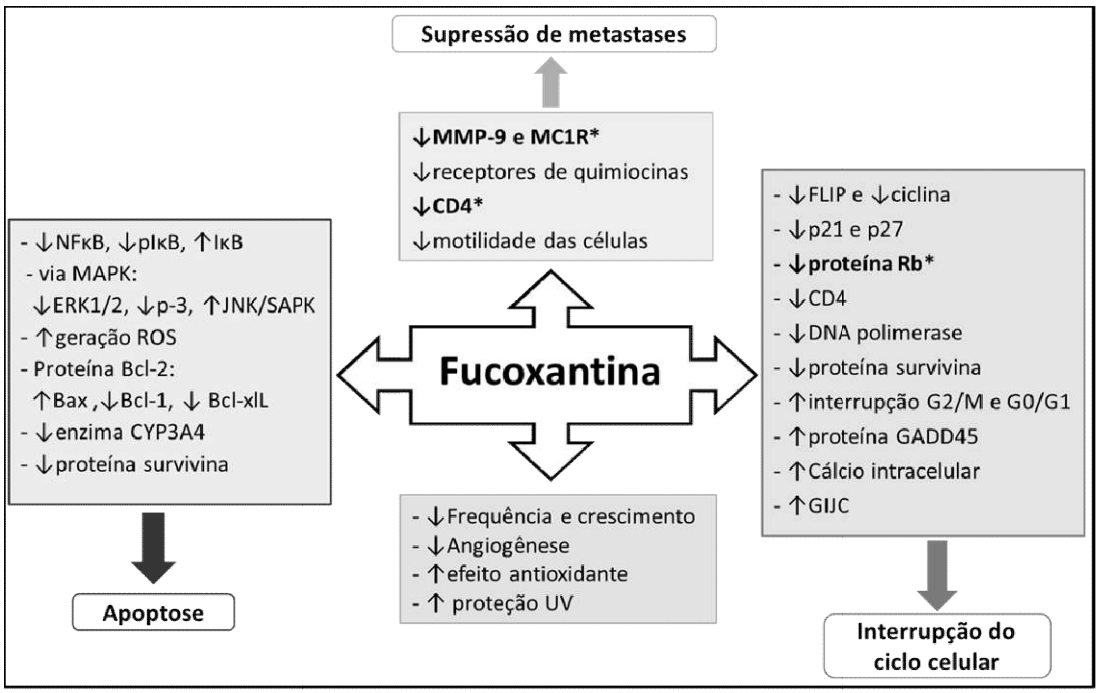
A interrupção do ciclo celular tem sido atribuída a diferentes vias e moléculas. Enquanto Yu e colaboradores (2001) observaram a parada do ciclo celular na fase da interfase G2 e fase mitótica, Liu e colaboradores (2009) relataram o efeito da FUCO à expressão aumentada de genes da junção da comunicação intracelular

(GIJC) e ao aumento dos íons de cálcio intracelular. Além disso, a FUCO interrompeu o crescimento celular na fase da interfase G1 e isso foi acompanhado por alteração na expressão de mais de 50 genes (SATOMI e NISHINO, 2007). Entre estes genes, houve um aumento das proteínas GADD45 (LIEBERMANN et al., 2011), proteínas p21 e p27 (DAS et al., 2005; SATOMI e NISHINO, 2009), proteína FLIP (KOTAKE-NARA et al., 2001) e diminuição da proteína de susceptibilidade ao retinoblastoma (pRb) (DAS et al., 2005; YAMAMOTO et al., 2011), da survinina (WANG et al., 2012) e da enzima DNA polimerase (MURAKAMI et al., 2002). Ishikawa e colaboradores (2008) encontraram diminuição da expressão da proteína ciclina e linfócitos TCD4 no tratamento com FUCO na leucemia.

O efeito que a FUCO exerce na apoptose de células cancerosas, como na interrupção do ciclo celular, também envolve diferentes vias e moléculas. A FUCO exerce ação sobre as proteínas quinases ativadas por mitógenos (MAPK), diminuindo a expressão das proteínas p38 e ERK1/2 e aumentando a expressão da proteína JNK/SAPK, resultando na apoptose de células no câncer de próstata (SATOMI e NISHINO, 2007; JOHNSON e LAPADAT, 2002). Nakazawa e colaboradores (2009) compararam os efeitos das formas total-*trans* e *cis* da FUCO e observaram uma diminuição das proteínas Bcl-2 (célula-B do linfoma 2), que foi associada à apoptose das células. Neste mesmo sentido, Kotake-Nara e colaboradores (2001) mostraram que houve diminuição na expressão das proteínas Bcl-2 e um aumento da expressão da proteína Bax, que é pró-apoptótica. O fator nuclear κB (NF-κB) possui propriedades pró-apoptóticas, e em um estudo, a FUCO reduziu a fosforilação de NF-κB e pI-κB e aumentou a expressão da proteína inibitória κB (I-κB) (YAMAMOTO et al., 2011). A expressão do gene survinina diminuiu com a administração da FUCO em células T adultas leucêmicas (ISHIKAWA et al., 2008).

Liu e colaboradores (2009) pesquisaram o possível papel da FUCO como adjuvante para prevenir ou superar a resistência aos fármacos induzida pela rifampicina em células com câncer de fígado e células com câncer colorretal humano. No seu estudo, houve a diminuição da atividade e da expressão da enzima citocromo P450 3A4 (CYP3A4) e da atividade do gene promotor do CYP3A4. Assim, os resultados indicam que a FUCO pode desempenhar um papel importante como agente quimioterápico.

Como parte da avaliação de segurança da FUCO, um estudo de toxicidade em ratos foi realizado, por via oral, em dose única (1,0 e 2,0 g/kg) e em doses repetidas (0,50 e 1,0 g/kg) por 30 dias. Em ambas as avaliações, não houve mortalidade e não foram observadas anomalias. No estudo de doses repetidas, a histologia não apresentou mudanças anormais nos tecidos do fígado, rim e do baço, concluindo que a FUCO não demonstra qualquer efeito tóxico relevante após quatro semanas diárias de tratamento (BEPPU et al., 2009a). Os mesmos autores conduziram outro estudo, no qual avaliaram a mutagenicidade do fucoxantinol, o principal composto formado após a ingestão oral da FUCO, pelo teste de Ames, e da FUCO pelo teste de micronúcleos. No teste de Ames, a mutação reversa bacteriana foi avaliada utilizando estirpes de *Salmonella typhimurium* e de *Escherichia coli*, e o resultado foi considerado negativo em todos os casos. No teste de micronúcleos, foram administrados oralmente doses de 0,5; 1,0 e 2,0 g/kg da FUCO em ratos. Após 24 horas, não foram observadas alterações. Com base nos dados do estudo pode-se presumir que a FUCO administrada via oral é um composto seguro em termos de mutagenicidade (BEPPU et al., 2009b).



↑ e ↓ indicam o aumento e diminuição dos fatores;

* fatores envolvidos no câncer de pele

Figura 6. Fatores (moléculas e mecanismos) que são regulados pela fucoxantina, resultando em efeitos anticarcinogênicos (Adaptado de KUMAR, MASASHI e KAZUO, 2013 e MARTIN, 2015).

3.4.3 Tratamento e prevenção do câncer

Na Figura 6, estão destacados alguns fatores envolvidos no câncer de pele. A FUCO inibiu a expressão e secreção de metaloproteína de matris-9 (MMP-9), ligada à invasão e à migração de tumores. Além disso, também reduz as expressões da glicoproteína da superfície celular (CD44) e receptores de quimiocina, conhecidos por estarem envolvidos na migração, invasão e adesão celular (ASAI, YONEKURA e NAGÃO, 2008). Do mesmo modo, a FUCO causa a interrupção do ciclo celular de células de melanoma através da diminuição das expressões da pRb (KIM et al., 2010; KIM et al., 2013).

A FUCO, em uma concentração que não apresenta efeito citotóxico (30 μM), suprimiu a invasão de células B16-F10 de melanoma em camundongos, bem como a migração celular em um ensaio de cicatrização de feridas. Estes resultados foram acompanhados por uma diminuição de MMP-9, CD44 e do receptor de quimiocina 4,

que são conhecidos por desempenharem papéis cruciais na migração e invasão do câncer, bem como na redução da formação de fibras de actina nas células, demonstrando que a FUCO suprime a metástase de células B16-F10 de melanoma altamente metastáticas *in vitro* e *in vivo* (CHUNG et al., 2013).

Em um estudo conduzido por Shimoda e colaboradores (2010), a aplicação cutânea da FUCO (1%) inibiu a atividade da tirosinase e da melanogênese em melanoma induzido por radiação UVB, além de suprimir a ciclooxigenase 2 (COX-2) e o receptor de melanocortina 1 (MC1R), que são os estimulantes da melanogênese das células epiteliais. Do mesmo modo, foi demonstrado efeito protetor da FUCO frente à radiação UVB, demonstrando também o efeito antioxidante da FUCO (HEO e JEON, 2009; URIKURA, SUGAWARA e HIRATA, 2011).

Neste contexto, Martin (2015) evidencia a baixa toxicidade da FUCO em células normais e o grande potencial como agente quimiopreventivo e/ou agente quimioterápico no tratamento do câncer. Além disso, Muthuirulappan e Francis (2013) sugerem o desenvolvimento de nanopartículas contendo FUCO, pois há evidências científicas dos efeitos terapêuticos e de sua estabilidade limitada.

3.5 Matérias-primas de origem vegetal da Amazônia

O Brasil está entre os 17 países mega diversos do mundo, com exuberante diversidade biológica tanto em número de espécies quanto na variedade e na complexidade. A floresta Amazônica é o maior reservatório natural de plantas no mundo e os materiais extraídos são uma importante fonte de pesquisa que visam a descoberta de novas substâncias com atividades farmacológicas. A indústria farmacêutica tem usado compostos de origem natural tanto como ativos em si quanto como base para o desenvolvimento de novas moléculas (BUTLER, 2004; OLIVEIRA e do AMARAL, 2004; ALVES et al., 2008; PIMENTEL et al., 2015).

Desta forma, a biodiversidade brasileira pode representar uma nova estratégia para a indústria, como fonte de novos insumos farmacêuticos, associados a métodos modernos de *drug delivery*, como as nanopartículas.

Neste contexto, tem-se o bacuri (*Platonia insignis* Mart., Clusiaceae), que é uma árvore cujos os frutos são usados para a produção da menteiga e do óleo de bacuri. Popularmente, usado para fins fitoterápicos é bem difundido como sendo um remédio contra picadas de aranha e cobra, para problemas de pele e contra o

reumatismo e artrite. A manteiga de bacuri é absorvida alguns minutos depois que é aplicada e a pele torna-se aveludada ao toque, além de remover manchas e reduzir cicatrizes. Estes efeitos são devido ao seu alto nível de tripalmitina (50% a 55%), que penetra na pele rapidamente. Da mesma forma, a elevada quantidade de ácido palmitoleico (5%) confere ao bacuri propriedades emolientes, que também pode ser usado como um agente hidratante (MORAIS e GUTJAHR, 2009; RUFINO et al., 2010; SILVA et al., 2015; UEKANE et al., 2017). Além disso, a família Clusiaceae representa uma rica fonte de xantonas e benzofenonas poli-isopreniladas, responsáveis por várias atividades biológicas, destacando-se os efeitos antioxidantes e cicatrizantes (DIDEROT, SILVERE e ETIENNE 2006; ACUNA, JANCOVSKI e KENNELLY, 2009; RUFINO et al., 2010; KUMAR, SHARMA e CHATTOPADHYAY, 2013; LUSTOSA et al., 2016).

O tucumã (*Astrocaryum vulgare*, Arecaceae) é nativo da região amazônica, possivelmente do estado do Pará, onde tem o seu centro de dispersão, até a Guiana Francesa e Suriname. A fruta possui um caroço que é recoberto externamente de uma polpa alaranjada, de consistência oleosa. Popularmente, o tucumã possui muitas utilidades: o caroço é utilizado no artesanato, as folhas fornecem uma fibra bastante resistente e a polpa do fruto é consumida *in natura* ou em forma de bebida, contendo uma das mais elevadas concentrações de provitamina A, o β-caroteno. O óleo é empregado na cozinha e em massagens e é extraído da polpa que contém 25,6% de ácidos graxos saturados e 74,4% de ácidos graxos insaturados compostos por ácidos palmítico, esteárico, oleico e linoleico. Como é rico em ômega 3, 6 e 9, é um bom hidratante e é usado em cosméticos em hidratantes para a pele, loções para o corpo e produtos para cabelos danificados. O óleo é uma excelente fonte de carotenoides, contendo 21 tipos destes, e de vitamina B2 (riboflavina), além de apresentar compostos bioativos, como catequina e quercetina (BORA et al., 2001; DE ROSSO e MERCADANTE, 2007; MORAIS e GUTJAHR, 2009; KODAMA et al., 2010).

4. CAPÍTULO I - Caracterização da fucoxantina e do seu isômero e o desenvolvimento de método analítico indicativo de estabilidade por CLAE

4.1 Introdução

Qualidade, segurança e eficácia são os atributos mais relevantes de um produto farmacêutico. No entanto, considerando que as substâncias ativas compreendem um amplo espectro de compostos, variando de pequenas moléculas naturais ou sintéticas a grandes produtos biológicos, devem ser realizadas abordagens para garantir a qualidade destes (MAGGIO, VIGNADUZZO e KAUFMAN, 2013).

Uma condição essencial para o desenvolvimento de novas formas farmacêuticas, tanto do ponto de vista científico quanto regulamentar, é a elucidação e caracterização química da substância ativa (GANDHI et al., 2002). O *International Council for Harmonization* (ICH) (2005) menciona que a pureza da substância ativa utilizada é de extrema importância para o desenvolvimento e validação de uma metodologia analítica.

A escolha de uma metodologia analítica adequada também é de fundamental importância para o procedimento de controle de qualidade. Os métodos analíticos utilizados devem ser devidamente validados, desde a matéria-prima até o produto acabado, incluindo todas as fases do desenvolvimento do fármaco, desde a pesquisa até o controle de qualidade (BOUABIDI et al., 2010; GIL, 2010). O desenvolvimento de um indicativo de estabilidade é um processo que pode ser separado em três estágios. Primeiramente, requer-se a obtenção da substância ativa adequada, em seguida a seleção da técnica e da detecção correta, que compreende também o desenvolvimento e otimização do método e, finalmente, a validação do método (MAGGIO, VIGNADUZZO e KAUFMAN, 2013).

Deste modo, no Capítulo I está descrito o desenvolvimento de um método analítico indicativo de estabilidade por cromatografia líquida de alta eficiência (CLAE). Inicialmente, foi adquirido o padrão da FUCO e a matéria-prima em duas apresentações, incorporada em um óleo e na forma de pó. Portanto, foi realizada a caracterização das duas matérias-primas pelas técnicas de espectrometria de massas (EM), ressonância magnética nuclear de hidrogênio (RMN ^{1}H) e RMN bidimensional (COSY). Por cromatografia gasosa (CG), objetivou-se caracterizar o óleo ao qual a FUCO foi incorporada. Estas caracterizações foram realizadas visando o uso da FUCO em estudos futuros, pois sabe-se que variações na

isomeria da molécula podem diferir consideravelmente na sua eficácia biológica (CRUPI et al., 2013). Por fim, houve a validação do método analítico indicativo de estabilidade por CLAE para detecção e quantificação da FUCO, seguindo os parâmetros oficiais (BRASIL, 2003, ICH, 2005; USP, 2017). O trabalho está disposto na forma de artigo científico, de acordo com as normas da revista na qual foi publicado.

4.2 Artigo científico

Characterization and analysis of fucoxanthin and its isomers

Publicado no periódico *Journal of Pharmaceutical Science and Bioscientific Research, v.5, n. 7, p. 322-334, 2017.*

Characterization and analysis of fucoxanthin and its isomers

Leticia Malgarim Cordenonsi*[a], Andressa Santer[a], Rafaela Martins Sponchiado[a], Martin Steppe[a], Renata Platcheck Raffin[b], Elfrides Eva Scherman Schapoval[a]

[a] Programa de Pós-Graduação em Ciências Farmacêuticas, Faculdade de Farmácia, Universidade Federal do Rio Grande do Sul, 90610-000 Porto Alegre - RS, Brasil.
[b] Programa de Pós-Graduação em Nanociências, Centro Universitário Franciscano, 97010-032 Santa Maria – RS, Brasil.

*Corresponding author: Leticia Malgarim Cordenonsi,
Post Graduation Program in Pharmaceutical Sciences, Faculty of Pharmacy /
Federal University of Rio Grande do Sul (UFRGS),
Av. Ipiranga 2752, sala 402 Porto Alegre-RS, Brazil, CEP 90610-000
Phone: +55 51 33085214
Email: leticiacordenonsi@hotmail.com

Abstract

Fucoxanthin (FUCO) is extremely instable and occur in nature as different isomers which may differ considerably in their biological effectiveness. Therefore, the aim of this work was to identify the FUCO isomers in oil and powder samples by LC-MS and NMR analyses and then to develop a precise, reliable, and rapid HPLC-DAD method for quantifying them; moreover, the effect of heating, basic and acid medium and light on their stability was measured. FUCO and isomers were identified as all-*trans* and 9'-*cis* fucoxanthin with MS and NMR spectra. Different chromatographic parameters were carefully optimized and the method was specific, linear (1-40 µg mL^{-1}; r>0.99), precise (standard deviation values <0.7%), accurate (mean recovery = 103.25%), low limit of quantification (0.1 µg mL^{-1}). Moreover, the robustness was investigated using the Box–Behnken experimental design and factors studied simultaneously were: pH of mobile phase, wavelength and column temperature, each at three levels, producing results within the acceptable range. This proposed method was successfully applied the analysis of FUCO, emphasizing thus the advantages of the method: high efficiency, reliable and rapid analysis. Our results suggested that method can be used for the quality control of FUCO and its isomers.

Keywords: Marine carotenoids, fucoxanthin, isomers, study stability, validation, HPLC.

1. Introduction

Carotenoids are isoprenoid molecules, which are some of the first naturally occurring pigments and are responsible for the bright color of various fruits, vegetables, insects, and marine animals [1-3]. They are supposedly potential agents for the treatment of cancer, diabetes, and cardiovascular diseases [4-7].

Fucoxanthin (FUCO) (3'-acetoxy-5,6-epoxy-3,5'-dihydroxy-6',7'-didehydro-5,6,7,8,5',6'-hexahydro-β,β-caroten-8-one) is a marine carotenoid present in the chloroplasts of numerous classes of microalgae and brown macroalgae, such as wakame (*Undaria pinnatifida*), kombu (*Laminaria japonica*), hijiki (*Hijikia fusiformis*), arame (*Eisena bicyclis*), and *Sargassum fulvellum*. It is the most abundant of all carotenoids, accounting for more than 10% of the estimated total natural production [8-10]. Currently there is great interest in isolating novel bioactive compounds from the marine environment, which contains rich natural resources, such as algae [1].

The complete structure of FUCO including chirality was determined by Englert and co-workers [11]. This carotenoid has a distinctive structure with an uncommon allenic bond and 5,6-monoepoxide in its molecule and further includes oxygenic functional groups, such as hydroxyl, epoxy, carbonyl, and carboxyl groups in addition to its polyene chain (Figure 1) [12-13].

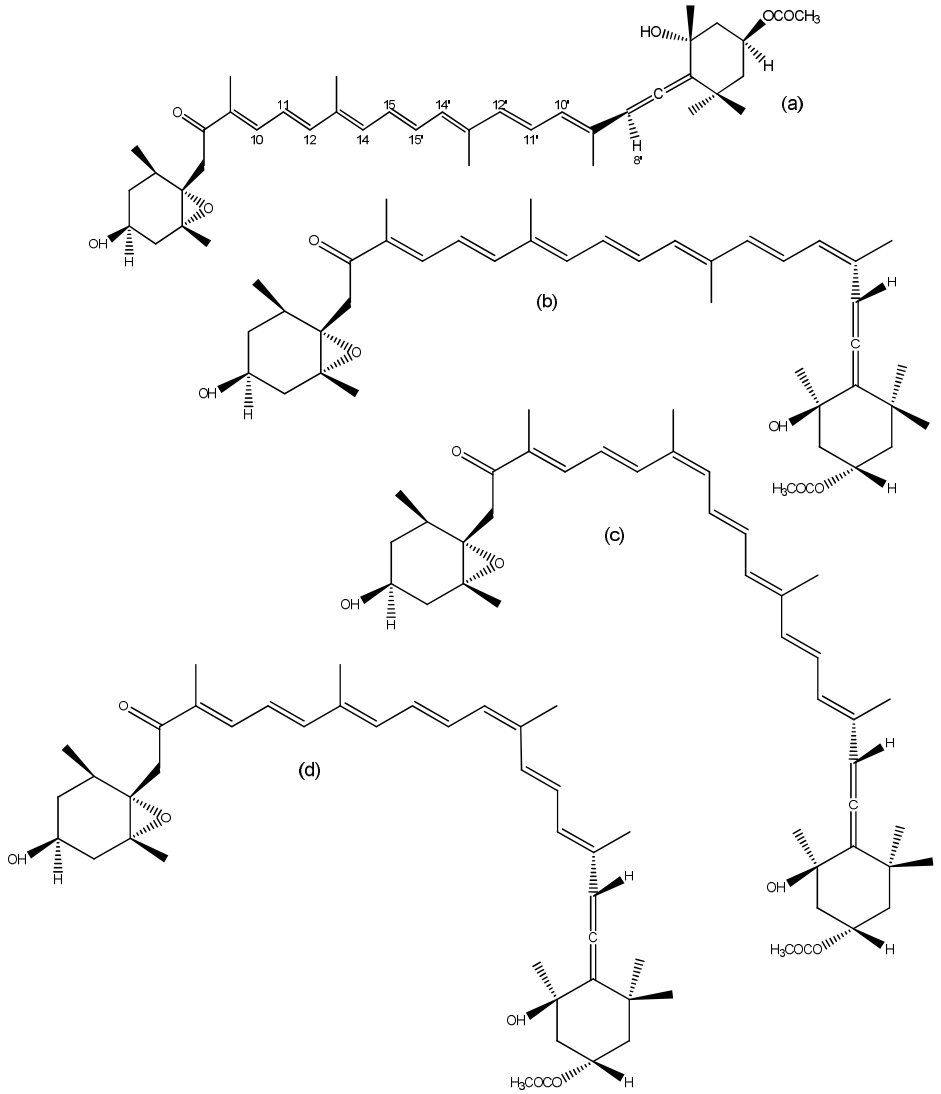


Figure 1. Structure of (a) all-*trans* fucoxanthin, (b) 9'-*cis* fucoxanthin (c) 13-*cis* fucoxanthin, and (d) 13'-*cis* fucoxanthin ($C_{42}H_{58}O_6$).

FUCO rich brown seaweeds have traditionally been used in the Southeast and is a promising option for the prevention and treatment of cancer and a wide variety of related pathologies, including obesity and diabetes [14-17]. Cancer preventing influences of FUCO are mediated through different signaling pathways, as the caspases, different proteins and enzymes. Furthermore, other molecules are involved in cell cycle arrest, apoptosis and anti-angiogenesis or inhibition of metastasis [18-21].

This carotenoid is extremely instable and occur in nature as different isomers which may differ considerably in their biological effectiveness [2]. Therefore, the aim of this work was to identify the FUCO isomers in oil and powder samples by LC-MS and NMR analyses and then to develop a precise, reliable, and rapid HPLC-DAD method for quantifying them; moreover, the effect of heating, basic and acid medium and light on their stability was measured.

2. Materials and Methods

2.1 Materials

A reference standard of FUCO ($C_{42}H_{58}O_6$) with purity of >95%, was supplied by Cayman Chemical Company® (Ann Arbor, MI, USA). Samples of FUCO in powder and oil were assigned a content of 30% and 2%, respectively, were kindly donated by Shaanxi Jiahe Phytochem Co., Ltd. (Xian, China). All chemicals used were of pharmaceutical or analytical grade. Ultrapure water was obtained from a Milli-Q apparatus (Millipore®, USA).

2.2 Identification of fucoxanthin in oil and powder

2.2.1 Liquid chromatography coupled to mass spectrometry (LC-MS/MS)

LC-MS/MS measurements were carried out using an Agilent 1100 Series chromatographic system coupled to an AB Sciex API 5000 triple quadrupole mass spectrometer with an electrospray source in positive ionization mode (ESI+). The conditions used were collision energy 10 eV, declustering potential 100 eV and source temperature 300 °C. Instrument control and data processing were carried out by means of Analyst 1.6.1 software. Separation was achieved in a Symmetry C18 LC column (75 x 4.6 mm; 3.5 mm particle diameter) from Waters. The injection volume was 6 µL, with flow rate adopted was 0.4 µL min^{-1} and mobile phase is composed by acetonitrile and water (9.5:0.5 *v/v*). Separately, FUCO in oil and powder were prepared in acetonitrile at 5.0 µg mL^{-1}.

2.2.2 Nuclear magnetic resonance (NMR) analysis

Previously, several solvents (methanol, ethanol, acetone, and n-hexane), solvent volume and extraction temperature were tested to determine the optimal conditions for FUCO extraction. Every procedure was performed under dark

conditions to prevent pigment degradation. Separately, approximately 10 mg of FUCO in oil and powder were spiked with 2 mL of n-hexane. The mixtures were centrifuged at 3,000 rpm for 5 min (Centrifuge Excelsa®). Supernatants were separated and the extraction procedure was repeated twice using 1 mL of n-hexane. The n-hexane was evaporated to dryness at room temperature. The residue of FUCO was dissolved in 1 mL deuterated methanol (CD3OD) and used for NMR spectroscopy. The proton NMR (^{1}H NMR) and two-dimensional COSY spectra of FUCO in oil and powder were recorded on a Bruker® AVANCE600 (Rheinstetten, Germany). Chemical shifts were adjusted with δ (ppm) referring to the solvent peak δH 3.31 for CD3OD. Data were processed with the MestRe Nova program, interpreted and compared with data in the literature.

2.2.3 Gas Chromatography

For preparation of FUCO, into 0.5 g oil containing FUCO were added and then shaken 5.0 mL methanol and 0.1 mL methanolic potassium hydroxide. The mixture was heated at 100 ºC for 15 min in a water bath. After cooling, 2.5 mL hexane were added and occasionally shaken; 5.0 mL saturated sodium chloride solution were added and shaken vigorously. The organic layer was separated and analyzed. The chemical composition was analyzed by gas chromatography–mass spectrometry (GC–MS) (Shimadzu®, quadrupole MS system QP5000, at 70 eV). A silica capillary column of VF-23 Varian® (30 m x 0.25mm x 0.25 m, coated with DB-5) was used to separate constituents. Injector and detector temperature were set at 220 °C and 250 °C, respectively; the oven temperature was programmed as 50-260 ºC at 3 °C min^{-1}, using helium as carrier gas at a flow rate of 1.0 mL^{-1}. The injection volume was 1.0 µl (splitless mode). The identification of compounds was based on the comparison of retention indices and their mass spectra, with authentic standards and with data taken from the literature [22] or by comparison with mass spectra recorded in the database. Relative amounts of the components were calculated based on GC peak areas.

2.3 HPLC-DAD system

An HPLC Agilent® model 1200 UV/LC system (Santa Clara, USA), consisting of a quaternary pump, a degasser, a column thermostat, a diode array detector

(DAD) and a thermostated auto sampler was used. System control and data analysis were performed using ChemStation software. Chromatographic identification and quantification of FUCO was achieved on an Agilent® Eclipse Plus C18 analytical column (4.6 mm x 150 mm, 5.0 µm). All separations were obtained in isocratic mode using acetonitrile and water, pH adjusted to 7.0 with sodium hydroxide 0.1 *M* (NaOH) (9.5:0.5 *v/v*). The system was programmed at 40 ºC for the column oven, 450 nm for the detection wavelength, flow rate was 1.0 mL min^{-1} and 50 µL for the injection volume.

The stock solutions of reference standard and sample solutions of FUCO in oil were prepared in order to optimize the experimental procedure and decrease the chance of analytical errors. The solutions were prepared with acetonitrile and the dilutions were done with acetonitrile and water, pH adjusted to 7.0 with NaOH 0.1 *M* (9:1 *v/v*). All analyses were performed under dark conditions.

2.4 Validation of HPLC-DAD method for fucoxanthin in oil

The method was validated based on the International Council on Harmonization (ICH) guidelines [23-24] and United States Pharmacopeia (USP) requirements [25], following the validation parameters: specificity, linearity, precision, accuracy, limit of detection, limit of quantification, and robustness. A Box-Behnken design with three factors was planned for robustness evaluation.

Specificity. Forced degradation studies were performed in order to provide an indication of stability. FUCO in acetonitrile, at 30.0 µg mL^{-1}, was subjected to degradation under acidic (hydrochloric acid - HCl 0.01 *M*), basic (NaOH 0.01 *M*), photolytic (UV-A radiation - 352 nm and UV-C radiation - 254 nm), oxidative (hydrogen peroxide - H_2O_2 0.3%), and thermal (65 °C) stress conditions. The acidic and basic conditions were carried out at room temperature for 4 h and the solutions were neutralized with base or acid before injection. The oxidation reaction with H_2O_2 0.3% was performed out at room temperature for 3 h before injection. For the photolytic degradation study, aliquots of FUCO were transferred to a 1 cm quartz cell, for 4 h. The cells were exposed, positioning them horizontally to have the maximum exposure area, under the direct incidence of UV-A radiation (Blacklight blue lamp – Orion, 352 nm/ 30 W) and UV-C radiation (Light Express lamp LE UV, 254 nm/30 W), in a glass chamber that is mirrored internally (100 × 16 × 16 cm). For the thermal

degradation study, FUCO was placed at a constant temperature of 65 ºC for 1 h. All samples were analyzed by HPLC-DAD to ensure the purity of the FUCO peak in all the stressed sample solutions.

Linearity. Linearity was determined by three analytical curves (peak area versus concentration), each one with nine concentrations for reference standard of FUCO, in the range of 1.0-40.0 μg mL^{-1} (1.0; 3.0; 5.0; 10.0; 15.0; 20.0; 25.0; 30.0 and 40.0 μg mL^{-1}).

Precision. The precision of the method was evaluated by injection of six preparations of FUCO at a concentration of 30.0 μg mL^{-1}, quantified against a reference standard. The results were expressed by repeatability (intra-day) and intermediate precision (inter-day) and the relative standard deviation (RSD, %) was calculated.

Accuracy. The accuracy of the method was evaluated in triplicate by adding standard solution at three concentration levels, low, medium, and high (5.0, 20.0, and 40.0 μg mL^{-1}, respectively) by the standard addition technique. The percentage of recovery was calculated at each level.

Limit of detection (LOD) and limit of quantification (LOQ). The limits were obtained based on the signal-to-noise by the ChemStation software. The LOD and LOQ for each sample were estimated at a concentration level in which the signal-to-noise ratio reached 3:1 and 10:1, respectively. The precision of LOQ was evaluated and the RSD were calculated.

Robustness. The robustness was investigated using the Box–Behnken experimental design. Three experimental parameters range in three levels were tested, pH range +/- 0.2 pH unit; temperature column +/- 2 ºC, and wavelength +/- 2 nm. Three replicates were used in the experiment and Minitab® software was used for modeling.

2.5 Kinetic degradation of fucoxanthin in oil

Degradation kinetics study was carried out under oxidative (H_2O_2 0.3%), stress conditions at room temperature, at pre-established times (0, 15, 30, 45, 60, 90, 120, 150 and 180 min). In this study, kinetic rate of FUCO degradation in oil was determined by plotting the drug concentration (zero order process), the log (first-order process), and the reciprocal (second-order process) of concentration versus

time. The determination coefficients (R^2) were obtained and the best observed fit indicated the reaction order. The kinetic parameters, such as the apparent order degradation rate constant (*k*), half-life time ($t_{1/2}$), and $t_{90\%}$ (time where 90% of original concentration of the drug is left), were obtained.

2.6 Analysis using HPLC-DAD method of fucoxanthin in powder

After identifying FUCO in powder, the sample was analyzed by HPLC-DAD using the method previously described in item 2.3. Stability studies were performed according to described forced degradation studies for FUCO in oil.

2.7 Statistical analysis

Data were analyzed by one-way ANOVA, a value of $p<0.05$ was considered statistically significant. The experimental designs was performed by the Minitab 14 (Minitab Inc, State College, PA, USA) data analysis software system.

3. Results and discussion

3.1 Identification of fucoxanthin in oil and powder

Several studies were conducted for the extraction and purification for FUCO from algae employing the use of different methods, modifying the solvent type, extraction time, temperature and extraction technology (maceration, ultrasound-assisted extraction, Soxhlet extraction, and pressurized liquid extraction). These methods, however, can induce oxidation, producing degradation products and isomers [26-28]. The correct identification of isomers is a fundamental point for the development of a stability indicating HPLC-DAD method, because accurate analysis is a prerequisite, since isomers differ substantially in their biochemical activity [29-30].

In the present study, FUCO isomers were identified by LC-MS/MS. Daughter ions obtained from protonated molecular ions of FUCO in oil ([M + H] 659.2 *m/z*) included main ions from each compound at *m/z* 641.6, 581.4, 429.4, 411.5 and 213.3. In powder, daughter ions obtained from protonated molecular ions ([M + H] 659.3 *m/z*) included main ions from each compound at *m/z* 641.3, 581.4, 497.7, 297.4 and 213.3. The mode scanning at *m/z* 641, 659, and 581 corresponding to $[M + H - nH_2O]^+$, $[M + H]^+$ and $[M + H - H_2O\text{-}AcOH]^+$, respectively. These three

fragments ions and dehydrated product ions from protonated molecules [M + H - nH2O]+ are observed for all hydroxylated carotenoids, such FUCO. Moreover, intensities of the dehydrated product ions may vary and reveal the structural characteristics of the hydroxylated end groups of isomeric carotenoids, allowing the distinction between structural isomers. FUCO and its isomers possess the same molecular formula, $C_{42}H_{58}O_6$, but the results showed differences in the fragments ions in LC-MS spectra [9-31].

The pure compounds from the extractions were subjected to ^{1}H NMR and two-dimensional COSY analysis. Chemical shift values for each FUCO isomer corroborated with previously reported values (Table 1). Furthermore, a detailed comparison of these data, particularly focusing on the olefinic protons in the COSY spectra (Figure 2), revealed that strong cross peaks between H8' and H11' and between H19' and H10', proved the 9'-*cis* isomer. The purified FUCO in oil was identified as all-*trans* fucoxanthin and FUCO in powder was identified 9'-*cis* fucoxanthin [11-32,33].

Table 1. ^{1}H NMR chemical shifts of the olefinic protons (in ppm, CD3OD) of fucoxanthin.

	H10	**H11**	**H12**	**H14**	**H15**	**H15'**	**H14'**	**H12'**	**H11'**	**H10'**	**H8'**	**H19'**
Oil	7.50	6.70	6.98	6.63	6.80	7.38	6.41	6.50	6.74	6.19	6.10	1.87
Powder	7.49	6.68	6.98	6.63	6.82	7.34	6.40	6.43	7.03	6.15	7.00	4.75

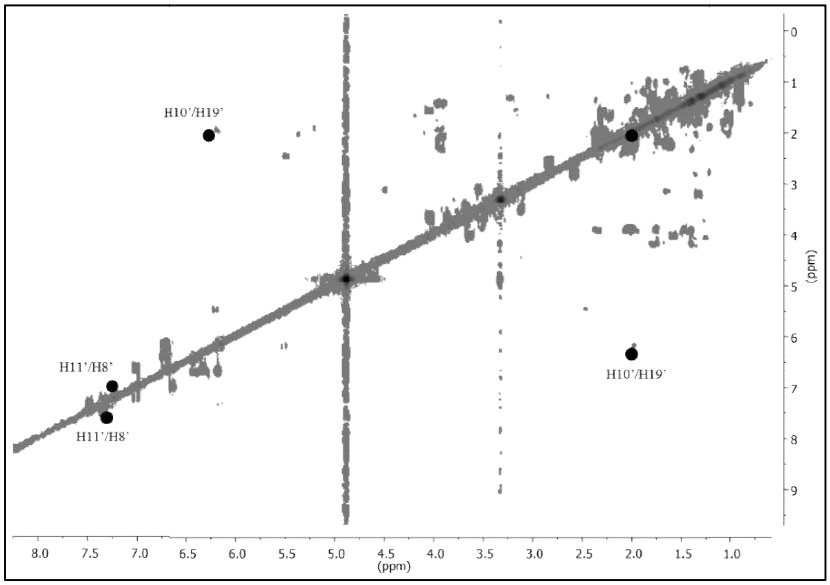


Figure 2. COSY spectrum of fucoxanthin in powder. Only relevant cross-peaks were assigned, between H8'/H11' and H19'/H10'.

In order to identify the components of oil by GC–MS, a representative chromatogram of FUCO in oil is provided in Figure 3. Seven integratable peaks were observed, four compounds were identified like as fatty acid, caprilic acid (49.4% in 13.1 min) and capric acid (36.1% in 20.5 min) were largest components. Although present in relatively small amounts are palmitic (37.6 min) and γ-linolenic acid (46.8 min). Three peaks were observed as fragments of FUCO, 13.4% of total peak area in 51.4, 57.4, and 60.2 min. Identification of fragments were made by comparison with mass spectrum with data taken from the literature.

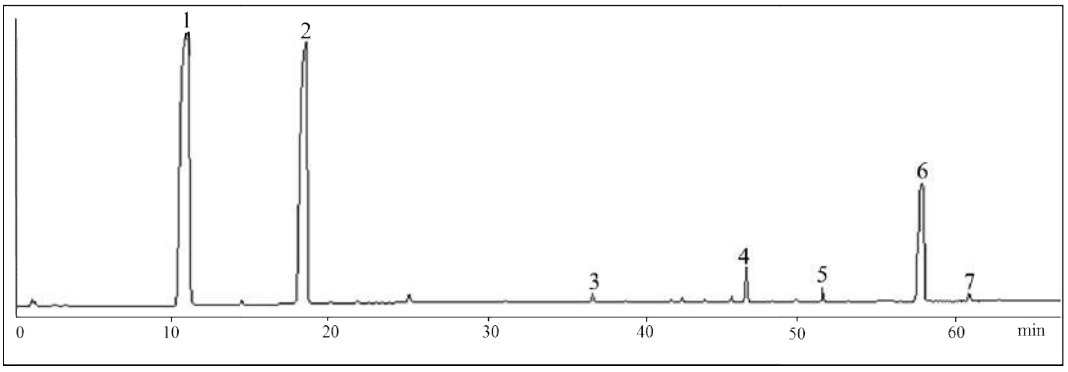


Figure 3. GC chromatogram of the FUCO in oil: (1) caprilic acid, (2) capric acid, (3) palmitic acid, (4) γ-linolenic acid and (5-7) fragments of FUCO.

The information provided by MS is of great help since it allows differentiation of carotenoids, because give rise to molecular weight and characteristic fragmentation patterns. On the other hand, carotenoids and its isomers are very similar in their chemical composition, having the same molecular weight and differences in the fragments ions [34]. In these cases, the information provided by and NMR and HPLC-DAD analyses contributes to unequivocal identification. In conclusion, FUCO in oil was identified as all-*trans* fucoxanthin and FUCO in powder was identified 9'-*cis* fucoxanthin. In addition, the oil has been identified like as fatty acid.

3.3 Optimization of chromatographic conditions

The main problem in carotenoid analysis arises from their instability. This means precautionary to avoid quantitative losses, such as completion of the analysis within the shortest possible time, protection from light, avoiding high temperature and contact with acid [3].

The physical and chemical properties of FUCO, such as polarity and solubility will be considered for determination by HPLC. Likewise, various experimental conditions were tested and optimized by using different column temperature, flow rate, ratios of acetonitrile/water, and pH values.

Acetonitrile was selected because FUCO is insoluble in water and soluble in organic solvents and DMSO. The flow rate was altered between 0.9, 1.0, and 1.2 mL min^{-1} to shorten the time of analysis, but it was observed that the resolution was not drastically affected by increasing the flow rate. The column was heated to temperatures of 40 ºC, thus reducing the pressure, because the viscosity of the mobile phase strongly depends on the temperature. It was reported that FUCO has good thermostability, between 80 – 100 °C, for 1 h [3,35].

After selection of column temperature, flow rate and ratio of acetonitrile/water, the next step is to optimize pH in the mobile phase. According to the USP requirements, system suitability tests are an integral part of methods. These tests are used to verify that the chromatographic system is adequate for the intended analysis. Parameters affecting the chromatographic response were studied, such as number of plates (column efficiency), retention time, tailing factor, retention factor, and

resolution compared with different pH values, 3.0, 5.0, 7.0, and 9.0 (Figure 4). At higher pH values, separation occurred with decreased retention times, but pH 7.0 is more efficient with a high number of plates. Resolution and tailing factor do not change at different pHs.

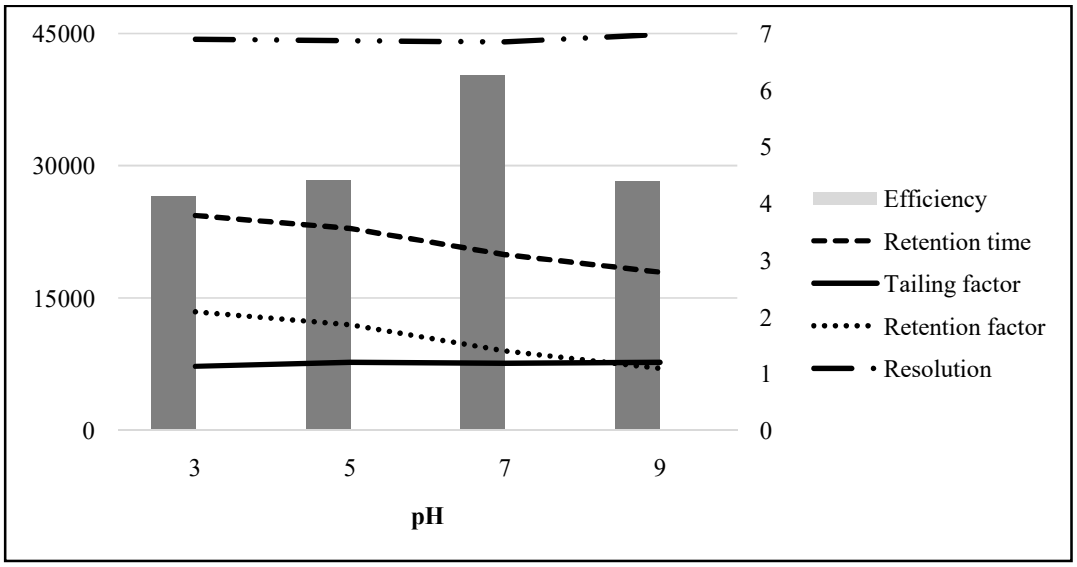


Figure 4. The effect of pH 3.0, 5.0, 7.0 and 9.0 on plates (column efficiency), retention time, tailing factor, retention factor and resolution of FUCO.

Based on the previous studies by Muthuirulappan and Francis [36] and Yip and co-workers [37], when FUCO was extracted from Malaysian brown seaweed, the stability tests showed that is most stable in pH 5.0-7.0, stored in conditions of darkness. In addition, according to Hii [38], FUCO is less stable in an acidic pH condition.

In Figure 5a shows the chromatograms obtained by HPLC-DAD and UV absorption spectra of reference standard and FUCO; FUCO eluted after 3 min, with a retention time identical to the standard reference and the purities of all the peaks were greater than 99.9%, indicating homogenous peaks. FUCO and reference standard showed an absorption spectrum with maximum at 332, 447 and 468 nm. Most carotenoids absorb maximally at three wavelengths, resulting in three peaks and the greater the number of conjugated double bonds, the higher the wavelength maximum values [3]. Other minor peak appears (retention time of 4.4 min) around the

FUCO peak and the UV-VIS spectrum of this peak showed a hypochromic shift (Figure 5b).

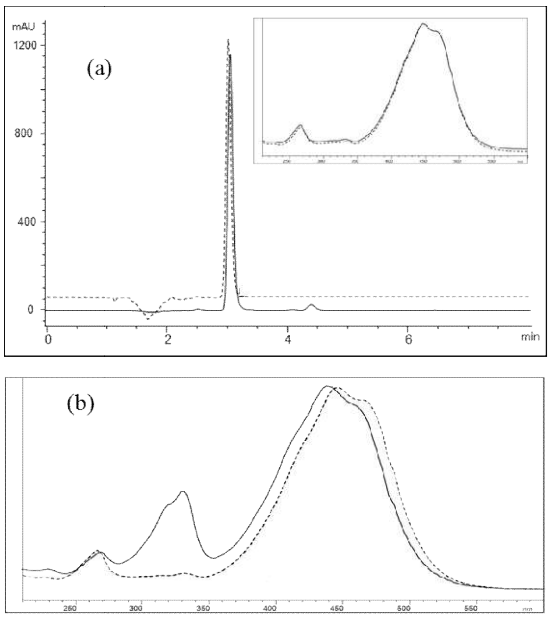


Figure 5. (a) HPLC-DAD chromatogram and UV absorption spectra (30.0 µg mL^{-1}) of reference standard (trace) and FUCO (line); **(b)** HPLC-DAD chromatogram and UV absorption spectra of FUCO (trace) and minor peaks (line).

3.3 Method validation for fucoxanthin in oil

The purpose of developing an analytical method is to provide a qualitative and quantitative result with an acceptable uncertainty level. In addition, the validation is needed to assure high quality, so that the products will be accepted by the regulatory agencies and obey the mandatory requirements for the registration of any pharmaceutical product [39,40]. The method validation parameters have been defined in different national and international committees. However, some of the definitions vary between the different organizations and an attempt was made to harmonize them for pharmaceutical applications [24].

Forced degradation studies

Forced degradation studies can help to identify the likely degradation products, which can in turn help establish the degradation pathways, intrinsic stability of the molecule, and presence of its potential impurities [41]. The specificity of the

developed method was determined by injecting sample solutions, 30.0 μg mL^{-1}, which was prepared under stress conditions. Table 2 summarizes the forced degradation results and chromatograms of the stress tests are shown in Figure 6.

After exposure to acid and alkaline conditions, approximately 48% and 65% of FUCO were degraded, respectively. The FUCO peak was recorded at 3.2 min, under the same condition and additional peaks were seen in the chromatogram. FUCO was found to be highly labile to oxidative degradation, after 3 h, approximately 60% drug degradation was observed. Under photolytic conditions, decreases in FUCO concentration from acetonitrile solution were observed. After 4 h of exposition to UV-A irradiation approximately 26% of FUCO degradation was detected and after only 45 min of UV-C, 72% of FUCO was degraded. FUCO was found to be stable at 65 °C, indeed after 1 h, only 1.6% degraded. The minor peak (retention time of 4.4 min) maintained its area. In addition, the resolution of peaks was calculated. This value of 2.0 or greater between two peaks will ensure that the sample may be accurately measured. Analyzing the chromatograms and values expressed in the table, all peaks were separated by this method with satisfactory resolution.

Alkaline condition and light irradiation (UV-C) were the main accelerators for the degradation of FUCO and other peaks appear in the chromatograms of the forced degradation study, demonstrating that the degradation products were detected using the optimized chromatographic conditions. During the analysis, bleaching solution of FUCO was observed under all stress conditions. Loss or change of color at any time during the analysis provides an immediate indication of degradation or structural modification [3].

Table 2. Summary of forced degradation results of FUCO in oil subjected to degradation under acidic (HCl 0.01 *M*), basic (NaOH 0.01 *M*), photolytic (UV-A and UV-C radiation), oxidative (H_2O_2 0.3%), and thermal (65 °C) conditions.

Stress Condition	Time	Degradation	Resolution	Remarks
Reference standard	-	-	-	-
FUCO	0	-	-	-
Acidic	4 h	48.2%	6.28*	Increase area of minor peaks
Alkaline	4 h	65.2%	2.7/5.71**	Increase area of minor peaks and degradation products formed
Oxidative	3 h	59.8%	5.38*	Increase area of minor peaks
UV-A radiation	4 h	26.6%	5.52*	Increase area of minor peaks and degradation products formed
UV-C radiation	45 min	71.9%	6.03*	Significant degradation observed, increase area of minor peaks and degradation products formed
Temperature	1 h	1.6%	5.83*	-

* Resolution from the FUCO peak (3.2 min) and peak about 4.4 min

** Resolution from the FUCO peak (3.2 min) and peaks about 2.2 and 4.4 min

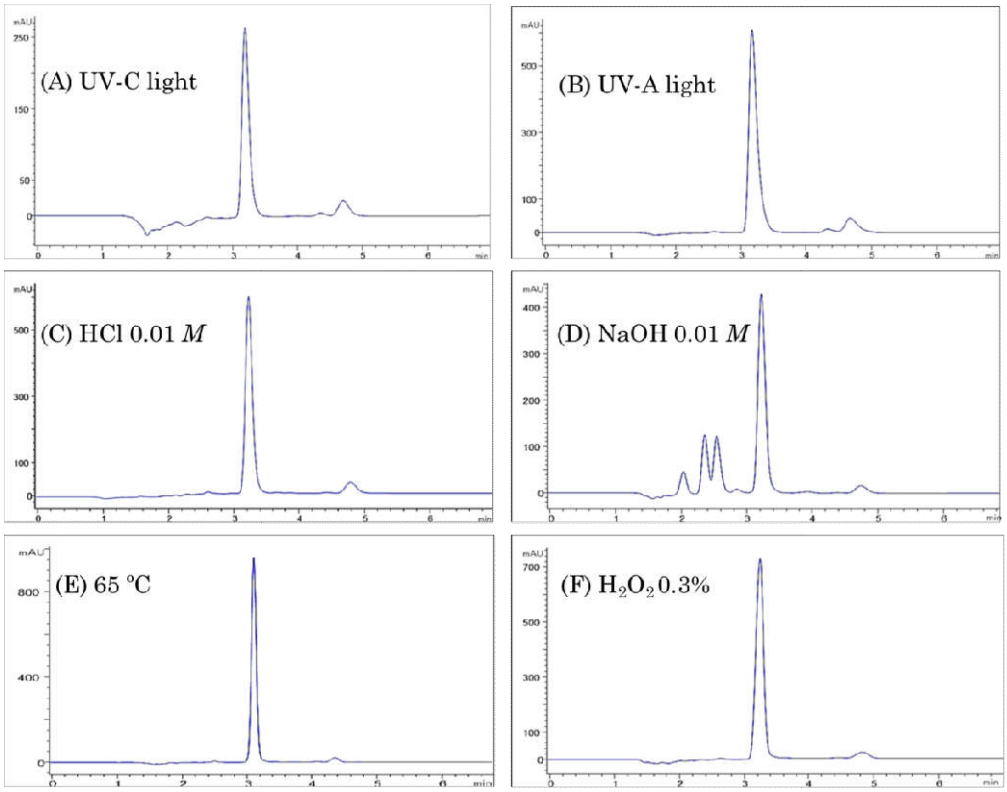


Figure 6. HPLC chromatograms obtained after forced degradation: (A) UV-C light for 45 min; (B) UV-A light for 4 h; (C) HCl 0.01 *M* for 4 h; (D) NaOH 0.01 *M* for 4 h; (E) 65 ºC during 1 hour; (F) H_2O_2 0.3% for 3 h.

Like other carotenoids, FUCO can be degraded when exposed to heat, light, oxygen and other pro-oxidant molecules, due to an extensive system of conjugated double bonds (polyene chain) [42]. The formation of some *cis* isomers by isomerization would happen which was related to treatment conditions. FUCO usually resulted in one main peak consisting of the *trans* form along with its isomers [13] and small fragments are also generated through breakdown at various carbon-carbon double bonds in the polyene chain, such as apocarotenoids (carotenoids with a shortened carbon skeleton) [43] (Figure 7).

The presence of a *cis* double bond carotenoid molecule creates greater steric hindrance between nearby hydrogen atoms and/or methyl groups, so that *cis* isomers are generally less stable thermodynamically than the *trans* form. With some double bonds, steric hindrance is relatively small so that isomers with *cis* double bonds in these positions are relatively easily formed and relatively stable. Therefore, 9'-*cis*, 13-

cis, and 13'-*cis* isomers were formed as main isomers during the incubation of all *trans* FUCO [30,44]. In this respect, isomerism has an effect on the absorption spectrum, with a new maximum appearing in the UV spectra (around 320–340 nm), retention time in chromatograph, melting points, solubility and molecule stability [45].

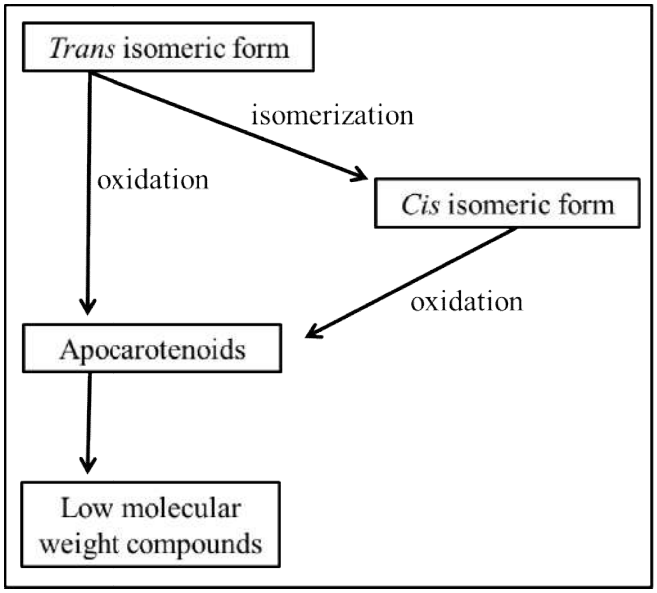


Figure 7. Possible scheme for the carotenoid degradation (Adapted from Yahia and Ornelas, [46]).

A spectrophotometric analysis of FUCO in canola oil was performed and results showed that heating caused the degradation of all-*trans* when exposed to a temperature of 25-100 ºC. By increasing the temperature, the formation of 13-*cis* and 13'-*cis* and the degradation of 9'-*cis* would also be promoted. The degradation of all-*trans* and 13-*cis* and 13'-*cis* FUCO was synergistically promoted when exposed to both air and light [47].

Linearity. Method linearity was observed over the concentrations range of 1.0 to 40.0 μg mL^{-1} at 450 nm, with significantly high coefficient correlation values (r=0.9994) for FUCO. The validity of the assay was verified by means of ANOVA, which demonstrated significant linear regression ($F_{calculated}<F_{critical}$ = 4.23; $p<0.05$) and non-significant linearity deviation ($p>0.05$), shown in Table 3.

LOD and LOQ. LOD with a signal-to-noise ratio of 3:1 was found to be 0.03 μg mL^{-1} and LOQ with a signal-to-noise ratio of 10:1 was found to be 0.10 μg mL^{-1}. These results indicate the adequate sensitivity of the method.

Precision. Precision evaluated as the repeatability (intra-day) and intermediate precision (inter-day) of the method was determined by calculating the RSD for six determinations at a concentration of 30 μg mL^{-1}. The experimental values obtained are presented in Table 3. The results indicate low RSD obtained for the repeatability and intermediate precision and showed the good precision of the method in both samples.

Accuracy. Determination of accuracy allows estimating the extent to which systematic errors affect the analytical method [40]. The accuracy of the method to quantify FUCO was calculated by percentage of recovery. The mean values were found to be 103.25% (RSD= 0.92%). These results showing satisfactory accuracy of the proposed method.

Table 3. Validation parameters of the stability-indicating HPLC-DAD method.

Parameters	Fucoxanthin
Retention time of standard (min)	3.01
Retention time of fucoxanthin (min)	3.14
Linearity	
Working range (μg mL^{-1})	1.0 – 40.0
Equation	y = 66,503x + 16,853
Coefficient correlation	0.9994
LOD (μg mL^{-1})	0.03
LOQ (μg mL^{-1})	0.10
Repeatability (RSD, %)	0.46
Accuracy (%)	103.25
Intermediate precision (RSD, %)	0.69

Robustness. The robustness refers to the signal drug's ability to remain unaffected by small and deliberate variations in method parameters. In order to evaluate the simultaneous variations of the factors in the responses considered, a multivariate approach using experimental design is recommended [40]. A response surface Box-

Behnken design was applied with focus on the pH of the mobile phase, wavelength, and column temperature. According to the ANOVA of the regression model, both linear and quadratic terms were significant, with $p<0.05$ and showed a good correlation ($r>0.96$). There were no significant interaction effects and no evidence of inadequacy was detected by the lack-of-fit test ($p>0.05$). These results indicated that the stability indicating the HPLC-DAD method was robust since the variations applied to the experimental parameters did not produce any statistically significant effects.

3.4 Kinetic degradation

Considering preliminary stability tests, the degradation kinetics of FUCO was performed under basic conditions. FUCO degradation shows a first-order kinetics (r= 0.9918) under the experimental conditions applied. This reaction consider that the reaction velocity is directly proportional to the drug concentration. With this information, through mathematical calculations, a constant value of the decomposition of FUCO was k = 0.0363 min, the $t_{1/2}$ and $t_{90\%}$ were 19.08 and 2.92 min, respectively. The kinetics reactions were useful to determine the concentration changes as a function of time and the kinetics run parameters. These data, applied to decomposition speed and probable reaction mechanisms involved, allow discussing the parameters related to formulation, stabilization, and administration of drugs [48].

3.5 Analysis using HPLC-DAD method of *fucoxanthin* in powder

For the HPLC-DAD analysis, the same chromatographic conditions were used, as described in item 2.3. In Figure 8 is showed the HPLC-DAD chromatogram and UV absorption spectra of reference standard and FUCO in powder (line).

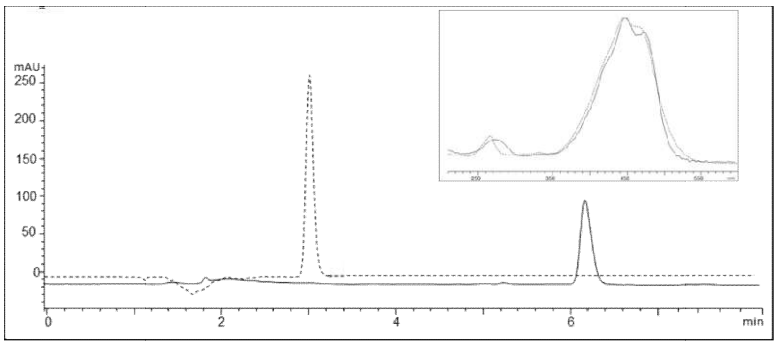


Figure 8. HPLC-DAD chromatogram and UV absorption spectra (30.0 μg mL^{-1}) of reference standard (trace) and FUCO in powder (line).

Figure 8 shows that the retention time for reference standard was 3.0 min and the retention time of FUCO in powder was 6.1 min. The maximum absorption wavelengths of both standard and FUCO in powder were similar. This peak, with retention time of 6.1 min, is believed to be *cis* isomer of FUCO, as suggested by previous studies [2,32]. Different retention times between reference standard and FUCO in powder may be due to the polarity. As reversed phase HPLC system was used, the more polar, reference standard, elute before the 9'-*cis* fucoxanthin.

It was also observed, during the analyses that the color of FUCO in powder was less intense. *Cis* isomerization of double bond causes a slight loss in color, small hypsochromic shift and hypochromic effect, accompanied by the appearance of a *cis* peak in or near the ultraviolet region. Moreover, the intensity of the *cis* band is greater as the *cis* double bond is nearer the center of the molecule [3].

Table 4 summarizes six degradations of FUCO in powder analyzed by HPLC-DAD. In the chromatograms, no additional peak was detected during the analyses. FUCO in oil, when compared with FUCO in powder, showed greater stability. Usually, *cis* isomers are thermodynamically less stable.

Table 4. Summary of forced degradation results of FUCO in powder subjected to degradation under acidic (HCl 0.01 *M*), basic (NaOH 0.01 *M*), photolytic (UV-A and UV-C radiation), oxidative (H_2O_2 0.3%), and thermal (65 °C) conditions.

Stress Condition	Time (min)	Degradation	Purity factor
FUCO in powder	**-**	**-**	99.9%
Acidic	60	85.7%	89.0%
Alkaline	60	84.5%	73.7%
Oxidation	60	75.5%	83.4%
UV-A radiation	60	43.5%	80.6%
UV-C radiation	30	90.9%	81.4%
Temperature	90	35.6%	99.8%

Conclusion

The purified FUCO in oil was identified as all-*trans* fucoxanthin and FUCO in powder was identified as 9'-*cis* fucoxanthin. An HPLC-DAD method has been developed for detection and quantification of FUCO. The method was validated according to current ICH guidelines and demonstrated specificity, linearity precision, accuracy, and robustness within the validated range. Furthermore, response surface and factorial designs was successfully used to test the robustness of the HPLC procedures. In forced degradation studies, all-*trans* and 9'-*cis* fucoxanthin differ substantially in their stability. The degradation kinetics of FUCO was determined, allowing kinetic parameters of basic degradation, such as rate constants (*k*) $t_{1/2}$ and $t_{90\%}$ to be calculated. The method is advantageous, because, besides being fast, good resolution, efficient it can be used for quantification of FUCO and its isomers. These results suggested that method can be used for the quality control of FUCO and the results will be employed of future studies in our research group for the development of nanoparticles.

References

(1) Christaki E, Bonos E, Giannenas I and Florou□Paneri P. Functional properties of carotenoids originating from algae. J. Sci. Food. Agric, 2013; 93:5-11.

(2) Crupi P, Toci AT, Mangini S, Wrubl F, Rodolfi L, Tredici MR and Antonacci D. Determination of fucoxanthin isomers in microalgae (Isochrysis sp.) by high performance liquid chromatography coupled with diode array detector multistage mass spectrometry coupled with positive electrospray ionization. Rapid Commun. Mass Spectrom, 2013; 27:1027-1035.
(3) Rodriguez-Amaya DB. A guide to carotenoid analysis in foods. 1.ed. Washington, DC: ILSI press.2001.
(4) Bolhassani A, Khavari A and Bathaie, SZ. Saffron and natural carotenoids: Biochemical activities and anti-tumor effects. Biochimica et Biophysica Acta, 2014; 1845:20-30.
(5) Meinke MC, Friedrich A, Tscherch K, Haag SF, Darvin ME, Vollert H and Rohn J. Influence of dietary carotenoids on radical scavenging capacity of the skin and skin lipids. Eur. J. Pharm. Biopharm, 2013; 84:365-373.
(6) Fiedor J and Burda K.Potential role of carotenoids as antioxidants in human health and disease. Nutrients, 2014; 6:466-488.
(7) Gammone MA, Riccioni G and D'Orazio N. Carotenoids: potential allies of cardiovascular health? Food Nutr. Res, 2015; 59:26762.
(8) Miyashita K, Nishikawa S, Beppu F, Tsukui T, Abe M and Hosokawa M. The allenic carotenoid fucoxanthin, a novel marine nutraceutical from brown seaweeds. J. Sci. Food. Agric, 2011; 91:1166-1174.
(9) Kim SM, Jung YJ, Kwon ON, Cha KH, Um BH, Chung D and Pan CH. A potential commercial source of fucoxanthin extracted from the microalga Phaeodactylum tricornutum. Appl. Biochem. Biotechnol, 2012; 166:1843-1855.
(10) Shimoda H, Tanaka J, Shan SJ and Maoka T. Anti□pigmentary activity of fucoxanthin and its influence on skin mRNA expression of melanogenic molecules. J. Pharm. Pharmacol, 2010; 62:1137-1145.
(11) Englert G, Bjørnland T and Liaaen□Jensen S. 1D and 2D NMR study of some allenic carotenoids of the fucoxanthin series. Magn. Reson. Chem, 1990; 28:519-528.
(12) Kumar SR, Hosokawa M and Miyashita K. Fucoxanthin: A marine carotenoid exerting anti-cancer effects by affecting multiple mechanisms. Mar. drugs, 2013; 11:5130-5147.
(13) Zhang H, Tang Y, Zhang Y, Zhang S, Qu J, Wang X and Liu Z. Fucoxanthin: A promising medicinal and nutritional ingredient. J. Evidence Based Complementary Altern. Med, 2015; 2015.
(14) Yan X, Chuda Y, Suzuki M and Nagata N. Fucoxanthin as the major antioxidant in Hijikia fusiformis a common Edible Seaweed. Biosci. Biotechnol. Biochem, 1999; 63:605-607.
(15) Hosokawa M, Kudo M, Maeda H, Kohno H, Tanaka T and Miyashita K. Fucoxanthin induces apoptosis and enhances the antiproliferative effect of the PPARγ ligand, troglitazone, on colon cancer cells. Biochim. Biophys. Acta, Gen. Subj, 2004; 1675:113-119.
(16) Maeda H, Hosokawa M, Sashima T, Funayama K and Miyashita K. Fucoxanthin from edible seaweed, Undaria pinnatifida, shows antiobesity effect through UCP1 expression in white adipose tissues. Biochem. Biophys. Res. Commun, 2005; 332:392-397.
(17) Martin LJ. Fucoxanthin and its metabolite fucoxanthinol in cancer prevention and treatment. Mar. drugs, 2015; 13:4784-4798.

(18) Liu CL, Huang YS, Hosokawa M, Miyashita K and Hu ML. Inhibition of proliferation of a hepatoma cell line by FUCO in relation to cell cycle arrest and enhanced gap junctional intercellular communication. Chem. Biol. Interact, 2009; 182:165–172.
(19) Rokkaku T, Kimura R, Ishikawa C, Yasumoto T, Senba M, Kanaya F and Mori N. Anticancer effects of marine carotenoids, fucoxanthin and its deacetylated product, fucoxanthinol, on osteosarcoma. Int. J. Oncol, 2013; 43:1176–1186.
(20) Chung TW, Choi HJ, Lee JY, Jeong HS, Kim CH, Joo M and Ha KT. Marine algal fucoxanthin inhibits the metastatic potential of cancer cells. Biochem. Biophys. Res. Commun, 2013; 439:580-585.
(21) Ganesan P, Matsubara K, Sugawara T and Hirata T. Marine algal carotenoids inhibit angiogenesis by down-regulating FGF-2-mediated intracellular signals in vascular endothelial cells. Mol. Cell. Biochem, 2013; 380:1-9.
(22) Adams RP. Identification of Essential Oils Components by Gas Chromatography/Quadrupole Mass Spectroscopy. Allured, Carol Stream, IL,USA. 2001.
(23) International Conference on Harmonization. Technical Requirements for the Registration of Pharmaceutical for Human Use, Stability Testing of New Drugs Substance and Products Q1A (R2). 2003.
(24) International Conference on Harmonization. Technical Requirements for the Registration of Pharmaceutical for Human Use, Validation of Analytical Procedures: Text and Methodology Q2 (R1). 2005
(25) USP 39. THE UNITED STATES Pharmacopoeia. 39. ed. Rockville: United States. Pharmacopeial Convention, 2016.
(26) Van Leeuwe MA, Villerius LA, Roggeveld J, Visser RJW and Stefels, J. An optimized method for automated analysis of algal pigments by HPLC. Mar. Chem, 2006; 102:267-275.
(27) Xia S, Wang K, Wan L, Li A, Hu Q and Zhang C. Production, characterization, and antioxidant activity of fucoxanthin from the marine diatom Odontella aurita. Mar. drugs, 2013; 11:2667-2681.
(28) Vieira FA, Guilherme RJ, Neves MC, Abreu H, Rodrigues ER, Maraschin M and Ventura SP. Single-step extraction of carotenoids from brown macroalgae using non-ionic surfactants. Sep. Purif. Technol, 2017; 172:268-276.
(29) Zhang Y, Fang H, Xie Q, Sun J, Liu R, Hong Z, Yi R and Wu H. Comparative Evaluation of the Radical-Scavenging Activities of Fucoxanthin and Its Stereoisomers. Molecules, 2014; 19:2100-2113.
(30) Nakazawa Y, Sashima T, Hosokawa M and Miyashita K. Comparative evaluation of growth inhibitory effect of stereoisomers of fucoxanthin in human cancer cell lines. J. Funct. Foods, 2009; 1:88-97.
(31) Maoka T, Fujiwara Y, Hashimoto K and Akimoto, N. Rapid Identification of Carotenoids in a Combination of Liquid Chromatography/UV-Visible Absorption Spectrometry by Photodiode-Array Detector and Atomospheric Pressure Chemical Ionization Mass Spectrometry (LC/PAD/APCI-MS). J. Oleo Sci, 2002; 51:1-9.
(32) Haugan JA, Englert G, Glinz E and Liaacn-Jensen S. Algal carotenoids. 48. Structural assignments of geometrical isomers of fucoxanthin. Acta Chem. Scand, 1992; 46:389-395.
(33) Haugan JA and Liaaen-Jensen S. Isolation and characterisation of four allenic (6′ S)-isomers of fucoxanthin. Tetrahedron Lett, 1994; 35:2245-2248.

(34) Breemen RB van. Electrospray liquid chromatography-mass spectrometry of carotenoids. Anal. Chem, 1995; 67:2004-2009.
(35) Teutenberg T, Tuerk, J, Holzhauser M and Giegold S. Temperature stability of reversed phase and normal phase stationary phases under aqueous conditions. J. Sep. Sci, 2007; 30:1101-1114.
(36) Muthuirulappan S and Francis SP. Anti-cancer mechanism and possibility of nano-suspension formulations for a marine algae product fucoxanthin. Asian. Pacifi. J. Cancer. Prev, 2013; 14:2213-2216.
(37) Yip WH, Joe LS, Mustapha WAW, Maskat MY, Said M (2014) Characterization and Stability of Pigments Extracted from Sargas sumbinderi Obtained from Semporna, Sabah. Sains Malays 43:1345-1354
(38) Hii SL, Choong PY, Woo KK, Wong CL and Wong A. Stability studies of FUCO from Sargas sumbinderi. Aust. J. Basic & Appl. Sci, 2010; 4:4580–4584
(39) Taverniers I, De Loose M and Van Bockstaele E. Trends in quality in the analytical laboratory. II. Analytical method validation and quality assurance. TrAC, Trends Anal. Chem, 2004; 23:535-552.
(40) Rambla-Alegre M, Esteve-Romero J and Carda-Broch S. Is it really necessary to validate an analytical method or not? That is the question. J. Chromatogr. A, 2012; 1232:101-109.
(41) Thompson M, Ellison SL and Wood R. Harmonized guidelines for single-laboratory validation of methods of analysis (IUPAC Technical Report). Pure Appl. Chem, 2002; 74:835-855.
(42) Mínguez-Mosquera MI, Hornero-Méndez D and Pérez-Gálvez A. Carotenoids and provitamin A in functional foods, in: Hurst, W.J. (1.ed) Methods of analysis for functional foods and nutraceuticals, CRC Press, 2002.101-157.
(43) Sugimura R, Suda M, Sho A, Takahashi T, Sashima T, Abe M and Miyashita K. Stability of fucoxanthin in dried Undaria pinnatifida (Wakame) and baked products (scones) containing wakame powder. Food Sci. Technol. Res, 2012; 18:687-693.
(44) Kawee-ai A, Kuntiya A and Kim SM. Anticholinesterase and antioxidant activities of fucoxanthin purified from the microalga Phaeodactylum tricornutum. Nat. Prod. Commun, 2013; 8:1381-1386.
(45) Tanaka T, Shnimizu M and Moriwaki H. Cancer chemoprevention by carotenoids. Molecules, 2012; 17:3202-3242.
(46) Yahia EM and Ornelas-Paz JDJ. Chemistry, stability and biological actions of carotenoids. Fruit Veg Phytochem, 2010; 1:177-222.
(47) Zhao D, Kim SM, Pan CH and Chung D. Effects of heating, aerial exposure and illumination on stability of fucoxanthin in canola oil. Food chem, 2014; 145:505-513.
(48) Watson GD. Pharmaceutical Analysis: A textbook for pharmacy students and pharmaceutical chemist.s 2nd ed. Churchill Livingstone: London. 2005.

5. CAPÍTULO II - Desenvolvimento de nanopartículas lipídicas inovadoras contendo uma combinação de manteiga de bacuri e óleo de tucumã

5.1 Introdução

No início dos anos 90, foram desenvolvidas as nanopartículas lipídicas (NL) baseadas em emulsões O/A como um sistema de liberação alternativo aos lipossomas, devido a sua instabilidade, e às nanopartículas poliméricas, devido à toxicidade dos solventes orgânicos empregados na produção. As NL possuem diâmetro médio na faixa de 150 a 300 nm, porém valores até 1 µm são aceitos para aplicações específicas. Em sua composição, além da utilização de lipídeos, as NL são constituídas de tensoativos não tóxicos que recobrem a superfície das partículas e, desse modo, estabilizam a dispersão (SIEKMANN e WESTESEN, 1994; MULLER, MAÉDER e GOHLA, 2000; MULLER e PARDEIKE, 2007; ALMEIDA e SOUTO, 2007; SHAH et al., 2007; SVILENOV e TZACHEV, 2014).

Atualmente, NL utilizando lipídios naturais foram preparadas e caracterizadas com sucesso (MANDAWGADE e PATRAVALE, 2008; HAJJ ALI et al., 2015). Nesse contexto, as matérias-primas vegetais provenientes da região Amazônica são potencialmente interessantes para produtos farmacêuticos devido às atividades farmacológicas que apresentam. Além disso, a extração de matérias-primas de fontes que são renováveis contribuem para o desenvolvimento sustentável da região 9 (MORAIS e GUTJAHR, 2009). A manteiga de bacuri e o óleo de tucumã são matérias-primas que possuem propriedades de interesse farmacológico. A manteiga de bacuri possui alto nível de tripalmitina e ácido palmitoleico, enquanto o óleo de tucumã contém ácidos graxos e insaturados, além de ser rico em ômega 3, 6 e 9 (MORAIS e GUTJAHR, 2009; PIMENTEL et al., 2015).

A preparação de NL pode ser realizada por diversas técnicas, e estas, por sua vez, interferem em diversas características das partículas, como a sua morfologia. Na homogeneização de alto cisalhamento, o lipídio fundido é disperso em uma solução aquosa com a ajuda de um homogeneizador de alto cisalhamento, como o Ultra-turrax®. Logo após, a emulsão obtida é resfriada em temperatura ambiente. Este método apresenta a vantagem de ser simples e rápido, proporcionar ótimas condições para transposição de escala e também por não ser necessária a utilização de solventes orgânicos (MEHNERT e MADER, 2001).

Nesse contexto, foram preparadas NL inovadoras com uma combinação de manteiga de bacuri e de óleo de tucumã utilizando homogeneização de alto cisalhamento para a preparação, sem o uso de solvente orgânico. As formulações

foram produzidas variando a proporção da manteiga de bacuri e do óleo de tucumã, mantendo as mesmas concentrações dos tensoativos. Posteriormente, foi realizada a caracterização físico-química das mesmas pelas técnicas de tamanho de partícula, índice de polidispersão (pdI), potencial zeta, pH, viscosidade, número de partícula por volume, microscopia eletrônica de transmissão (MET) e calorimetria exploratória diferencial (DSC). Concomitantemente, foi realizado o monitoramento da estabilidade das formulações produzidas, durante dois meses à temperatura ambiente (25 ± 2 ºC), pelas técnicas descritas anteriormente.

O trabalho está disposto na forma de artigo científico, de acordo com as normas da revista à qual foi submetido.

5.2 Artigo científico

Controlled formation of nanosized colloidal suspensions by combination of bacuri butter and tucumã oil

Submetido à publicação no periódico *Journal of Controlled Release*.

Controlled formation of nanosized colloidal suspensions by combination of bacuri butter and tucumã oil

Leticia Malgarim Cordenonsi[a], Andressa Santer[a], Rafaela Martins Sponchiado[a], Renata Platcheck Raffin[b] and Elfrides Eva Scherman Schapoval[a]

[a] Programa de Pós-Graduação em Ciências Farmacêuticas, Faculdade de Farmácia, Universidade Federal do Rio Grande do Sul, 90610-000 Porto Alegre - RS, Brasil.
[b] Programa de Pós-Graduação em Nanociências, Centro Universitário Franciscano, 97010-032 Santa Maria – RS, Brasil.

Abstract

The aim of this investigation was to evaluate the potential of a combination of bacuri butter and tucumã oil for producing novel lipid nanoparticles (LN) as new skin drug delivery systems. They were prepared using a rapid and simple high shear homogenization, without the use of organic solvent. Hence, different concentrations of bacuri butter and tucumã oil were tested, and these novel LN were characterized. Novel LN had an average size of 255 nm, a uniform size distribution and a relatively high zeta-potential, between -11 mV and -24 mV, enough to prevent droplet coalescence. Spherical shape and size were confirmed using transmission electron microscopy analyses. Moreover, the novel LN obtained showed good stability for at least two months. In conclusion, bacuri butter and tucumã oil are new actives and new excipients for production LN prepared with a very simple technique. The results of this study emphasize the potential of novel LN as new skin drug delivery systems.

Keywords: Nanoparticle, lipid nanoparticles, tucumã oil; bacuri butter.

1. Introduction

The biological activity of plants from all over the world, based on the popular use of different species have been reported. The Brazilian Amazon forest has a huge biodiversity of plant species that can be considered excellent sources of new biologically active compounds [1,2].

Bacuri (*Platonia insignis* Mart., Clusiaceae) is native from Brazilian Amazon and Northeast Regions. Bacuri butter is absorbed a few minutes after it is applied and the skin becomes velvety to the touch; it also removes spots and reduces scarring. This is due to its high level of tripalmitin (50% to 55%), which penetrates the skin quickly. The high amount of fatty palmitoleic acid (5%) makes the bacuri a good emollient that also be used as a moisturizing agent [3-6]. Moreover, the family Clusiaceae represents a rich source of polyisoprenylated xanthones and benzophenones, which are responsible for several biological activities, such as antioxidant effects, wound healing, and cytotoxic properties [6-10].

Tucumã (*Astrocaryum vulgare*, Arecaceae) is native from Amazonian region, possibly from Pará, a Brazilian state. The oil extracted from the pulp contains 25.6% saturated fatty acids and 74.4% unsaturated fatty acids composed of palmitic, stearic, oleic, and linoleic acids. This oil is also rich in omega 3, 6, and 9, it is a good moisturizer and is used in body lotions, and products for damaged hair. It is also an excellent, easily spread emollient. The orange oil is an excellent source of carotenoids, it contains 21 different types, including β-carotene, the precursor of vitamin A. It is also a major source of vitamin B2 (riboflavin) and presents bioactive compounds such as catechin and quercetin [11-14].

In recent years, applications of nanotechnology using natural products have received increasing attention, mainly in the cosmetics and pharmaceutics industry [15-17]. In particular, lipid nanoparticles (LN) have become an alternative carrier to liposomes, and emulsions due to advantages such as improved stability, release modulation, no biotoxicity of the compounds, efficient incorporation of lipophilic and hydrophilic drugs, avoidance of organic solvents and ease of scaling up and manufacturing [18-23].

LN are prepared from a lipid, such as triglycerides, glycerides, fatty acids and waxes, and are stabilized with surfactant on the surface, co-surfactants, and coating materials. Antioxidants, electrolytes, preservatives, viscosity-enhancing agents, and

other excipients can also be used [24-25]. In addition, LN made of natural lipids were successfully prepared and characterized [26-29].

The techniques for LN preparation include high-pressure homogenization, microemulsification, solvent evaporation, and phase inversion [25]. High-pressure homogenization is one of the first techniques used in the preparation of LN and its advantage is the absence of organic solvents, but special equipments needed [30]. High shear homogenization is a very simple and widely used technique; Colomé [28] described the use of high shear homogenization for the production of LN, although organic solvent is used in the production.

Due to its biological effects, bacuri and tucumã attract great interests for pharmaceutical purposes. Moreover, all these present works to a large extent support that bacuri and tucumã has potential to be used as new actives with pharmacological properties and new excipients for innovative formulations [6-14]. Preparing novel LN with these natural, biodegradable, non-expensive materials, and easily available will promote their potential use in several applications, like dermatology [18-20, 23, 31]. Therefore, in this study, we propose the first application of a combination the bacuri butter and tucumã oil for preparation novel LN. As far as we know, there are no studies describing the use of the combination of bacuri e tucumã in nanoparticles, especially for dermal use. In this study, the Amazonian lipids are both excipient for LN formation as well as the actives that will perform the efficacy of the formulation.

The aim of this investigation was to evaluate the potential of a combination of bacuri butter and tucumã oil for producing novel LN using a simple and rapid high shear homogenization for preparation, without organic solvent, as new skin drug delivery systems. This further supports the need for developing this study since these compounds may exhibit pharmacological activity of interest in the pharmaceutical industry. Hence, formulations with different concentrations of bacuri butter and tucumã oil were developed and characterized, in order to avoid the use of organic solvents and special equipment. The physical and chemical stabilities of the novel LN were also monitored during storage for two months.

2. Materials and Methods

2.1 Materials

Bacuri butter and tucumã oil were kindly donated by Amazon Oil Industry (Brazil). Polysorbate 80 was obtained from Delaware (Porto Alegre, Brazil) and sorbitan monooleate was purchased from Sigma-Aldrich (São Paulo, Brazil). All other chemicals were of analytical grade.

2.2 Preparation of novel lipid nanoparticles

Experiments were performed for the purpose of determining the best composition, with a variety of proportions of compounds, temperatures, surfactant concentration, stirring speed, and time. Later on, the optimal composition was employed for the production of novel LN with different concentrations of bacuri butter and tucumã oil, resulting in six formulations (Table 1).

Novel LN were prepared using high shear homogenization. In short, the lipid phase was composed of bacuri butter (3-9%), tucumã oil (2-6%), and sorbitan monooleato (2%). The aqueous phase was composed of polysorbate 80 (4%) and water. The lipid phase and aqueous phase were simultaneously heated at 65 °C under constant magnetic stirring, until all components were melted. Then, the aqueous phase was poured over the lipid phase under agitation under controlled temperature. The suspension was subjected to shaking using an Ultra-turrax® T10 Basic (Ika, Germany) mixer at 24,000 rpm during 20 minutes and, finally, the novel LN were obtained after cooling.

2.3 Physicochemical characterization of novel lipid nanoparticles

Particle size measurements

LN were characterized in terms of mean particle size and particle size distribution. The mean particle size and polydispersity indexes (pdI) were investigated by dynamic light scattering (DLS) using a Zetasizer® Nano ZS, model ZEN 3600 (Malvern Instruments, UK). The samples were diluted 500 times (*v*/*v*) in ultra-pure water, which was performed at 25 °C and the results reported are the average of three measurements.

The particle size distribution was determined by laser diffraction using a Microtrac FLEX (Microtrac Inc., PA, USA) in order to obtain information on the

nanometric and micrometric ranges of the dispersions. The size distribution was also expressed by the SPAN factor, calculated by Equation (Eq) (1).

$$Span = (d_{0.9} - d_{0.1}) / d_{0.5}$$

Where *d*(0.9), *d*(0.1) and *d*(0.5) are the diameter sizes and the given percentage value is the percentage of particles smaller than that size. A high SPAN value indicates a wide size distribution [32].

Zeta-potential and conductivity

The zeta-potential and conductivity were determined by electrophoretic mobility (Zetasizer®, model ZEN 3600, Malvern Instruments) after the samples were diluted 500 times (*v*/*v*) with 10 m*M* sodium chloride solution, which was performed at 25 °C and the results reported are the average of three measurements.

pH values

The pH values of the LN suspensions were determined using a potentiometer, model DM-22 (Digimed Analytical, Brazil), directly in the formulations at 25 °C.

Viscosity

The viscosity was determined using a rotary viscometer (LV-DVII + Pro, Brookfield, Brookfield, USA), at 25 °C with the ULA spindle at a shear rate of 6.11 s−1 (50 rpm).

Number of Particles per Volume in the formulations

The number of particles per milliliter was estimated by turbidimetry according to the method described by Zattoni and co-workers [33]. Briefly, the samples were diluted with ultra-pure water to produce five different concentrations that presented absorbance values between 0.2 and 0.8 analyzed at the wavelength 600 nm (where there is no absorption) using a UV-1800 spectrophotometer (Shimadzu, Japan).

The turbidity (τ, cm^{-1}) of the sample is an experimental quantity that can be obtained from the analytical signal of the UV detector that operates as a turbidimeter Eq. (2):

$$\tau = \frac{1}{b} \ln(10)\, A$$

Here *b* (cm) is the optical cell path length, and *A* is the instrumental absorbance signal. Turbidity (τ) can be expressed as Eq. (3):

$$\tau = \ln(10)\ KC$$

Where *c* (g cm^{-3}) is the sample concentration, and *K* (cm^2 g^{-1}) is the sample extinction coefficient.

In a sufficient dispersion of spherical particles turbidity, τ is a function of the particle diameter *d* (cm), number concentration of particles *N* (particles cm^{-3}), and the dimensionless quantity *W*, the extinction efficiency Eq. (4).

$$\tau = \frac{\pi}{4} d^2\ N\mathrm{W}$$

A fundamental property of *W* states that, at constant particle shape, *W* is a function of the type *W* (*x*,*m*), where *x* is the size parameter defined as *x* = πd /λ , in which λ (cm) is the incident wavelength in the dispersing medium, which is $\lambda=\lambda_0/n$ (cm) where λ_0 (cm)is the wavelength in the vacuum and *n* the refractive index of the dispersing medium. Then, by combining Eq. 3 and Eq. 4, with fixed relative refractive index, W can be obtained by the relation below Eq. (5).

$$W = K\ 2\ln(10) \propto \frac{d}{3}$$

where α (g cm^{-3}) is the particle density [33].

Nanoparticle morphology

Transmission electron microscopy (TEM) was used to observe the surface morphology of novel LN and to further confirm particle diameter by DLS. Observations were made with TEM (JEM 1200 Exll) operating at 80 kV (Centro de Microscopia da UFRGS). Diluted (10x-ultra-pure). All formulations were dripped on specimen grids (Formvar-Carbon supportfilm, Electron Microscopy Sciences) and negatively stained with uranyl acetate solution (2% *w/v*).

Differential scanning calorimetry (DSC)

The thermograms of formulation and pure materials were determined using a differential scanning calorimetry Shimadzu (Shimadzu, Japan), model DSC-60, with FC-60 flow controller, 60 WS integrator, and TA 60. Before the analysis, nanoparticle suspensions were dried at room temperature. Approximately 1.50 mg of each sample

was heated in aluminum pans from 20–200 °C and the scanning rate was conducted at 10 °C min^{-1}.

2.4 Preliminary stability studies

The six formulations of novel LN were placed in vials immediately after preparation and kept at room temperature (25±2 ºC) during preliminary stability studies. The macroscopic and physicochemical evaluations were carried out after 15, 30, 45, and 60 days, in triplicate. Macroscopic evaluations consisted of visual inspections in order to verify the occurrence of color change, phase separation, and aggregation, while the physicochemical measurements were particle size, pdI, zeta-potential, conductibility, and pH were performed at the start of the stability period evaluation and after two months period at normal storage conditions

2.5 Statistical analysis

All data are expressed as mean ± standard deviation (SD). The level of significance was analyzed by one-way ANOVA with Tukey's post-hoc test. A value of $p<0.05$ was considered to be statistically significant.

3. Results and discussion

3.1 Influence of the tucumã oil and bacuri butter concentrations on the physicochemical characteristics of novel lipid nanoparticles

In the present study, novel LN containing a combination of bacuri butter and tucumã oil were prepared by high shear homogenization, without the use of organic solvent. There is an increasing attention in lipid based drug delivery systems due to factors such as formulation versatility and the choice of different drug delivery systems [34]. With the ability to combine the beneficial characteristics of component fatty acids, lipid modifications may enhance the role fats or lipids play in drug delivery applications. LN are tailor made with improved properties compared with the individual components. A novel approach is herein presented, to harness a combination the bacuri butter and tucumã oil, for novel LN using products from the Brazilian Amazon. More, such LN may be incorporated in gels and cream.

In fact, this study introduces new possibilities for encapsulation and applications using novel natural ingredients. These compounds have two functions:

(a) new actives with pharmacological properties, and (b) new excipients that form LN. As a new actives, bacuri has high level of tripalmitin, and fatty palmitoleic acid, moreover, represents a rich source of polyisoprenylated xanthones and benzophenones. Tucumã is rich in omega 3, 6, and 9, carotenoids and it is also a major source of vitamin B2. As excipient, bacuri and tucumã are emollient and can also be used as a moisturizing agent [3,7,9,11].

High shear homogenization is a simple, rapid, easy to handle and feasible technique to prepare LN, since it requires low cost equipment which allows obtaining particles of nanometric size [35]. It is advantageous to employ lipids, since it has been shown to increase control over the release kinetics of encapsulated drug and to improve the stability of incorporated sensitive lipophilic compounds [36]. Regarding the topical use, LN can be prepared using 5 to 40% of lipids [37].

For the purpose of determining the best composition, six combinations of butter and oil have been formulated and effects on novel LN have been investigated. Novel LN formulations were composed of sorbitan monooleate and polysorbate 80 as emulsifier (Table 1). Polysorbate 80 is non-ionic stabilizer, formed by mono and diglycerides exceedingly prone to emulsion by water molecules, entrapped in lipid matrix [38].

All the suspensions of LN exhibited a milky and opaque appearance. Figure1 shows the effect of butter and oil ratio of LN on the particle size, pdI, and SPAN factor after preparation. Overall, the mean particle diameters of LN varied from 138.0±2.0 nm to 254.5±0.9 nm. The results indicate that particle size was influenced by the concentration of butter and oil.

There are different expressions for calculating size e distribution and those used most correspond to SPAN factor and pdI. For the SPAN calculation, the diameters of the volume averaged at 90%, 10%, and 50% of the total droplet population are required. The pdI used as an indication for the width of particle size distribution, in order to indicate the uniformity of the vesicle size within the formulation. The pdI is the ratio of standard deviation to mean droplet size and it is generally accepted samples with pdI below <0.2 are considered a narrow size distribution [39,40]. However, some formulations were between 0.2 and 0.29, corresponding also to a uniform distribution [41]. The SPAN factor of all LN are low (<1.0), suggesting low polydispersity and a narrow size distribution [42].

Different concentrations of tucumã oil (2.0; 4.0; and 6.0%) were observed with a significant change ($p<0.05$) in the particle size of LN. Increasing the oil content led to an increase of the particle size, because the excess oil was expelled during the lipid crystallization process. Nevertheless, this phenomenon may depend on many factors, such as the chemical structure of the lipids used and their chemical interaction [43]. On the other hand, an insignificant change ($p>0.05$) in the pdI and SPAN factor of LN was observed when they were prepared with different concentration of tucumã oil, however, pdI and SPAN factor were increased upon increasing the concentration of tucumã oil.

The particle size in the system composition was consistent with the expected results since smaller particles were obtained for low bacuri butter percentage and an identical surfactant content. A significant change ($p<0.05$) in the particle size of LN was observed when they were prepared with different concentrations of bacuri butter (3.0; 7.0; and 9.0%); the particle size increased with the increasing concentration of butter. Larger particle size could be attributed to the decrease in emulsifying efficiency and the increase in particle agglomeration [37]. Moreover, Siekmann and Westesen [44] described that low lipid concentration leads to LN with reduced particle size. An insignificant change ($p>0.05$) in the pdI and SPAN factor of LN was observed when they were prepared with different concentration of bacuri butter, however, the SPAN factor were increased upon increasing the concentration of tucumã oil, and pdI was decreased.

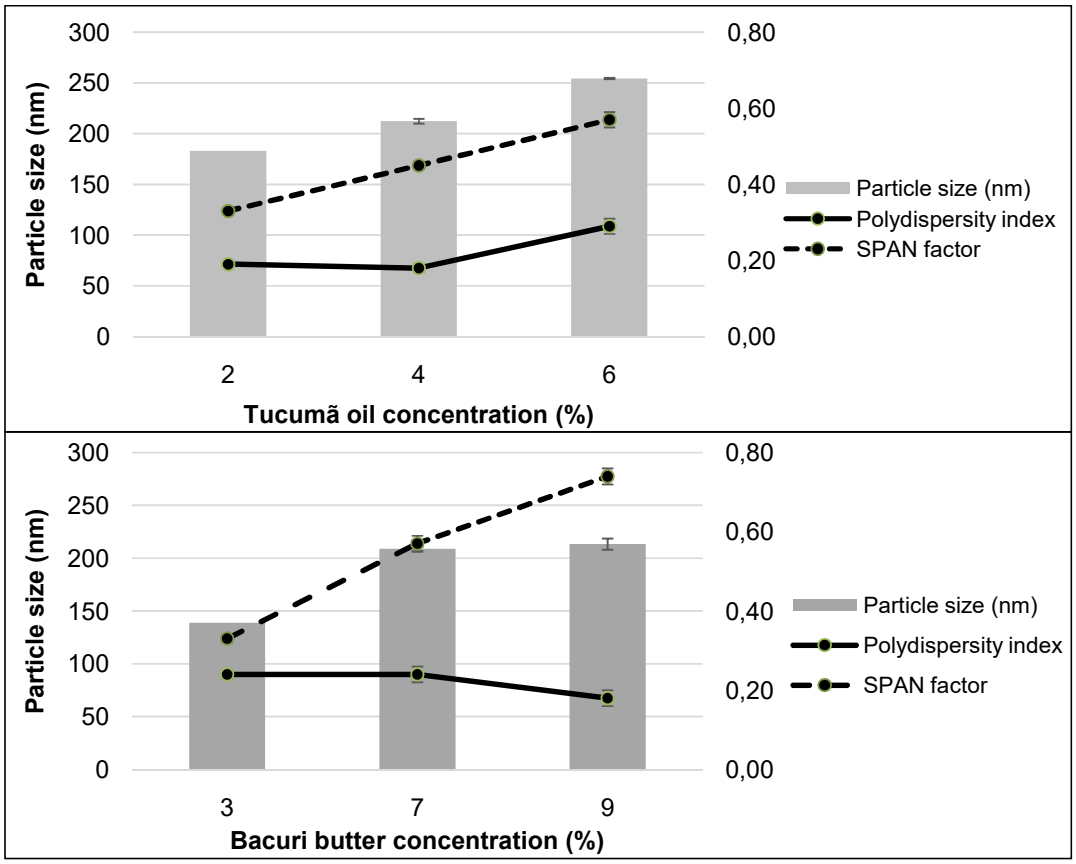


Figure 1. Effect of tucumã oil and bacuri butter concentration on the characteristics of novel LN after preparation. *Each point represents mean ± SD

Table 1 summarizes the results of zeta-potential, pH values, number of particles per volume in the formulations and viscosity after preparation. The measurement of the zeta potential allows the estimation of LN storage stability. Usually nanoparticle aggregation is less likely to occur for particles with high zeta potential, due to electric repulsion. In general, LN are negatively charged on the surface [45-47]. Based on the zeta-potential obtained for LN, the stability could be ranked by order as follows: LN-2 > LN-6 > LN-5 >LN-4>LN-1= LN-3.A significant change ($p<0.05$) was observed between formulations LN-2, LN-5, and LN-6, the variation indicates the different interfacial properties of these particles. Similar LN was reported by Kheradmandnia and co-workers [48] in LN prepared from a mixture of beeswax and carnauba wax using polysorbate 80, the zeta-potential of these LN varied in the range of –15 mV to –17 mV, suggesting the presence of similar interface properties, between polysorbate 80 and fatty acids.

The slightly acid pH values varied from 5.44 to 5.64 and no significant change ($p>0.05$) was observed.

Results showed that turbidimetric analysis depends upon the percentage of bacuri butter and tucumã oil in the formulations. A significant change ($p<0.05$) was observed between formulations LN-3, and LN-6 and an increase in particle concentration is observed in direct proportion to the quantity of butter and oil in formulations.

The LN formulations presented viscosity between 4.0 and 6.8. An increase in viscosity was observed in direct proportion to the quantity of butter in formulations and a significant change ($p<0.05$) was found regarding the higher bacuri butter concentration (9%).

Table 1. Composition and physicochemical characteristics of novel LN.

Formulation	Bacuri butter	Tucumã oil	Zeta-potential[1*]	pH*	N [2*]	Viscosity[3]
LN-1	5%	2%	-11.0±0.56	5.59±0.04	1.82 x10^{13}	4.8
LN-2	5%	4%	-24.2±0.20	5.64±0.01	2.48 x10^{13}	4.4
LN-3	5%	6%	-11.0±0.05	5.44±0.04	3.37 x10^{13}	4.4
LN-4	3%	2%	-11.9±0.25	5.62±0.04	1.84 x10^{13}	4.0
LN-5	7%	2%	-18.0±0.43	5.55±0.01	2.37 x10^{13}	5.2
LN-6	9%	2%	-20.3±0.32	5.46±0.03	5.09 x10^{13}	6.8

*Data represent the mean ± SD

[1] Zeta-potential (mV)

[2] Number of particles per milliliter (particles.cm^{-3}) was estimated by turbidimetry

[3] Viscosity in pascal-seconds (Pa·s) at 50 rpm

TEM studies were carried out to improve the understanding of the LN morphology, and revealed spherical nanoparticles, even with the use of different concentration of oil and butter (Figure 2). The particle sizes were found to be in the range of 180 to 255 nm and the uniformity in particle size distribution correlates with the small pdI obtained via DLS.

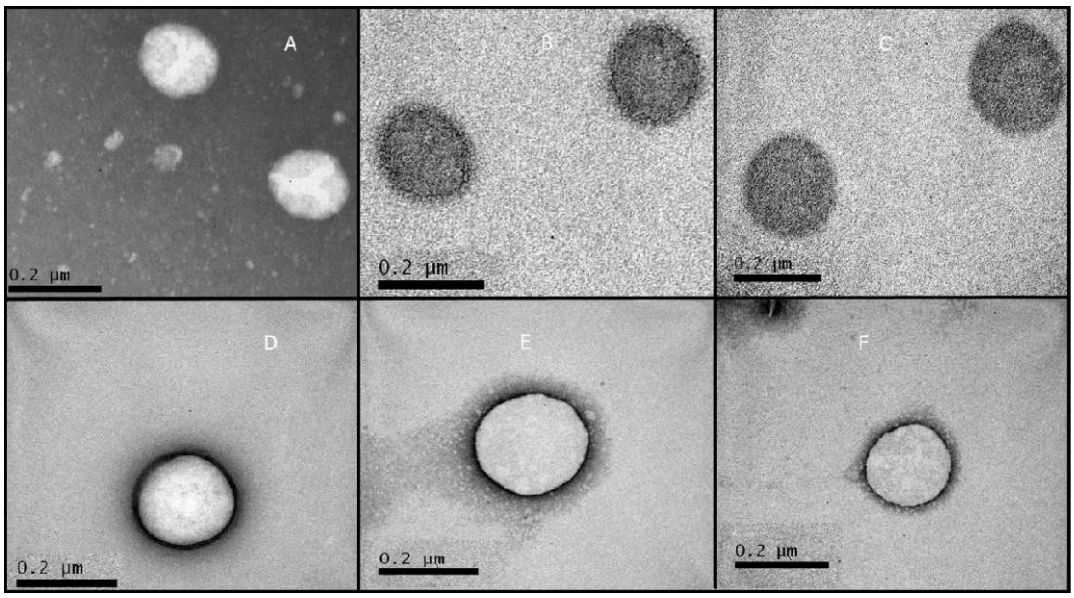


Figure 2. Transmission electron microscopic images of LN containing bacuri butter and tucumã oil: LN-1 (A), LN-2 (B), LN -3 (C) LN-4 (D), LN-5 (E) and LN-6.

The crystallinity of the novel LN obtained by a combination of tucumã oil and bacuri butter was investigated using DSC. Figure 3 shows the DSC thermograms of raw materials and LN formulations. The melting event location were shifted towards lower temperatures compared to raw materials, and there was a decrease of the shoulder at the left. This can be attributed to the colloidal dimension of the particles in particular to their large surface to volume ratio, and explained by the Thomson equation [49]. The thermograms of LN with different concentrations of oil and butter indicate that crystallinity of the samples changes with the concentration. Likewise, thermograms of LN with different ratios of beeswax in lipid matrices indicate that sample crystallinity increased by decreasing beeswax content in the lipid mixture [48]. The endothermic peak around 115 to 120 °C is the flash point of polysorbate80 and, its structures begins the degradation process around 140 °C [50].

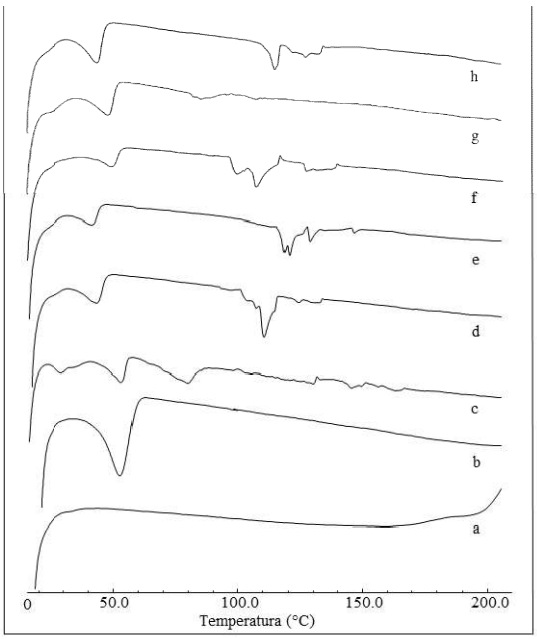


Figure 3. DSC heating curves of the tucumã oil (A), bacuri butter (B), LN-1(C), LN-2 (D), LN-3 (E), LN-4 (F), LN-5 (G) and LN-6 (H).

3.2 Preliminary stability studies

The physical properties of LN formulations during storage can be determined by monitoring changes in appearance, particle size, SPAN factor, zeta-potential, pH, and conductivity as the function of time. In general, suspensions of LN showed good stability during a stability study, no visual precipitation and phase separation was observed. All remained homogenous after 3,000 rpm centrifugation, with a macroscopic homogeneity. The absence of phase separation is a positive factor in the stability evaluation.

After production the LN were stored at room temperature (25±2 °C) during two months and Figure 4 showed results of physicochemical characteristics. For all formulations, measurements showed that the particle size remained lower than 260 nm, two months after production. A significant change ($p<0.05$) was observed within formulations LN-3, LN-5, and LN-6, during the storage. The pdI value remained around 0.3 and results showed no statistical difference ($p>0.05$), indicating the homogeneity of the population. These results were in agreement with Müller [24], who described the same behavior, with low pdI value indicating higher stability and

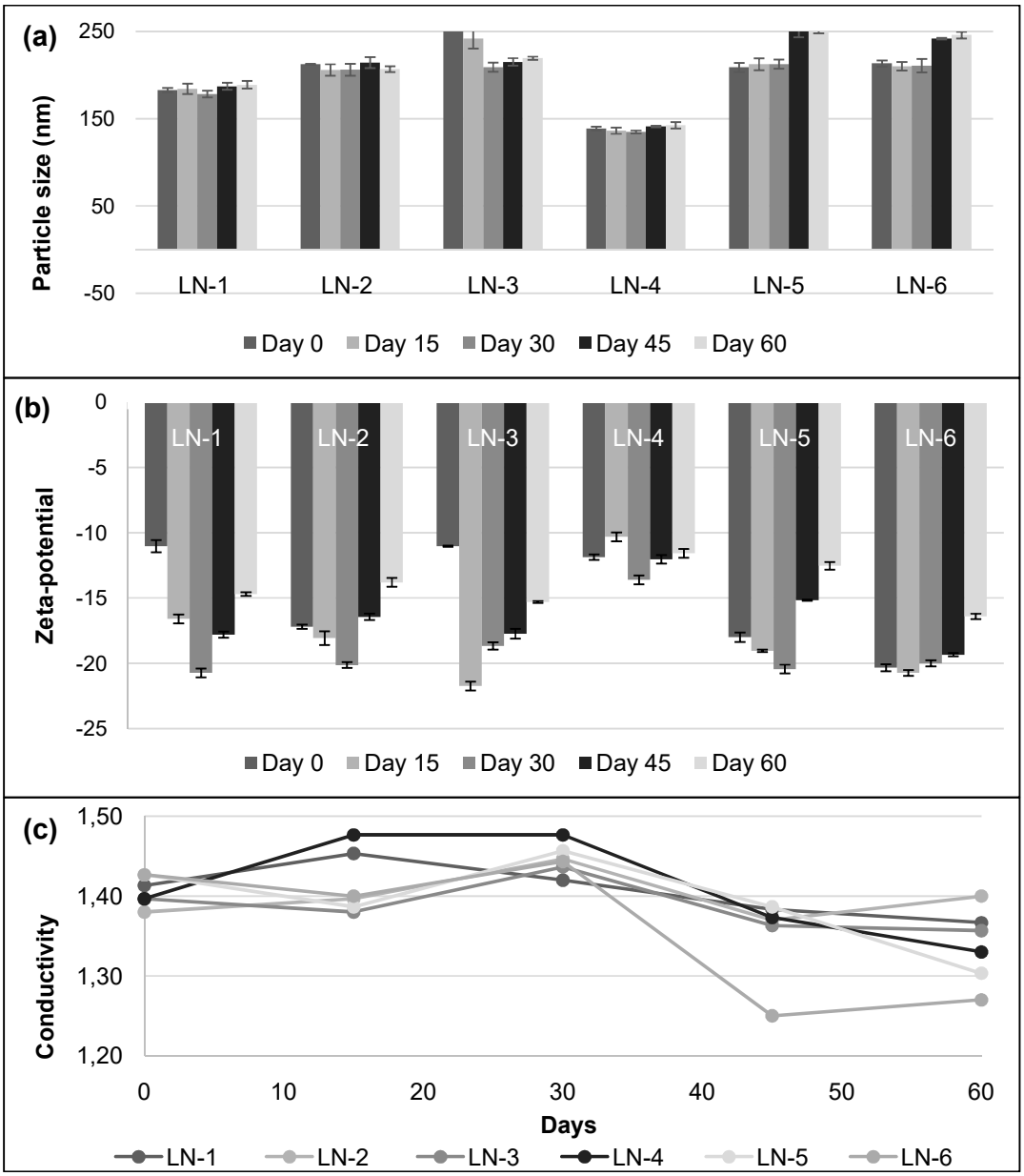
therefore maintenance of the initial and good values, showing higher stability through storage time.

Zeta-potential is important for evaluating the stability of colloidal dispersions and the value increased during the storage due the accommodation and stabilization of the system [46,51]. The zeta-potential of all formulations presented a significant change ($p<0.05$). However, polysorbate 80 employed in this work provided stearic stability to achieve stable, but decrease the zeta potential due the shift in the shear plane of the particle [31, 45].

For conductivity values, a significant change ($p<0.05$) was observed between formulations LN-1, LN-4, LN-5, and LN-6, during the storage. Determination of electrical conductivity is the most common procedure to investigate phase inversion. When this process occurs the conductivity decreases strongly. However, it is difficult to assess the stability only using conductivity as there is no linear relationship between this parameter and the instability process [51,52].

Formulations of LN remained with acid pH and a significant change ($p<0.05$) was observed between formulations LN-1 and LN-5, during the storage The pH control plays an important role in stability, significant changes in value, may indicate formulation instability.

All formulations of LN showed an increase in SPAN factor, except LN-2, which showed very similar values (0.45 and 0.47) two months after production and stored at room temperature. These findings suggested that LN-2 was more stable than all formulations.


(a)
Particle size (nm)
250
150
50
-50
LN-1
LN-2
LN-3
LN-4
LN-5
LN-6
Day 0
Day 15
Day 30
Day 45
Day 60
(b)
Zeta-potential
0
-5
-10
-15
-20
-25
LN-1
LN-2
LN-3
LN-4
LN-5
LN-6
Day 0
Day 15
Day 30
Day 45
Day 60
(c)
Conductivity
1,50
1,40
1,30
1,20
0
10
20
30
40
50
60
Days
LN-1
LN-2
LN-3
LN-4
LN-5
LN-6

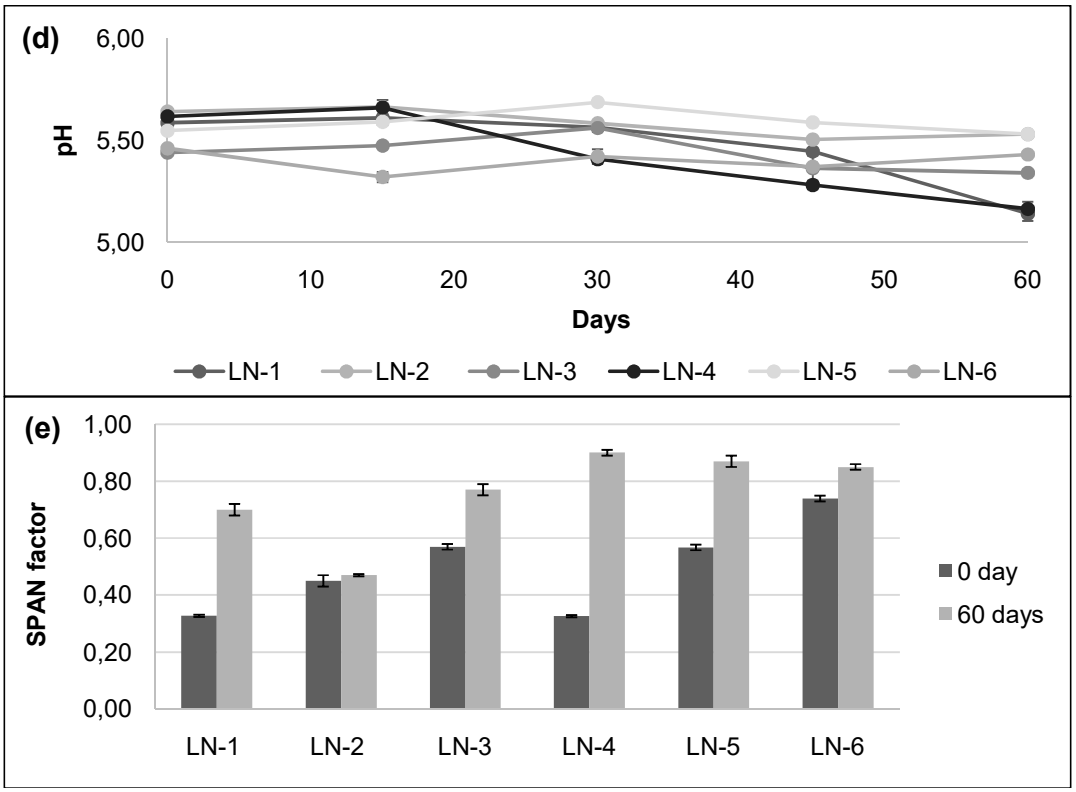


Figure 4. Physicochemical characteristics of LN during storage: (a) particle size, (b) zeta-potential, (c) conductibility, (d) pH and (e) SPAN factor.

Conclusion and future perspectives

The present study has shown that it is possible to produce novel LN by a simple and rapid high shear homogenization method using a combination of tucumã oil and bacuri butter. The results of the characterization and evaluation established the suitability and compatibility of compounds, hitherto unexplored in the novel drug delivery. The experimental results reveal that LN with 5% of bacuri butter and 4% of tucumã oil, showed better results in terms of the studied parameters within the evaluated period. In conclusion, bacuri butter and tucumã oil are new actives and new excipients for production LN prepared with a very simple technique. The results of this study emphasize the potential of novel LN as new skin drug delivery systems.

References

[1] M. Lahlou, Screening of natural products for drug discovery. Expert Opin. Drug Discovery. 2 (2007) 697-705.

[2] B.V. Bonifácio, P.B. da Silva, M.A. dos Santos Ramos, K.M.S. Negri, T.M. Bauab, M. Chorilli, Nanotechnology-based drug delivery systems and herbal medicines: a review. Int. J. Nanomed. 9 (2014) 1-15.
[3] L.R.B. Morais, E. Gutjahr, Química de oleaginosas: Valorização da biodiversidade amazônica. Brasília: Agência de Cooperação Técnica Alemã (GTZ), 83p, 2009.
[4] A.P. Silva, C.L.S. Filho Jose Carlos, J.S. da Costa Júnior, W.J. Peláez, M.S. Faillace, A.B.F. Ferraz, J.M. David, R.M. Freitas. Toxicological Study Employing Repeated Doses of Garcinielliptone FC, a Polyisoprenylated-Benzophenone Isolated from Seed of Platonia Insignis Mart. J. Pharm. Pharmacol. 3 (2015) 316-330.
[5] T.M. Uekane, L. Nicolotti, A. Griglione, H.R. Bizzo, P. Rubiolo, C. Bicchi, C.M. Rezende, Studies on the volatile fraction composition of three native Amazonian-Brazilian fruits: Murici (Byrsonima crassifolia L., Malpighiaceae), bacuri (Platonia insignis M., Clusiaceae), and sapodilla (Manilkara sapota L., Sapotaceae). Food Chem. 219 (2017) 13-22.
[6] M.S.M. Rufino, R.E. Alves, E.S. de Brito, J. Pérez-Jiménez, F. Saura-Calixto, J. Mancini-Filho, Bioactive compounds and antioxidant capacities of 18 non-traditional tropical fruits from Brazil. Food Chem. 121 (2010) 996-1002.
[7] U.M. Acuna, N. Jancovski, E.J. Kennelly, Polyisoprenylated benzophenones from clusiaceae: potential drugs and lead compounds. Curr. Top. Med. Chem. 9 (2009) 1560–1580.
[8] S. Kumar, S. Sharma, S.K. Chattopadhyay, The potential health benefit of polyisoprenylated benzophenones from Garcinia and related genera: ethnobotanical and therapeutic importance. Fitoterapia. 89 (2013) 86–125.
[9] A.K.M. Lustosa, D.D. Arcanjo, R.G. Ribeiro, K.A.F. Rodrigues, F.F.B Passos, C.A. Piauilino, F.A.A Carvalho, Immunomodulatory and toxicological evaluation of the fruit seeds from Platonia insignis, a native species from Brazilian Amazon Rainforest. Rev. Bras. Farmacogn. 26 (2016) 77-82.
[10] N.T. Diderot, N. Silvere, T. Etienne, Xanthones as therapeutic agents; chemistry and pharmacology. Adv. Phytomed. 2 (2006) 273-298.
[11] V.V De Rosso, A.Z. de Mercadante, Identification and quantification of carotenoids, by HPLC-PDA-MS/MS, from Amazonian fruits. J. Agric. Food Chem. 55 (2007) 5062-5072.

[12] G.C.H.M. Maia, M.S. Campos, J.B. Monteiro, J.E.L. Castillo, M.S. Faleiros, Effects of Astrocaryum aculeatum Meyer (Tucumã) on Diet-Induced Dyslipidemic Rats. J. Nutr. Metab. (2014) 1-9.
[13] P.S. Bora, N. Narain, R.V.M. Rocha, A.C. De Oliveira Monteiro, R. De Azevedo Moreira, Characterization of the oil and protein fractions of Tucuma (Astrocaryum Vulgare Mart.) fruit pulp and seed kernel. Ciencia y Technologia Alimentaria. 3 (2001) 111-116.
[14] D.H. Kodama, A.E.D.S.S. Gonçalves, F.M. Lajolo, M. Genovese, Flavonoids, total phenolics and antioxidant capacity: comparison between commercial green tea preparations. Food Sci. Technol. 30 (2010) 1077-1082.
[15] H. Chen, C. Khemtong, X. Yang, X. Chang, J. Gao, Nanonization strategies for poorly water-soluble drugs. Drug Discovery Today. 16 (2011) 354-360.
[16] S. Kalepu, M. Manthina, V. Padavala, Oral lipid-based drug delivery systems – an overview. Acta Pharm. Sin. B3 (2013) 361–372.
[17] B.V. Bonifácio, M.A. dos Santos Ramos, P.B. da Silva, K.M.S. Negri, É. de Oliveira Lopes, L.P de Souza, T.M. Bauab, Nanostructured lipid system as a strategy to improve the anti-Candida albicans activity of Astronium sp. Int. J. Nanomed. 10 (2015) 5081–5092.
[18] W. Mehnert, K. Mäder, Solid lipid nanoparticles: production, characterization and applications. Adv. Drug Delivery Rev. 64 (2012) 83-101.
[19] R.H. Muller, M. Radtke, S.A. Wissing, Solid lipid nanoparticles (SLN) and nanostructured lipid carriers (NLC) in cosmetic and dermatological preparations. Adv. Drug Delivery Rev. 54 (2002) S131-S155.
[20] E.B. Souto, A.J. Almeida, R.H. Muller, Lipid nanoparticles (SLN®, NLC®) for cutaneous drug delivery: structure, protection and skin effects. J. Biomed. Nanotechnol. 3 (2007) 317-331.
[21] A.J. Almeida, E. Souto, Solid lipid nanoparticles as a drug delivery system for peptides and proteins. Adv. Drug Delivery Rev. 59 (2007) 478–490.
[22] R.H. Muller, W. Mehnert, J.S. Lucks, C. Schwarz, Solid lipid nanoparticles (Sln) – an alternative colloidal carrier system for controlled drug-delivery. Eur. J. Pharm. Biopharm. 41 (1995) 62–69.
[23] K.A. Shah, A.A. Date, M.D. Joshi, V.B. Patravale, Solid lipid nanoparticles (SLN) of tretinoin: potential in topical delivery. Int. J. Pharm. 345 (2007), 163-171.

[24] R.H. Muller, K. Maéder, S. Gohla, Solid lipid nanoparticles (SLN) for controlled drug delivery–a review of the state of the art. Eur. J. Pharm. Biopharm. 50 (2000) 161-177.
[25] H. Svilenov, C. Tzachev, Solid Lipid Nanoparticles–A Promising Drug Delivery System. In: Nanomedicine. One Central Press Manchester, 2014. 187-237.
[26] S.D. Mandawgade, V.B. Patravale, Development of SLNs from natural lipids: application to topical delivery of tretinoin. Int. J. Pharm. 363 (2008) 132-138.
[27] H.H. Ali, F. Michaux, B. Ntsama, I. Sandrine, P. Durand, J. Jasniewski, M. Linder, Shea butter solid nanoparticles for curcumin encapsulation: Influence of nanoparticles size on drug loading. Eur. J. Lipid Sci. Technol. (2015).
[28] L.M. Colomé, R.P. Raffin, E.R. Assumpção, A.R. Pohlmann, S.S. Guterres, Theospheres based on theobroma grandiflorum seed butter: Development of innovative nanoparticles for skin application. Soft Materials. 8 (2010) 72-88.
[29] R.P. Raffin, A. Lima, R. Lorenzoni, M.B. Antonow, C. Turra, M.P. Alves, S.B. Fagan, Natural lipid nanoparticles containing nimesulide: synthesis, characterization and in vivo antiedematogenic and antinociceptive activities. J. Biomed. Nanotechnol. 8 (2012) 309-315.
[30] E.B. Souto, R.H. Muller, Lipid nanoparticles (SLN and NLC) for drug delivery, Handb. Exp. Pharmacol. 197 (2007) 115–141.
[31] Hoeller S, Sperge, A, Valenta C. Lecithin basednanoemulsions: A comparative study of theinfluence of non-ionic surfactants and the cationicphytosphingosine on physicochemical behavior and skin permeation. Int. J. Pharm. 2009; 370:181–186

[32] R.H. Parikh, R.R. Dubey, Studies of PLGA microspheres. Pharm. Tech. Eur. 16 (2004) 23–34.
[33] A. Zattoni, E.L. Piccolomini, G. Torsi, P. Reschiglian, Turbidimetric detection method in flow-assisted separation of dispersed samples. Anal. Chem. 75 (2003) 6469-6477.
[34] M. Stuchlık, S. Zak, Lipid-based vehicle for oral drug delivery. Biomed. Papers 145 (2001) 17–26.
[35] W. Mehnert, K. Mäder, Solid Lipid Nanoparticles: Production, Characterization and Applications. Adv. Drug Delivery Rev. 47 (2001) 165-196.

[36] T. Helgason, T.S. Awad, K. Kristbergsson, D.J. McClements, J. Weiss, Effect of surfactant surface coverage on formation of solid lipid nanoparticles (SLN). J. Colloid Interface Sci. 334 (2009) 75–81.
[37] A. Lippacher, R.H. Muller, K. Mader, Liquid and semisolid SLN e dispersions for topical application: rheological characterization. Eur. J. Pharm. Biopharm. 58 (2004) 561–567.
[38] E.B. Souto, R.H. Muller, Lipid nanoparticles: effect on bioavailability and pharmacokinetic changes Handbook of Experimental Pharmacology, Springer, 2010. 115–141
[39] V. Centis, P. Vermette, Physico-chemical properties and cytotoxicity assessment of PEG-modified liposomes containing human hemoglobin. Colloids Surf B. 65 (2008) 239–46.
[40] M. Sanchez-Dominguez, C. Rodriguez-Abreu, Nanocolloids: A Meeting Point for Scientists and Technologists. Elsevier, 2016.
[41] S. Das, W.K. Ng, R.B.H. Tan, Are nanostructured lipid carriers (NLCs) better than solid lipid nanoparticles (SLNs): development, characterizations and comparative evaluations of clotrimazole-loaded SLNs and NLCs? Eur. J. Pharm. Sci. 47 (2012) 139-151.
[42] N. Mondal, A. Samanta, T.K. Pal, S.K. Ghosal, Effect of different formulation variables on some particle characteristics of poly (DL-lactide-co-glycolide) nanoparticles. Yakugaku Zasshi. 128 (2008) 595–601.
[43] X. Lin, X. Li, L. Zheng, L. Yu, Q. Zhang, W. Liu, Preparation and characterization of monocaprate nanostruc tured lipid carriers, Colloids Surf. A Physicochem. Eng. Asp. 311 (2007) 106-111.
[44] B. Siekmann, K. Westesen, Melt-homogenized solid lipid nanoparticles stabilized by the nonionic surfactant tyloxapol. I. Preparation and particle size determination, Pharm. Pharmacol. Lett. 3 (1994) 194–197.
[45] R.H. Müller, Zetapotential und Partikelladung in der Laborpraxis — Einführung in die Theorie, praktischeMeßdurchführung, Dateninterpretation, Wissenschaftliche Verlagsgesellschaft, Stuttgart, 1996.
[46] C. Schwarz, W. Mehnert, Solid lipid nanoparticles (SLN) for the controlled drug delivery. II. Drug incorporation and physicochemical characterization, J. Microencapsul. 16 (1999) 205–213.

[47] Wu, L., Zhang, J., & Watanabe, W. (2011). Physical and chemical stability of drug nanoparticles. Advanced drug delivery reviews, 63(6), 456-469.
[48] B. Siekmann, K. Westesen, Thermoanalysis of the recrystallization process of melt-homogenized glycerid nanoparticles. Colloids Surf B. 3 (1994) 159–175.
[49] S. Kheradmandnia, E. Vasheghani-Farahani, M. Nosrati, F. Atyabi, Preparation and characterization of ketoprofen-loaded solid lipid nanoparticles made from beeswax and carnauba wax. Nanomedicine. 6 (2010) 753-759.
[50] J.Y. Fang, C.L. Fang, C.H. Liu, Y.H. Su, Lipid nanoparticles as vehicles for topical psoralen delivery: Solid lipid nanoparticles (SLN) versus nanostructured lipid carriers (NLC). Eur. J. Pharm. Biopharm. 70 (2008) 633–640.
[51] V.B. Junyaprasert, V. Teeranachaideekul, E.B. Souto, P. Boonme, R.H. Müller, Q10-loaded NLC versus nanoemulsions: Stability, rheology and in vitro skin permeation. Int. J. Pharm. 377 (2009) 207–214.
[52] D. Bernardi, T. Pereira, N. Maciel, J. Bortoloto, G. Viera, G. Oliveira, P.A. Rocha-Filho, Formation and stability of oil-in-water nanoemulsions containing rice bran oil: In vitro and in vivo assessments. J. Nanobiotechnol. 44 (2011) 1-9.

6. CAPÍTULO III - Desenvolvimento e caracterização de hidrogel contendo nanopartículas lipídicas inovadoras de fucoxantina para aplicação cutânea

6.1 Introdução

Como anteriormente descrito, a FUCO é um carotenoide marinho presente em microalgas e macroalgas marrons, com uma estrutura única, incluindo um grupo alênico e um grupo epóxido. Este carotenoide apresenta efeitos promissores no tratamento do câncer, como promotor da apoptose, indutor da interrupção do ciclo celular, supressor de metástases e ação cutânea na melanogênese induzida por raios UVB (SHIMODA et al., 2010; KUMAR, MASASHI e KAZUO, 2013).

As NL são carreadores de substâncias ativas com tamanho submicrométrico, constituídos por lipídios biocompatíveis e biodegradáveis. Para aplicação cutânea, as NL apresentam vantagens devido ao aumento da hidratação da pele, modificação da liberação da substância ativa, modulação da penetração da pele, formação de filme e efeito oclusivo. Além disso, as NL são apropriadas para uso na pele danificada ou inflamada, pois são baseadas em lipídios não irritantes e não tóxicos. Na maioria dos casos, a incorporação da suspensão de NL em bases semissólidas, como os géis, se faz necessária para obter uma formulação que possa ser administrada na pele (MULLER, RADTKE e WISSING, 2002; SOUTO, ALMEIDA e MULLER, 2007).

No entanto, como os outros carotenoides, o uso da FUCO é limitado, pois a molécula é extremamente instável (HII et al., 2010; ZHANG et al., 2015). O uso de NL em produtos tópicos apresenta vantagens e, aliado a isto, o uso de uma matriz lipídica com uma constituição balanceada de ácidos graxos permite uma maior eficiência na encapsulação da FUCO, além de promover um aumento na hidratação e, consequentemente, na penetração na epiderme e derme.

Nesse contexto, este capítulo descreve os resultados do desenvolvimento e caracterização físico-química das NL-FUCO para aplicação cutânea. A formulação de NL inovadoras contendo uma combinação de 5% de manteiga de bacuri e 4% de óleo de tucumã foi utilizada para incorporar a FUCO. As NL-FUCO foram caracterizadas e um método analítico por CLAE foi desenvolvido para detecção e quantificação da FUCO na formulação de NL. Posteriormente, as NL-FUCO foram incorporadas em um hidrogel de Carbopol 940® e caracterizadas. Foram realizados estudos de fotoestabiliade frente à luz UVA e estabilidade prelimiar nas temperaturas de 6 ºC, 25 ºC e 40 ºC. A fim de avaliar a formulação desenvolvida, foram realizados estudos de dissolução e permeação cutânea *in vitro.* O trabalho

está disposto na forma de artigo científico, de acordo com as normas da revista à qual foi submetido.

6.2 Artigo científico

Amazonia products in novel lipid nanoparticles for fucoxanthin encapsulation

Submetido à publicação no periódico *European Journal of Pharmaceutical Sciences*.

Amazonia products in novel lipid nanoparticles for fucoxanthin encapsulation

Leticia Malgarim Cordenonsi[a], Andressa Santer[a], Rafaela Martins Sponchiado[a], Renata Platcheck Raffin[b] and Elfrides Eva Scherman Schapoval[a]

[a] Programa de Pós-Graduação em Ciências Farmacêuticas, Faculdade de Farmácia, Universidade Federal do Rio Grande do Sul, 90610-000 Porto Alegre - RS, Brasil.
[b] Programa de Pós-Graduação em Nanociências, Centro Universitário Franciscano, 97010-032 Santa Maria – RS, Brasil.

Abstract

Abstract

Lipid nanoparticles (LN) are well-known systems that show effectiveness to improve skin hydration, being suggested for cutaneous use. However, LN suspensions have low viscosity, which is non-attractive for cutaneous application. To circumvent this drawback, the LN was incorporate in semi-solid formulation is easy manipulation. This study demonstrated that it is possible to obtain novel LN loaded fucoxanthin (LN-FUCO) for topical administration containing a combination of bacuri butter and tucumã oil prepared by high shear homogenization for improved stability. The particle size was found to be 243.0 nm and the entrapment efficiency was up to 98% of FUCO was incorporate, achieved confirmed of the suitability of formula. The LN-FUCO hydrogel showed characteristics compatible with dermal application: pH slightly acid, drug content was close to 100%, nanometric mean size. Photostability assay by UVA, LN-FUCO and LN-FUCO hydrogel improved photostability and conferred greater protection against FUCO degradation. The results obtained from *in vitro* skin permeation studies showed significant difference between LN-FUCO hydrogel and FUCO ($p<0.05$), and no drug was found in the receptor medium. Therefore, high shear homogenization is demonstrated to be a simple, available and effective method to prepare high quality LN-FUCO hydrogel for topical application.

Keywords: Lipid solid, tucumã oil; bacuri butter; fucoxanthin, hydrogel.

1. Introduction

Bacuri (*Platonia insignis* Mart., Clusiaceae) is a native of the Brazilian Amazon and Northeast Regions. Bacuri butter has high levels of tripalmitin (50% to 55%), which penetrates the skin quickly. The high amount of fatty palmitoleic acid (5%) makes bacuri emollient and it can also be used as a moisturizing agent (Morais and Gutjahr, 2009; Rufino et al., 2010; Silva et al., 2015; Uekane et al., 2017).

Tucumã (*Astrocaryum vulgare*, Arecaceae) is native to the Amazon region. The oil extracted from the pulp contains 25.6% saturated fatty acids and 74.4% unsaturated fatty acids composed of palmitic, stearic, oleic, and linoleic acids. As it is rich in omega 3, 6 and 9, it is a good moisturizer and is used in cosmetics such as skin moisturizers, body lotions, and products for damaged hair. The orange oil is an excellent source of carotenoids, its contains 21 different types of carotenoids including b-carotene, the precursor of vitamin A (Bora et al., 2001; De Rosso and Mercadante, 2007; Morais and Gutjahr, 2009).

Fucoxanthin (FUCO) is a major marine carotenoid present in microalgae and brown macroalgae, with a unique structure including an allenic bond and a 5,6-monoepoxide. It has also been reported that FUCO has considerable potential and promising applications in human health, because of its antioxidant and anti-inflammatory properties as well as anti-cancer activity (Miyashita et al., 2011; Kumar, Masashi e Kazuo, 2013). Shimoda and co-workers (2010) established that FUCO inhibited tyrosinase activity, melanogenesis in melanoma and ultraviolet B-induced skin pigmentation. The results suggested that FUCO showed anti-pigmentary activity by topical or oral application in ultraviolet B induced melanogenesis, possibly through the suppression of prostaglandin E2 synthesis and melanogenic stimulant receptors. Furthermore, it inhibited cell damage for pre-treated cells, indicating that it could protect skin against photodamage induced by ultraviolet B irradiation from sunlight (Heo and Jeon, 2009). However, like other carotenoids, there are a number of challenges that limit its potential application, as their instability (Hii et al., 2010; Crupi al., 2013).

Lipid nanoparticles (LN) are drug carriers in the submicron range size, between 50 nm and 1000 nm, made of biocompatible and biodegradable lipids. LN exhibits advantages for topical application, because of increased skin hydration, drug release modification, modulation of skin penetration, film forming, occlusivity and

increased efficiency of molecular UV blockers (Shidhaye et al., 2008; Kumar and Randhawa, 2013). In addition, LN are appropriate for use on damaged or inflamed skin because they are based on non-irritant and nontoxic lipids. In most cases, the incorporation of the LN suspension in semi-solid formulation (ex. ointment, cream or gel) is necessary in order to achieve a formulation which can be administered to the skin (Wissing and Muller, 2003; Souto et al., 2007).

The use of drug delivery systems such as nanoemulsion (Salvia-Trujillo et al., 2015), nanogels (Ravi e Baskaran, 2015) and microsphere (Quan et al., 2013) to encapsulate FUCO is reported in the literature. The encapsulation of FUCO with chitosan-glycolipid hybrid nanogels by ionic gelation method has been reported in previous research to improve stability of FUCO (Ravi e Baskaran, 2015). Likewise, Salvia-Trujillo (2015) studied the impact of three types of lipid carrier on the bioavailability of FUCO in nanoemulsions for use in *in vitro* gastrointestinal model.

In this study, we propose the first application of a combination of the bacuri butter and tucumã oil for preparation of novel LN for encapsulation of FUCO. Until now, as we know, there are no papers describing the use of combination of bacuri e tucumã in nanoparticles, especially for topical administration. Earlier, we reported that bacuri butter and tucumã oil have beneficial properties and can be the actives that will perform the efficacy of the formulation, as well are both excipients for LN formation. In addition, high shear homogenization is a simple, rapid, easy to handle and feasible technique to prepare LN, because it requires low cost equipment which allows obtaining particles of nanometric size. As a result, the objective of the present study was to prepare novel LN-FUCO for topical administration with a combination of bacuri butter and tucumã oil prepared by high shear homogenization for improved stability.

2. Materials and Methods

2.1 Materials

A reference standard of FUCO ($C_{42}H_{58}O_6$) with purity of >95%, was supplied by Cayman Chemical Company® (Ann Arbor, MI, USA). FUCO (2%) was kindly donated by Shaanxi Jiahe Phytochem Co., Ltd. (Xian, China). Phenypropanol and caprylyl glycol (Sharomix CPP®) were kindly donated by Sharon Laboratório (Brazil). Bacuri butter and tucumã oil were kindly donated by Amazon Oil Industry. Carbopol

940® and polysorbate 80 were obtained from Delaware (Porto Alegre, Brazil) and sorbitan monooleate was purchased from Sigma-Aldrich (São Paulo, Brazil). All chemicals used were of pharmaceutical or special analytical grade. Ultra-pure water was obtained from a MilliQ® apparatus (Millipore®, USA).

2.2 Preparation of LN-FUCO

Based on the results of the development of a novel LN containing a combination of bacuri butter and tucumã oil performed by our research group, the formulation that presented the best results was chosen for the incorporation of FUCO. LN-FUCO were prepared using high shear homogenization. In short, the lipid phase was composed of bacuri butter (5%), tucumã oil (4%), FUCO (0.05%) and sorbitan monooleate (2%). The aqueous phase was composed of polysorbate 80 (4%) and water. The lipid phase and aqueous phase were simultaneously heated at 65 °C under constant magnetic stirring, until all components were melted. Then, the aqueous phase was poured over the lipid phase under agitation and with controlled temperature. The suspension was subjected to shaking using an Ultra-turrax® T10 Basic (Ika, Germany) mixer at 24,000 rpm during 20 min and, finally, the novel LN-FUCO were obtained after cooling.

2.3 Preparation of LN-FUCO hydrogel

Carbopol 940® (0.25% *w/v*) was dispersed directly in suspension of LN-FUCO and allowed to hydrate for 24 h. Sharomix CPP® was added as preservative at a concentration of 1% (*w/v*). After 24 h, hydrogel was neutralized with triethanolamine to yield LN-FUCO based Carbopol hydrogel with a pH value of about 6.0. A similar hydrogel formulation containing FUCO, sorbitan monooleate and polysorbate 80, but using water in the place of the suspension of LN-FUCO was also prepared for comparison. In parallel, a hydrogel with neither FUCO nor LN-FUCO was also prepared as control.

2.4 HPLC-DAD analysis

HPLC-DAD was used to determine the FUCO concentration in the LN, with the same chromatographic conditions to quantify FUCO in other samples. This stability indicating method was developed in our research group (Cordenonsi et al., 2017).

The chromatographic analysis of the LN-FUCO was performed on a HPLC Agilent® model 1200 UV/LC system (Santa Clara, USA), using a Agilent® Eclipse Plus C18 analytical column (4.6 mm x 150 mm, 5.0 µm) as stationary phase and a mobile phase composed an isocratic mode using acetonitrile and water, pH adjusted to 7.0 with sodium hydroxide 0.1 *M* (NaOH) (9.5:0.5 *v/v*). The system was programmed at 40 ºC for the column oven, 450 nm for the detection wavelength; flow rate was 1.0 mL min-1 and 50 µL for the injection volume.

LN-FUCO was extracted by acetonitrile and quantified. Standard FUCO solutions were prepared in acetonitrile and the dilutions were done with acetonitrile and water, pH adjusted to 7.0 with NaOH 0.1 *M* (9:1 *v/v*). All analyses were performed under dark conditions.

2.5 Physicochemical characterization

2.5.1 Particle size and zeta-potential measurements

LN-FUCO and LN-FUCO hydrogel were characterized in terms of mean particle size and particle size distribution. The mean particle size and polydispersity indexes (pdI) were investigated by dynamic light scattering (DLS) using a Zetasizer® Nano ZS, model ZEN 3600 (Malvern Instruments, UK). The samples were diluted 5,000 times (*v*/*v*) in ultra-pure water, which was performed at 25 °C and the results reported are the average of three measurements.

The zeta-potential was determined by electrophoretic mobility (Zetasizer®, model ZEN 3600, Malvern Instruments) after the samples were diluted 5,000 times (*v*/*v*) with 10 m*M* sodium chloride solution, which was performed at 25 °C and the results reported are the average of three measurements.

2.5.2 pH values

The pH values of the LN-FUCO and LN-FUCO hydrogel were determined using a potentiometer, model DM-22 (Digimed Analytical, Brazil), directly in the formulations at 25±0.5 °C.

2.5.3 Nanoparticle morphology

Transmission electron microscopy (TEM) was used to observe the surface morphology of LN-FUCO and to further confirm particle diameter by DLS.

Observations were made with TEM (JEM 1200 Exll) operating at 80 kV (Centro de Microscopia da UFRGS). Diluted (10x- ultra-pure). All formulations were dripped on specimen grids (Formvar-Carbon support film, Electron Microscopy Sciences) and negatively stained with uranyl acetate solution (2% *w/v*).

2.5.4 Drug contents and entrapment efficiency (E.E.)

The drug contents were determined by HPLC-DAD under the conditions described. The association rate was determined by ultrafiltration–centrifugation technique (Ultrafree-MC 10.000 MW, Merck, Millipore®) at 8,000 rpm for 10 min. FUCO concentration associated with the LN was calculated considering the difference between the total concentration of FUCO in the formulation and the dissolved concentration in the aqueous phase of the dispersion.

2.6 Photostability assay

The photostability assay was performed by irradiating the samples in a mirrored chamber with a UVA light source. Aliquots of LN-FUCO and LN-FUCO hydrogel were transferred to a one cm quartz cell and exposed positioning them horizontally to have the maximum exposure area, at pre-established times (0, 30, 60, 90, 120, 180, and 240 min), and the quantification was verified by the HPLC-DAD method. Degradation kinetics study was carried and determined by plotting the drug concentration, the log and the reciprocal of concentration versus time. The determination coefficients (r^2) were obtained and the best observed fit indicated the reaction order. The kinetic parameters, such as the apparent order degradation rate constant (*k*), half-life time ($t_{1/2}$), and $t_{90\%}$ (time where 90% of original concentration of the drug is left) were obtained.

2.7 Accelerated stability studies

LN-FUCO were stored under controlled conditions: 6±2 ºC, 25±2 ºC, and 40±2 °C. Periodical testing of different parameters, such as particle size, zeta-potential, and drug content were performed during 45 days real-time stability studies were performed.

2.8 *In vitro* dissolution studies

For the dissolution studies, 1.0 mL of the LN-FUCO were suspended in 100 mL of phosphate buffer, pH 7.4, and incubated into a bath at 37±0.5 °C under magnetic stirring at 60 rpm. The sink conditions prevailed during the release studies. At appropriate intervals, 1.0 mL aliquots were withdrawn, filtrated through a Millipore 0.1 µm filter. The drug release/dissolved was assessed through HPLC analysis according to the method described above. The initial volume of medium was maintained by adding 1.0 mL of phosphate buffer after each withdrawal. All experiments were conducted in quadruplicate. The data obtained were fitted to the mathematical models using Scientist® 2.0 software (MicroMath®, St Louis, MO, USA). The model that best describes the drug release profile was selected through the model selection criteria (MSC), graphic adjustment, and the correlation coefficient.

2.9 *In vitro* skin permeation studies

2.9.1 Skin sample preparation

Fresh porcine ears were cleaned with water and skin samples removed (central region of the outer side of the auricle) using a scalpel and scissors. Skin samples were sliced into round pieces with 2 cm diameter, packed in PVC film surrounded by aluminum foil, and stored (-20 ºC) for up to 30 days. The ears were obtained from a local slaughterhouse and the following criteria were applied: they had to be from the same porcine race, age between 4-6 months, white and the excision procedure had to be done before the usual scalding of the animals. No skin with wounds, warts or hematomas was used.

2.9.2 Skin barrier-impairment

The method was adapted from Alnasif and co-workers (2014). The skin barrier impairment was induced by use of the tape stripping method. The skin was stripped using adhesive tape (Scotch Tape, 3M Company). Each tape was applied to the skin surface and removed from the test area in one gentle, continuous move. For each repeated strip, the tearing-off direction was varied to obtain a homogeneous removal of the stratum corneum cell layers. The stripping procedure was repeated for 20 and 40 strips.

2.9.3 Skin penetration studies of FUCO and LN-FUCO hydrogel

Skin permeation profiles of FUCO and LN-FUCO hydrogel into the intact and barrier-impaired skin, using Franz cell apparatus. The skin samples were placed on the Franz diffusion cell (Hanson Research, Chatsworth, USA) with the dermis facing the receptor compartment. Franz cell had a diffusion area of 1.77 cm^2 and stored 7.0 mL of receptor medium, composed of ethanol and water (50:50 *v/v*). FUCO solubility in the receptor phase was determined, achieving sink conditions to have a high capacity to dissolve and carry away the drug. After equilibrating the skin for 30 min receptor medium, formulation applied evenly on the skin surface using a spatula. At given times intervals (0.5, 1, 2, 4, 6 and 8 h) aliquots of 1.0 mL were collected to be analyzed and the same volume of receptor fluid was replaced. The receptor medium was maintained at 37 ºC, in order to keep the skin surface at 32 ºC (the ambient temperature was 21-25 ºC) and magnetically stirred at 500 rpm. All samples were filtered prior to HPLC injection and nine replicates of FUCO and LN-FUCO were performed for the intact and barrier-impaired skin.

After eight hours of experiment, the excess of formulation on the skin was removed with cotton, and the skin layers, epidermis, and dermis were separated using a scalpel. The skin layers were weighted and FUCO was extracted from epidermis and dermis using 2.0 mL of acetonitrile and placed in ultrasound bath for 30 min. The results are reported as means relative standard deviations (RSD) (n=9) and data were statistically analyzed using the t-test, after assuring the normal distribution. The level of significance was set at $\alpha = 0.05$.

2.9.4 Bioanalytical method validation

Prior to the skin permeation assay, the analytical methods for FUCO analysis was validated considering specificity, matrix effects, linearity, accuracy, precision, quantification and detection limits followed national and international guidelines (ICH, 2005).

Specificity: the chromatograms obtained from the extraction solution of epidermis and dermis in contact with LN-FUCO formulation were compared with the chromatogram from skin extraction solution.

Linearity: Linearity was evaluated through the construction of standard plots (n=3) with six concentrations in the range of 0.5–40.0 μg mL-1. The linearity was evaluated

by linear regression analysis that was calculated by the least square regression and by ANOVA for compliance of the linear model.

Detection and quantification limits (LOD and LOQ): LOD and LOQ were obtained based on the signal-to-noise by the ChemStation software. The LOD and LOQ were estimated at a concentration level in which the signal-to-noise ratio reached 3:1 and 10:1, respectively. The precision of LOQ was evaluated and the RSD were calculated.

Accuracy (recovery): Round skin samples, measuring 1.5 cm in diameter, had the epidermis (n=9) and dermis (n=9) separated, with a scalpel, by placing the skin into a water bath at 60 ºC during one min. Then, the skin layers were cut into small pieces and placed in tubes. These layers were spiked with a known amount of standard solutions and, after the solvent evaporated, diluting solvent was added. Samples placed in ultrasound bath. The amount of FUCO, after the solvent addition, corresponded to the theorical concentration of 0.5, 15.0 and 40.0 µg mL-1. Each concentration was prepared in triplicate in 3 days. The measured and nominal concentrations of the analytes in the matrix skin samples were compared. The results were expressed as the percentage of drug reference standard recovered from the sample.

Precision: The precision data was obtained from the recovery assay, analyzing the results from six independent sample preparations on the same day. The intermediate precision was tested by assaying freshly prepared sample solutions at different concentrations on another day. Precision was reported as RSD.

3. Results and discussion

3.1 Development and characterization of LN-FUCO

Previously identified and characterized by Cordenonsi and collaborators (2017), FUCO in oil was identified as all-*trans* FUCO. All-*trans* FUCO when compared with 9'-*cis* FUCO, showed greater stability. Usually, cis isomers are thermodynamically less stable. In addition, the correct identification of isomers is a fundamental point, since isomers differ substantially in their activity (Cordenonsi et al., 2017).

Studies have reported the preparation of nanoparticles as a nanocarrier for FUCO using microfluidizer and ionic gelation method (Salvia-Trujillo et al., 2015;

Ravi e Baskaran, 2015). Although successfully obtained, these methods present some limitations, such as residual traces from the organic solvents used in the production process and difficulties in increasing the scale of the production (Mehnert and Mader, 2001). In this paper, we prepared LN-FUCO by high shear homogenization. This method is relatively simple, without the use of organic solvent and energy-efficient, which requires low cost materials and allows large scale production.

This is the first study to show the encapsulation of FUCO containing a novel combination of bacuri butter and tucumã oil, two important compounds. The development of novel LN for cutaneous application was described by our research group. LN had an average size of 255 nm, a uniform size distribution and a high zeta-potential, sufficient to prevent droplet coalescence. Spherical shape and size were confirmed using transmission electron microscopy analysis. High shear homogenization is a very simple and widely used technique. In addition, organic solvent residues derived from preparation procedures such as the solvent evaporation technique often used for liposome and polymeric nanoparticles, can be present in the delivery system and could result in severe acceptability and toxicity problems (Souto, Almeida and Muller, 2007; Gasco, 2007).

Based on these results, FUCO was incorporated in the formulation with best results with 5% of bacuri butter and 4% of tucumã oil, and LN-FUCO was successfully produced. The results are summarized in Table 1.

Table 1. Summary of results from the characteristics of LN, LN-FUCO and LN-FUCO hydrogel.

	LN	**LN-FUCO**	**LN-FUCO hydrogel**
Average size (nm)*	212.4 ± 0.7	243.0 ± 1.6	220.1 ± 1.3
Polydispersity index*	0.18 ± 0.01	0.22 ± 0.01	0.22 ± 0.01
Zeta-potential (mV)*	-24.2±0.2	-44.9 ± 2.3	-25.5 ±1.1
pH*	5.64 ± 0.01	7.16 ± 0.05	5.95 ± 0.03
Drug content (%)*	-	103.65 ± 0.66	100.98 ± 0.81
Encapsulation efficiency (%)*	-	98.90 ± 0.32	-

* The values are expressed in mean ± SD.

Regarding the visual aspect, LN-FUCO formulation was orange colored and homogenous. The particle size distribution and mean particle diameter of the LN-FUCO were measured immediately after they were produced by high shear homogenization. LN-FUCO had a nanometric and monomodal size distribution, 243.0 nm and pdI values of 0.22, respectively. When FUCO was added, the particle size increased from 212 nm to 243.0 nm and pdI values increased from 0.18 to 0.22 nm. The pdI values were below 0.3 for all nanostructured carriers suggesting that each preparation method led to controlled size distributions. These results suggested that a good LN-FUCO could be formed by a novel combination of bacuri butter and tucumã oil. Puglia and co-workers (2008) described the potential of NL as carriers for topical administration. They developed a NL by hot high pressure homogenization and ultrasonication techniques, and the particle size was between 215-404 nm.

LN-FUCO formulations were negatively charged, the zeta-potential was -44.9 mV. LN produced without FUCO showed a zeta-potential of -24.2 mV. Thus, the addition of FUCO resulted in increased zeta-potential and high values contributed to the physicochemical stability of the formulations. Coulombic repulsion forces arise on the surface of highly charged nanoparticles, which can overcome the Van der Waals attractive force between them and prevent aggregation (Puglia et al, 2008; Muthu and Singh, 2008).

The pH value observed for LN-FUCO was 7.16. When FUCO was added, the pH values increased, from 5.64 to 7.16, which is adequate for cutaneous administration.

The total drug content and E.E. of LN-FUCO were estimated to be 103.65% and 98.90%, respectively. The E.E. depends on the size of nanoparticles and thus the stabilizer compositions. High value, approaching 100%, indicates the efficiency of the method for the preparation of LN and that no significant losses occurred during formulation and indicating that there was no degradation of the drug during the preparation (Sinha, Muller and Moschwitzer, 2013). In this way, bacuri butter was an adequate lipid to encapsulate FUCO, showing high drug loading and E.E. Previous study reported that the encapsulation efficiency of FUCO in chitosan-glycolipid hybrid nanogels was found to be 90% (Ravi et al., 2015).

The morphological study using TEM (Figure 1) revealed that the LN-FUCO are spherical in shape with a smooth surface. The particle size and distribution by TEM

correlated well with the results obtained from DLS. Souto and co-workers (2007) described the morphology of LN depend on the lipid selected. When using crude mixtures, spherical shape is preferentially formed, because in this case more crystallized lipid molecules are presents.

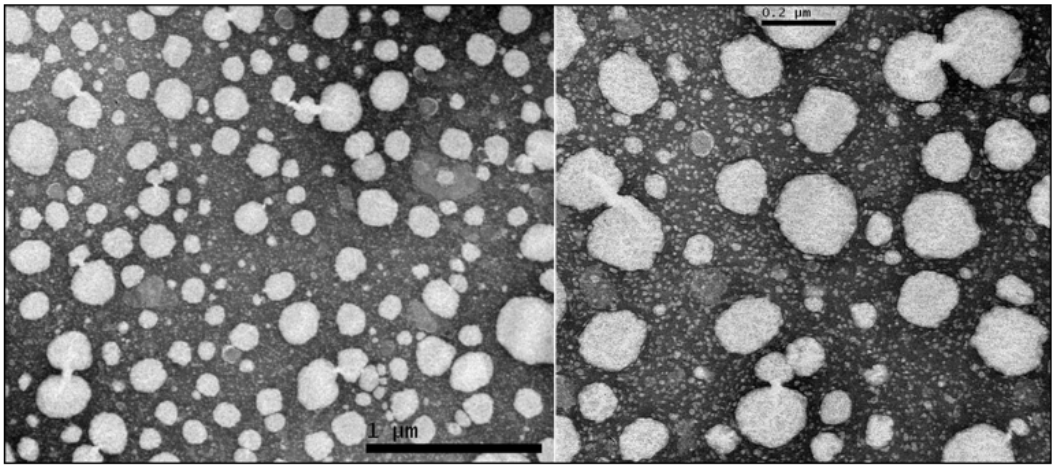


Figure 1. TEM photographs of LN-FUCO

3.2 Development and characterization of LN-FUCO hydrogel

The LN-FUCO possesses low viscosity and hence it is inconvenient for topical application. Hydrogel, as Carbopol gel, preparations are generally preferred because of their controlled release character, easy manipulation, flexibility, versatility and good tissue compatibility (Freitas and Muller, 1999).

For semi-solid formulation, the biggest challenge is using a natural preservative that is as efficacious as a chemical preservative but without the associated effect. Since the inclusion of parabens is nowadays poorly accepted by the consumers, Sharomix CPP® was included as the antimicrobial component and is composed of caprylyl glycol and phenylpropanol and is considered a “preservative free”, non-pH dependent and therefore, creating a highly efficient broad spectrum blend. As reported by Muller and co-workers (2002), LN can be formulated in topical administration, through their incorporation into existing products or by addition of a viscosity agent to LN or by direct production of highly concentrated dispersions.

In this study, the LN-FUCO are formulated in hydrogel for topical application using Carbopol 940®. The LN-FUCO hydrogel appeared opalescent, good stability

and properties of consistency and spreadability. The results of LN-FUCO hydrogel are summarized in Table 1.

The stability of LN-FUCO before and after their incorporation into hydrogel was monitored by particle size and pdI examination to investigate the possible aggregation of particles due to incompatibility or interactions between the gel forming ingredients. The analysis showed that the incorporation of LN-FUCO into hydrogel did not affect the pdI values. The mean zeta-potential values measured was -25.5 mV for LN-FUCO hydrogel. However, the zeta-potential of the LN-FUCO in aqueous suspension was larger (-44.9 mV) when compared to the particles dispersed in the hydrogel matrix.

The FUCO content of the LN hydrogel was found to be 100.98% of the theoretical value. Hydrogel formulations presented pH values close to 5.95, which is adequate for cutaneous application (Schmid-Wendtner and Korting, 2006).

3.3 Validation of the HPLC-DAD for LN-FUCO

Figure 2 shows the chromatograms obtained by HPLC-DAD of reference standard, LN-FUCO, and LN. LN-FUCO eluted after 3 min, with a retention time identical to the standard reference and the purities of all the peaks were greater than 99.9%, indicating homogenous peaks.

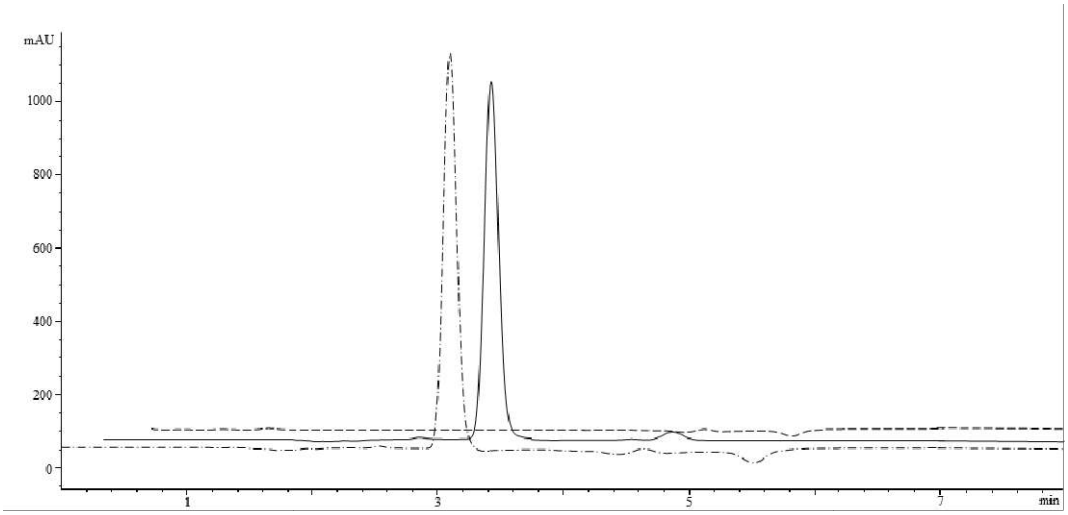


Figure 2. HPLC-DAD chromatogram of reference standard (line), LN-FUCO (trace-point) and LN (trace). Chromatographic conditions: Agilent® Eclipse Plus C18 column (4.6 mm x 150 mm, 5.0 µm), 40 °C; mobile phase: acetonitrile (ACN) and water, pH adjusted to 7.0 with sodium hydroxide 0.1 *M* (NaOH) (9.5:0.5 *v/v*); flow rate: 1.0 mL min-1; detection: 450 nm.

The analytical curves constructed for FUCO were found to be linear in the range 1.0-40.0 µg mL-1 ($r>0.99$), ANOVA showed non-significant linearity deviation ($p > 0.05$) and with adequate fitting ($p>0.05$). LN without FUCO injections were performed to demonstrate the absence of interference of the excipients components with the FUCO, as shown in Figure 2. LOD with a signal-to-noise ratio of 3:1 was found to be 0.03 µg mL-1 and LOQ with a signal-to-noise ratio of 10:1 was found to be 0.10 µg mL-1. These results indicate the adequate sensitivity of the method. Precision evaluated as the repeatability (intra-day) and intermediate precision (inter-day) of the method was determined by calculating the RSD for six determinations. The repeatability was RSD 0.86% and intermediate precision was 0.94%. The results indicate low RSD obtained for the repeatability and intermediate precision and showed the good precision of the method. Determination of accuracy allows estimating the extent to which systematic errors affect the analytical method (Rambla-Alegre et al., 2012). The accuracy of the method to quantify LN-FUCO was calculated by percentage of recovery. The mean values were found to be 102.15% (RSD= 0.63%). These results indicate low RSD, showing satisfactory accuracy of the

proposed method. Therefore, the results discussed show that the stability-indicating method for FUCO is specific and accurate and possesses very satisfactory linearity and precision, without any interference.

3.4 Photostability assay

FUCO is a drug which has a wide instability in the presence of light, making its use difficult. Photostability assay of FUCO was conducted in order to verify if a novel LN could protect the drug from radiation and accelerate possible degradation reactions that occur in this process.

The results for photostability assay of FUCO, LN-FUCO and LN-FUCO hydrogel are shown in Figure 3. Approximately 11% of LN-FUCO and LN-FUCO hydrogel were degraded within 240 min, while for the free FUCO, 27% was degraded. Nanoparticulate carriers offered significantly better photoprotection. This can be ascribed to the solid photoprotective lipid layer around the entrapped drug, thus protecting it from direct light (Raza et al., 2013). Based on these results, the importance of FUCO encapsulation to increase stability, especially, since it refers to a substance highly unstable and susceptible to degradation under light.

Considering photostability assay, the degradation kinetics of LN-FUCO was performed. LN-FUCO degradation shows a first-order kinetics (r= 0.988) under the experimental conditions applied (Figure 3b). This reaction consider that the reaction velocity is directly proportional to the drug concentration. With this information, through mathematical calculations, a constant value of the decomposition of FUCO was k = 0.0155 min, the $t_{1/2}$ and $t_{90\%}$ were 44.61 and 6.82 min, respectively. Previous study reported that the kinetics of saffron carotenoids encapsulated in different amorphous polymeric matrices follow first-order kinetics (Selim, Tsimidou and Biliaderis, 2000),

The chromatograms of FUCO were monitored by the appearance of additional peaks and the peak purity during the photostability study. The results showed no additional peaks in the chromatograms and the purities of all the peak was greater than 99%, indicating homogenous peaks.

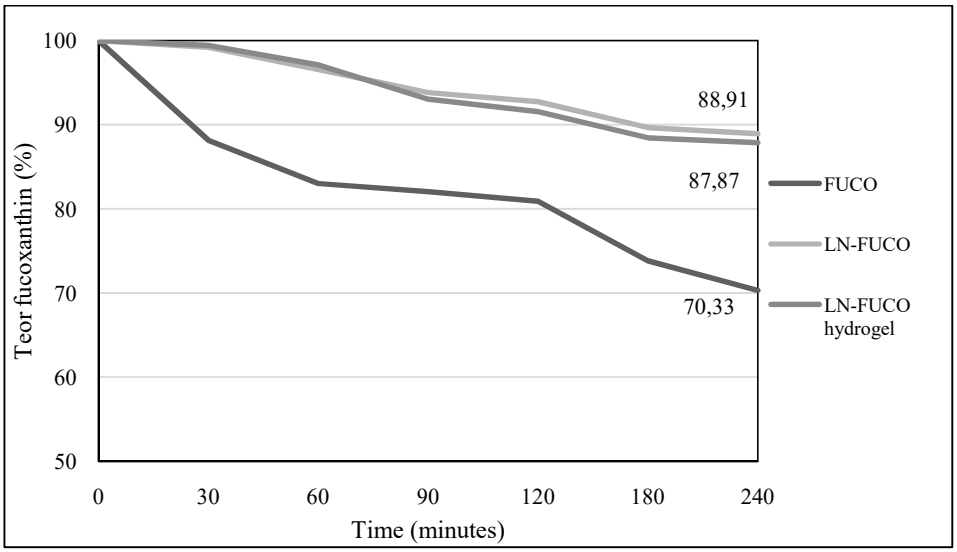


Figure 3. Photostability assay of FUCO, LN-FUCO and LN-FUCO hydrogel by UVA lamp.

3.5 Accelerated stability studies

The physical and chemical stability are common concerns for LN formulations. The initial particle size of LN were 247.29 ± 1.76 nm. Upon storage, slight increase in particle size was observed. The LN-FUCO did not show any macroscopic instability processes and their particle size remained in the nanoscale range. Clotrimazole loaded LN were prepared and the results showed that the particles remained in their colloidal state during 3 months of storage at 4 ºC, 20 ºC and 40 ºC (Souto et al., 2004). Likewise, Andrade and co-workes (2014) developed LN to deliver genistein to deeper skin layers. Stability studies demonstrated that mean diameter and pdI did not significantly change over 180 days at 4 ºC.

The zeta-potential is a key factor in order to obtain information about the stability of nanoparticles. Zeta-potential values were between −43.6 mV and −46.1 mV in the initial measurement (Figure 4b). After 45 days this parameter was close to −41 mV, which shows good physical stability of the dispersed systems, because high zeta-potential values ensure repulsion of droplets (Puglia et al., 2008).

After 45 day storage, the drug content in the LN-FUCO stored at 6 °C, 25 °C, and 40 °C were measured to be 100.5%; 101.0%; and 97,1%, respectively (Figure 4c). The results showed that the LN-FUCO performed good stability of FUCO during the storage for all temperatures. The melting point of the bacuri butter is 25 °C,

however the storage at 40 °C has not affected the stability. Furthermore, being an advantage, LN-FUCO can be stored at room temperature.

NL are innovative vehicles, show an improved drug entrapment efficiency, increased stability during storage, and exhibit high physical stability (Wissing and Muller, 2003; Souto et al., 2007; Puglia et al., 2008). The LN-FUCO were considered stable they continued inside acceptable parameters, what means inside the nanoscale droplet size range and macroscopically stable.

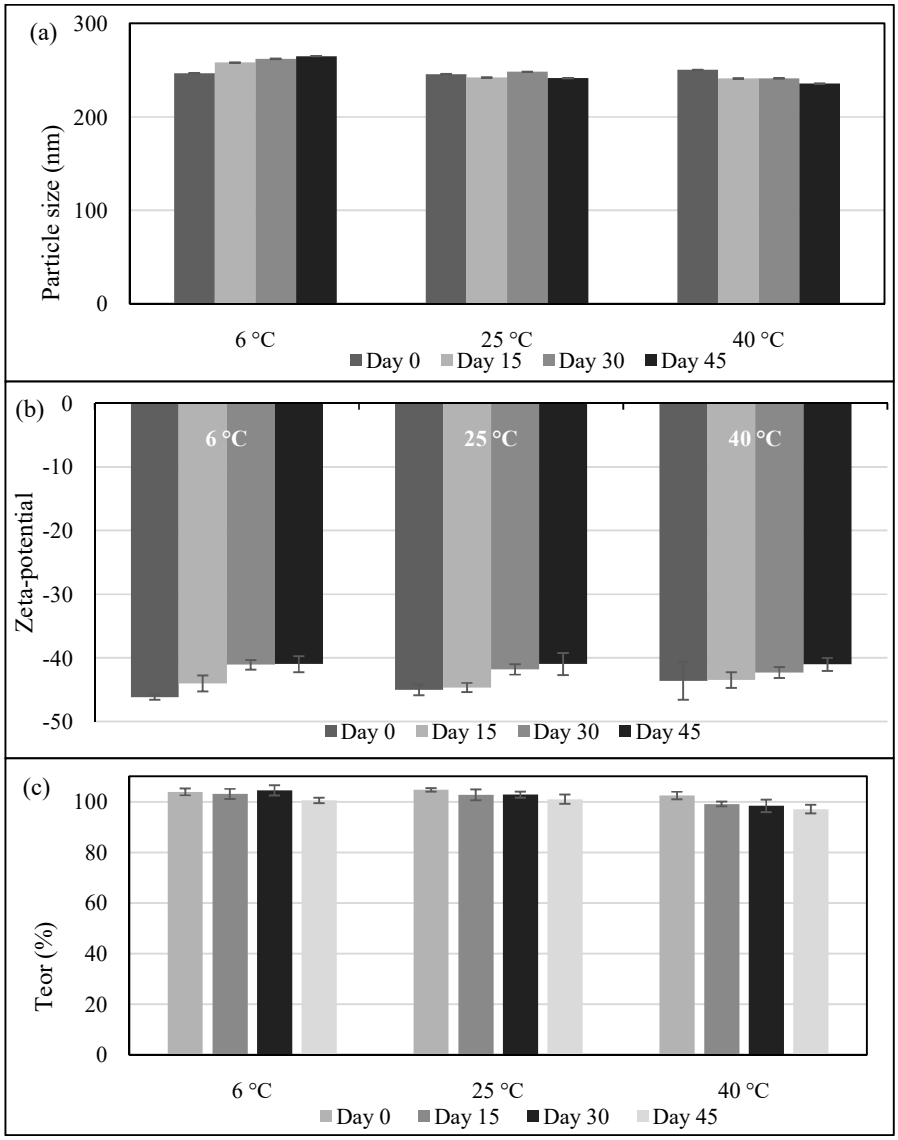


Figure 4. Particle size, zeta-potential, and drug content graphic of accelerated stability studies of LN-FUCO.

3.6 *In vitro* dissolution studies

In vitro dissolution studies are an essential tool for quality control purposes as well as for prediction of the *in vivo* performance of drug delivery systems. In the sample and separate methods, the nanoparticles are directly added into the release medium and sample separation techniques (such as ultrafiltration, ultracentrifugation, and centrifugal ultrafiltration) are used to separate the dispersed nanoparticles from the continuous phase at different time intervals. In some cases, the use of syringe filters with smaller pore size (0.1) has been used as a simple yet efficient way for sample separation (Wallace et al., 2012; Shen and Burgess, 2013).

In matrix systems, such as LN, the drug is incorporated in the lipid matrix either in dissolved or in dispersed form. Consequently, the solubility of the drug in the lipid matrix becomes important controlling factor for the release of drug from LN (Muller et al., 2002).

Figure 5 shows the FUCO release profiles from 243.0 nm nanoparticles. The quantification of the FUCO was performed using validated analytical method. In sink conditions, the release of LN-FUCO after 4 h was 81.50%, in contrast, FUCO non-encapsulated diffused 98.76% in 10 min. The statistical t-test showed significant difference ($p<0.05$). This statistical analysis indicated that the drug release of FUCO loaded LN was not similar to FUCO in solution and demonstrate the ability of LN to promote a controlled release of the FUCO. The ability of the LN to control and prolong the FUCO release was confirmed by mathematical modeling. The model selection was based on the best correlation coefficient and MSC value. The model that best described the drug release profile was the bi-exponential model ($r=0.9981$; MSC=5.45±0.25; k1=0.0246±0.0012; k2=0.00414±0.0003; t½ k1 =27.56±1.25 min; t½ k2 =247.13±25.56 min).

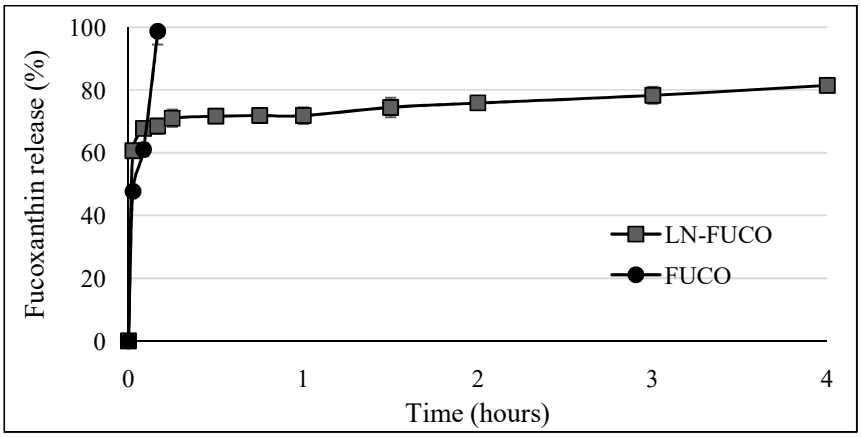


Figure 5. Release profiles of free FUCO and LN-FUCO in phosphate buffer, pH7.4, at 37°C during 4 h. Data are shown as mean ± S.D.

3.7 *In vitro* skin permeation studies

In vitro penetration studies were carried out on intact and barrier-impaired porcine skin in Franz diffusion cells to evaluate the influence of FUCO and LN-FUCO hydrogel on its skin permeation profile. The skin permeation model was established on the fact that pig epidermis can be histologically associated to human skin in terms of thickness and cellular structures, and that the information obtained could be correlated to a human skin behavior (Fernandez et al., 2000).

During the method validation for permeation studies, no interference from the skin matrix, extraction solutions, and excipients ingredients were observed in the chromatographic runs. The results showed linearity over the concentration range established and the r^2 was 0.9986. The analysis of variance revealed that the obtained results correspond to a linear regression with no deviation from linearity (α=0.05). LOQ and LOD were 0.1 and 0.03 µg mL-1, respectively. The RSD results for repeatability, presented maximum values of 2.23% and intermediate precision was 1.19%. The percentages of recovered were 99.89-101.37% for the epidermis and 98.57-102.46% for dermis. Therefore, the method was considered specific, linear, precise and accurate.

The results obtained from the permeation assay were analyzed as the amount of drug permeated by skin area and the amount of drug retained in each skin layer, epidermis, and dermis. Figure 6a represent FUCO distribution for FUCO and LN-FUCO hydrogel at different skin layers. The results demonstrated that LN-FUCO

hydrogel retained a higher amount of FUCO in skin layers. The retention in epidermis and dermis was considered statistically significant ($p<0.05$), and in the receptor compartment, no FUCO was found after 8 hours of experiment. Vitamin A loaded solid lipid nanoparticle were tested for drug penetration in porcine skin. These nanoparticle increase the penetration of vitamin A in skin due to occlusion effect (Jenning et al., 2000). Likewise, LN controlled genistein release and increased the drug penetration in skin layers, and these LN would seem to be a promising nanocarrier for the topical delivery of genistein (Andrade et al., 2014).

Figure 6b represents LN-FUCO distribution at different skin layers after removal of stratum corneum. Jesen and collaborates (2011) verified by histological examination of the excised pig ear skin after 0, 5, 15, 25 and 40 skin stripping. At baseline (0 stripping) the stratum corneum was abundant. After 15-25 stripping the stratum corneum was partly removed, and after 40 skin stripping the stratum corneum was completely removed.

Permeation assay demonstrated that the removal of stratum corneum by tape stripping facilitated LN-FUCO penetration into viable epidermis and dermis after 8 h. Significant differences can be observed in comparison to the results presented (Figure 6b).

It is essential to highlight that these results reflect the use of intact and skin barrier impairment, when the stratum corneum is partially/totally removed. This means that the results observed overestimate the permeation of FUCO in intact skin. In many clinical conditions, such cancer, the integrity of the stratum corneum is compromised and its removal is part of some *in vitro* protocols (Saija et al., 1998).

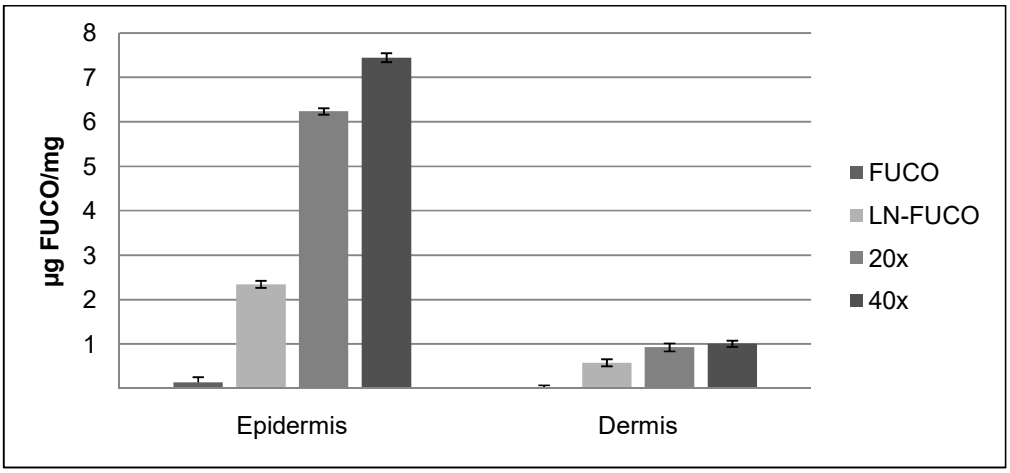


Figure 6. *In vitro* penetration studies were carried out on intact and barrier-impaired porcine skin in Franz diffusion cells. The results are relative to the total amount of FUCO recovered (n = 9)

Conclusion

This study demonstrated that it is possible to obtain LN-FUCO for topical administration with a novel combination of bacuri butter and tucumã oil prepared by high shear homogenization for improved stability. Optimizing the LN-FUCO composition with 5% of bacuri butter and 4% of tucumã oil a suitable formulation was developed. FUCO a highly lipophilic drug was successfully incorporated into the LN, because high total drug content and E.E. achieved confirmed the suitability of the formula. Photostability assay by UVA improved photostability and conferred protection against FUCO degradation. The LN-FUCO into paraben-free hydrogel showed characteristics compatible with dermal application: slightly acid pH, drug content close to 100%, particle size nanometric with low polydispersity and negative zeta-potential. The results obtained from *in vitro* skin permeation studies showed significant difference between LN-FUCO hydrogel and FUCO ($p<0.05$), and no drug was found in the receptor medium. The LN-FUCO hydrogel are promising for topical application.

References

Alnasif, N., Zoschke, C., Fleige, E., Brodwolf, R., Boreham, A., Rühl, E., Haag, R., 2014. Penetration of normal, damaged and diseased skin—an *in vitro* study on dendritic core–multishell nanotransporters. J Control Release. 185, 45-50.

Andrade, L.M., de Fátima Reis, C., Maione-Silva, L., Anjos, J.L.V., Alonso, A., Serpa, R.C., Taveira, S.F., 2014. Impact of lipid dynamic behavior on physical stability, in vitro release and skin permeation of genistein-loaded lipid nanoparticles. Eur J Pharm Biopharm. 88, 40-47.

Bora, P.S., Narain, N., Rochag, R.V.M., De Oliveira Monteiro, A.C., 2011. De Azevedo Moreira, R. Characterization of the oil and protein fractions of Tucuma (Astrocaryum Vulgare Mart.) fruit pulp and seed kernel. Ciencia y Technologia Alimentaria, v. 3, 111-116.

Cordenonsi, L.M., Santer, A., Sponchiado, R.M, Steppe, M., Raffin, R.P., Schapoval, E.V.S., 2017. Characterization and analysis of fucoxanthin and its isomers. J Pharm Sci Bioscientific Res. 7, 322-334

Crupi, P., Toci, A.T., Mangini, S., Wrubl, F., Rodolfi, L., Tredici, M.R., Antonacci, D., 2013. Determination of fucoxanthin isomers in microalgae (Isochrysis sp.) by high-performance liquid chromatography coupled with diode-array detector multistage mass spectrometry coupled with positive electrospray ionization. Rapid Commun Mass Spectrom. 27, 1027-1035.

De Rosso, V.V., Mercadante, A.Z., 2007. Identification and quantification of carotenoids, by HPLC-PDA-MS/MS, from Amazonian fruits**.** J Agric Food Chem, 55, 5062-5072.

Fernandez, C., Marti-Mestres, G., Ramos, J., Maillols, H., 2000. LC analysis of benzophenone-3: II application to determination of '*in vitro*'and 'in vivo' skin penetration from solvents, coarse and submicron emulsions. J Pharm Biomed Anal. 24,155–65.

Freitas, C., Muller, R.H., 1999. Stability determination of solid lipid nanoparticles in aqueous dispersion after addition of electrolyte. J microencap. 16, 59-71.

Gasco, M.R., 2007. Lipid nanoparticles: perspectives and challenges. Adv Drug Deliv Rev. 59, 377-378.

Heo, S.J., Jeon, Y.J., 2009. Protective effect of fucoxanthin isolated from Sargassum siliquastrum on UV-B induced cell damage. J Photochem Photobiol. 95, 101-107.

Hii, S.L., Choong, P.Y., Woo, K.K., Wong, C.L., 2010. Stability studies of fucoxanthin from Sargassum binderi. Aust J Basic Appl Sci. 4, 4580–4584.

ICH Guideline, 2005. Validation of analytical procedures: text and methodology Q2 (R1). In International Conference on Harmonization, Geneva, Switzerland (pp. 11-12).

Jenning, V., Gysler, A., Schäfer-Korting, M., Gohla, S.H., 2000. Vitamin A-loaded solid lipid nanoparticles for topical use: drug release properties. Eur. J. Pharm. Biopharm. 49, 211–218.

Jensen, L.B., Petersson, K., Nielsen, H.M., 2011. *In vitro* penetration properties of solid lipid nanoparticles in intact and barrier-impaired skin. Eur J Pharm Biopharm. 79, 68-75.

Kumar, S., Randhawa, J.K., 2013. High melting lipid based approach for drug delivery: Solid lipid nanoparticles. Mater Sci Eng C. 33, 1842–1852.

Kumar, S.R., Masashi, H., Kazuo, M., 2013. Fucoxanthin: A marine carotenoid exerting anti-cancer effects by affecting multiple mechanisms. Marine drugs. 11, 5130–5147.

Mehnert, W., Mader, K., 2001. Solid lipid nanoparticles: production, characterization and applications. Adv Drug Deliv Rev. 47, 165-196.

Miyashita, K., Nishikawa, S., Beppu, F., Tsukui, T., Abe, M., Hosokawa, M., 2011. The allenic carotenoid fucoxanthin, a novel marine nutraceutical from brown seaweeds. J Sci Food Agric. 91, 1166-1174..

Morais, L.R.B., Gutjahr, E., 2009. Química de oleaginosas: Valorização da biodiversidade amazônica. Brasília: Agência de Cooperação Técnica Alemã (GTZ), 83p.

Muller, R.H., Radtke, M., Wissing, S.A., 2002. Solid lipid nanoparticles (SLN) and nanostructured lipid carriers (NLC) in cosmetic and dermatological preparations. Adv Drug Deliv Rev. 54, S131-S155.

Muthu, M.S., Singh, S., 2008. Studies on biodegradable polymeric nanoparticles of risperidone: *in vitro* and in vivo evaluation. Nanomedicine. 3, 305-319.

Puglia, C., Blasi, P., Rizza, L., Schoubben, A., Bonina, F., Rossi, C., Ricci, M., 2008. Lipid Nanoparticles for prolonged topical delivery: An *in vitro* and in vivo investigation. Int J Pharm. 357, 295-304.

Quan, J., Kim, S.M., Pan, C.H., Chung, D., 2013. Characterization of fucoxanthin-loaded microspheres composed of cetyl palmitate-based solid lipid core and fish gelatin–gum arabic coacervate shell. Food Res Int. 50, 31-37.

Rambla-Alegre, M., Esteve-Romero, J., Carda-Broch, S., 2012. Is it really necessary to validate an analytical method or not? That is the question. J Chromat A. 1232, 101-109.

Ravi, H., Baskaran, V., 2015. Biodegradable chitosan-glycolipid hybrid nanogels: A novel approach to encapsulate fucoxanthin for improved stability and bioavailability. Food Hydrocoll. 43, 717-725.

Raza, K., Katare, O.P., Setia, A., Bhatia, A., Singh, B., 2013. Improved therapeutic performance of dithranol against psoriasis employing systematically optimized nanoemulsomes. J Microencap. 30, 225-236.

Rufino, M.S., Alves, R E., de Brito, E.S., Pérez-Jiménez, J., Saura-Calixto, F., Mancini-Filho, J., 2010. Bioactive compounds and antioxidant capacities of 18 non-traditional tropical fruits from Brazil. Food chem. 121, 996-1002.

Saija, A., Tomaino, A., Trombetta, D., Giacchi, M., De Pasqual,e A., Bonina, F., 1998. Influence of different penetration enhancers on *in vitro* skin permeation and in vivo photoprotective effect of flavonoids. Int J Pharm. 175, 85–94.

Salvia-Trujillo, L., Sun, Q., Um, B.H., Park, Y., McClements, D.J., 2015. *In vitro* and in vivo study of fucoxanthin bioavailability from nanoemulsion-based delivery systems: Impact of lipid carrier type. J Funct Foods. 17, 293-304.

Schmid-Wendtner, M.H., Korting, H.C., 2006. The pH of the skin surface and its impact on the barrier function. Skin Pharmacol Physiol. 19, 296-302.

Selim, K., Tsimidou, M., Biliaderis, C., 2000. Kinetic studies of degradation of saffron carotenoids encapsulated in amorphous polymer matrices. Food Chemistry. 7, 199-206.

Shen, J., Burgess, D.J, 2013. In vitro dissolution testing strategies for nanoparticulate drug delivery systems: recent developments and challenges. Drug Deliv. and Transl. Res. 3, 409–415.

Shidhaye, S.S., Vaidya, R., Sutar, S., Patwardhan, A., Kadam, V.J., 2008. Solid lipid nanoparticles and Nanostructured Lipid Carriers innovative Generations of Solid Lipid Carriers. Curr Drug Deliv. 5, 324-331.

Shimoda, H., Tanaka, J., Shan, S.J., Maoka, T., 2010. Anti-pigmentary activity of fucoxanthin and its influence on skin mRNA expression of melanogenic molecules. J Pharm Pharmacol. 62, 1137-1145.

Silva, A.P., Filho, J.C.C., da Costa Júnior, J.S., Peláez, W.J., Faillace, M.S., Ferraz, A.D.B.F., Freitas, R.M., 2015. Toxicological Study Employing Repeated Doses of Garcinielliptone FC, a Polyisoprenylated-Benzophenone Isolated from Seed of Platonia Insignis Mart. J Pharm Pharmacol. 3, 316-330.

Sinha, B., Muller, R.H., Moschwitzer, J.P., 2013. Bottom-up approaches for preparing drug nanocrystals: formulations and factors affecting particle size. Int J Pharm. 453, 126-141.

Souto, E.B., Almeida, A.J., Muller, R.H., 2007. Lipid nanoparticles (LN®, NLC®) for cutaneous drug delivery: structure, protection and skin effects. J Biomed Nanotechnol. 3, 317-331.

Souto, E.B., Wissing, S.A., Barbosa, C.M., Muller, R.H., 2004. Development of a controlled release formulation based on SLN and NLC for topical clotrimazole delivery Int. J. Pharm. 18, 71-77.

Uekane, T.M., Nicolotti, L., Griglione, A., Bizzo, H.R., Rubiolo, P., Bicchi, C., Rezende, C.M., 2017. Studies on the volatile fraction composition of three native Amazonian-Brazilian fruits: Murici (Byrsonima crassifolia L., Malpighiaceae), bacuri (Platonia insignis M., Clusiaceae), and sapodilla (Manilkara sapota L., Sapotaceae). Food Chemistry. 219, 13-22.

Wallace, S.J., Li, J., Nation, R.L,. Boyd, B.J., 2012. Drug release from nanomedicines: selection of appropriate encapsulation and release methodology. Drug Deliv Transl Res. 2, 284–92.

Wissing, S.A., Muller, R.H., 2003. Cosmetic applications for solid lipid nanoparticles. Int J Pharm. 254, 65-68.

7. CAPÍTULO IV - Avaliação toxicológica *in vitro* de nanopartículas lipídicas contendo fucoxantina e seus isômeros

7.1 Introdução

Nos últimos anos, uma gama de produtos farmacêuticos utilizando nanopartículas tem sido desenvolvidos e existe uma constante descoberta de novas aplicações. Adicionalmente, as nanopartículas apresentam propriedades físico-químicas diferentes de outros sistemas, como tamanho reduzido, composição química, cristalinidade, propriedades eletrônicas, reatividade de superfície, solubilidade, forma e agregação. Estas propriedades físico-químicas lhes conferem uma atividade biológica característica que, de certo modo, depende do seu tamanho e método de aplicação (NEL et al., 2006; KROLL et al., 2012).

No entanto, a ampla aplicação das nanopartículas aumentaram a exposição humana e, portanto, o potencial risco relacionado ao seu curto e longo prazo. Neste sentido, centros internacionais de pesquisa e validação como *Organisation for Economic Co-operation and Development* (OECD, 2010) recomendam a utilização de métodos alternativos a animais para avaliação toxicológica.

Atualmente, a maioria dos estudos para as avaliações toxicológicas de nanopartículas disponíveis está baseada em técnicas *in vitro*. Além disso, os dados existentes em experimentos de cultura de células ainda são difíceis de comparar, pois são realizados em linhagens celulares e tipos de células diferentes, com diferentes passagens e, ainda, os métodos utilizados possuem variações (OSTROWSKI et al., 2009; DOKTOROVOVA, SOUTO e SILVA, 2014).

Diante do exposto, o presente capítulo tem como objetivo explorar o efeito da FUCO e do seu isômero em células 3T3 através dos ensaios de citotoxicidade por MTT, (3-(4,5-dimetiltiazol-2-il)-2,5-difenil-2H tetrazolato de bromo), vermelho neutro (NR) e o método de exclusão com azul de Tripan. Concomitantemente, foram avaliadas as espécies reativas de oxigênio (ROS) e nitrogênio (RNS) e o potencial de membrana mitocondrial. Posteriormente, NL-FUCO foram preparadas e a toxicidade foi avaliada.

O trabalho foi desenvolvido em colaboração com o Laboratório de Toxicologia (LATOX) da Faculdade de Farmácia da UFRGS e está disposto na forma de artigo científico, de acordo com as normas da revista à qual foi submetido.

7.2 Artigo científico

In vitro biocompatibility of lipid nanoparticle loaded with fucoxanthin and its isomers

Submetido à publicação no periódico *Toxicology Letters*.

In vitro biocompatibility of lipid nanoparticle loaded with fucoxanthin and its isomers

Leticia Malgarim Cordenonsi[1], Andressa Santer[1], Rafaela Martins Sponchiado[1], Bárbara da Costa[2], Shanda Cattani[2], Marcelo Dutra Arbo[2], Solange Cristina Garcia[2], Renata Platcheck Raffinan[3], Elfrides Eva Scherman Schapoval[1]

[1] Laboratório de Controle de Qualidade Farmacêutico/Faculdade de Farmácia, Universidade Federal do Rio Grande do Sul (UFRGS), Av. Ipiranga 2752, Porto Alegre, Brasil.
[2] Laboratório de Toxicologia (LATOX)/Faculdade de Farmácia, Universidade Federal do Rio Grande do Sul (UFRGS), Av. Ipiranga 2752, Porto Alegre, Brasil.
[3] Laboratório de Nanociências, Centro Universitário Franciscano, Santa Maria, Brasil.

Abstract

The increasing of nanotechnology and their application in several areas requires a detailed understanding of their potential toxicity, because the impacts of nanoscale particles on organisms have not yet been thoroughly clarified. In this study, we investigated the effects of fucoxanthin (FUCO), its isomers, and a novel lipid nanoparticle loaded with FUCO (LN-FUCO) on 3T3 cells to explore the potential use in skin application. Cytotoxicity, production of free radicals and the mitochondrial membrane potential were evaluated. LN-FUCO was prepared by high shear homogenization and the particle size, polydispersity index, and zeta potential were suitable for skin application. LN-FUCO is biocompatible with 3T3 cells up to 80 µg/mL, suggesting its applicability in skin diseases.

Keywords: Tucumã oil; bacuri butter; fucoxanthin, cytotoxicity, lipid nanoparticles, nanotoxicity

1. Introduction

The increasing of nanotechnology and their application in several areas requires a detailed understanding of their potential toxicity. Lipid nanoparticles (LN) have been widely used in nanomedicine, such as in skin formulations (Pardeike et al., 2009) and for cancer treatment (Wang and Thanou, 2010). LN are prepared from a lipid, such as triglycerides, glycerides, fatty acids, and waxes, that preserves the solid state at room temperature, and are stabilized with surfactant on the surface, co-surfactants, and coating materials. Antioxidants, electrolytes, preservatives, viscosity-enhancing agents, and other excipients can also be used (Muller, Maéder and Gohla, 2000; Svilenov and Tzachev, 2014).

The matrix used in LN is frequently a physiological lipid with low acute and chronic toxicity (Muller, Maéder and Gohla, 2000). Due to the presence of surfactants and drugs loaded, the tolerability of the LN must be assessed via toxicity studies. Cell cultures appear as the most promising alternatives to evaluate the toxicity of compounds and the 3T3 murine embryonic fibroblast cell line has been used as model for toxicological studies with LN (Ridolfi et al., 2011; How, Abdullah and Abbasalipourkabir, 2013; Doktorovova, Souto and Silva, 2014).

Fucoxanthin (FUCO) is a marine carotenoid with a unique structure including an allenic bond and a 5,6-monoepoxide (Figure 1). It has also been reported that FUCO has considerable potential and promising applications in human health, because of its anti-cancer activity. In particular, FUCO has been shown to dramatically decrease metastatic potential of melanoma (one of the major malignant cancer) (Miyashita et al., 2011; Kumar, Masashi e Kazuo, 2013). However, like other carotenoids, there are a number of challenges that limit its potential application (Hii et al., 2010; Crupi et al., 2013).

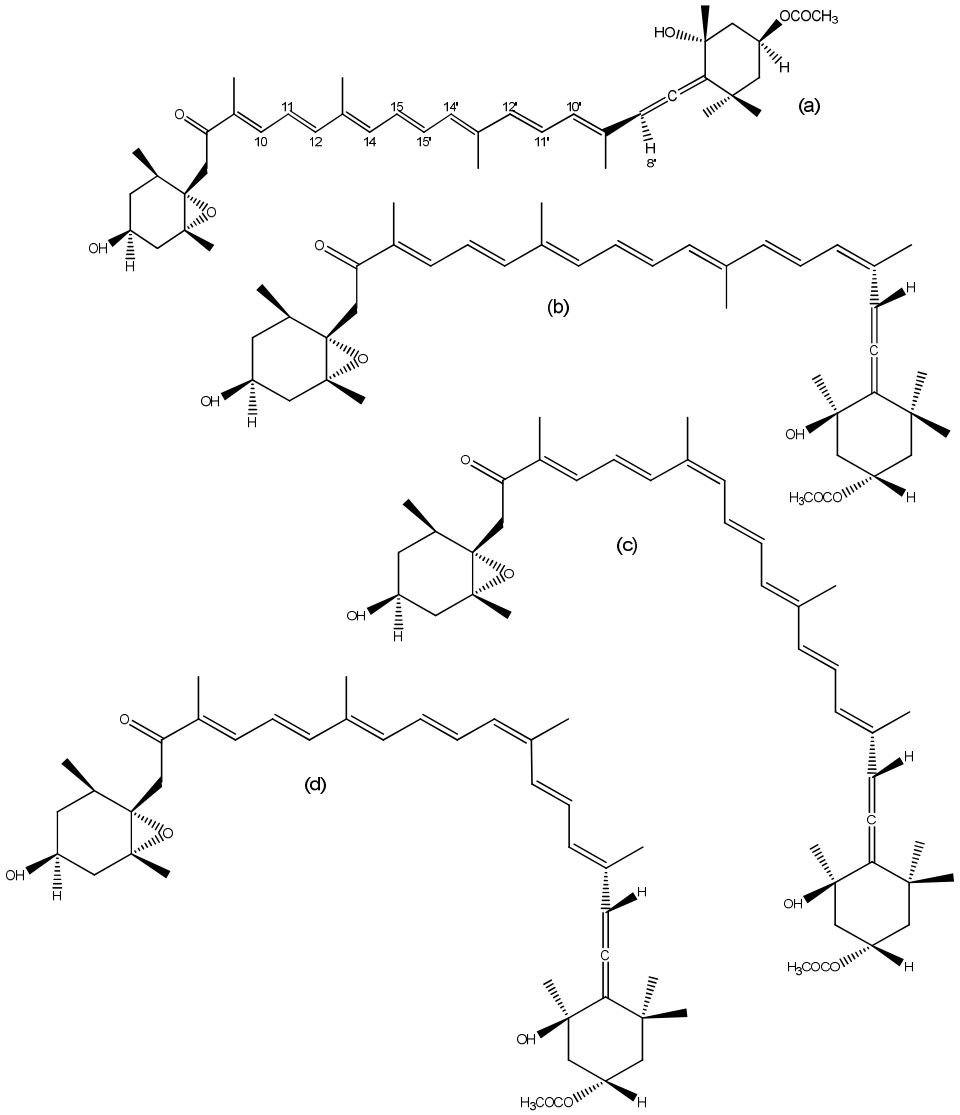


Figure 1. Structure of (a) all-*trans* fucoxanthin, (b) 9'-*cis* fucoxanthin (c) 13-*cis* fucoxanthin, and (d) 13'-*cis* fucoxanthin ($C_{42}H_{58}O_6$).

Here in, we proposed the first combination of the bacuri butter and tucumã oil for preparation of novel LN loaded with FUCO (LN-FUCO) as new skin drug delivery systems. Studies have shown that LN are advantageous in several skin applications, exhibiting an occlusive effect, which improves skin hydration, making them suitable to be applied to a damaged skin (Papakostas et al., 2011; De Louise, 2012). Bacuri butter (*Platonia insignis*) and tucumã oil (*Astrocaryum vulgare*) are Brazilian Amazon lipids. Bacuri butter in fatty acid is mainly composed of palmitic acid and represents a rich source of polyisoprenylatedxanthones and benzophenones, with antioxidant and

wound healing properties (Kumar, Masashi e Kazuo, 2013; Lustosa et al., 2016). Tucumã oil contains high amount of vitamin B2 (riboflavin) and polyphenols, such as catechin and quercetin, which also present antioxidant and wound healing properties (Bora et al., 2001; de Rosso and Mercadante, 2007). These lipids are excipient for LN formation as well as the actives that will perform the efficacy of the skin formulation.

The first aim of our study was to explore the effect of FUCO and its isomers on 3T3 cells using different cytotoxicity assays, measurement of intracellular reactive oxygen and nitrogen species, and assessment of mitochondrial membrane potential. Afterward, LN-FUCO were prepared and the cytotoxicity was evaluated.

2. Materials and Methods

2.1 Materials

Samples of FUCO in powder and oil were assigned a content of 30% and 2%, respectively, were kindly donated by Shaanxi Jiahe Phytochem Co., Ltd. (Xian, China). Bacuri butter and tucumã oil were kindly donated by Amazon Oil Industry. Polysorbate 80 was obtained from Delaware (Porto Alegre, Brazil) and sorbitan monooleate was purchased from Sigma-Aldrich (São Paulo, Brazil). All chemicals used were of pharmaceutical or special analytical grade. Ultrapure water was obtained from a Milli Q® apparatus (Millipore®, USA). The 3T3 cells were obtained from Rio de Janeiro Cell Bank (Rio de Janeiro, Brazil).

2.2 Fucoxanthin preparation

Stock solutions of FUCO in power and oil were made up in 1% dimethyl sulfoxide (DMSO). Working solutions were done by diluting the stock solution in cell culture medium. The concentration of DMSO in cell culture medium was never higher than 0.1%.

2.3 Bacuri butter and tucumã oil preparation

Preliminary tests were carried out in order to determine the ideal amount of samples in the extracts. The final masses used in the extracts from bacuri butter and tucumã oil were 2 g. The procedure used was developed by Larrauri collaborators (1997). Briefly, the samples were weighed in test tubes and 5 mL of 50% methanol

was added for the extraction. The tubes were homogenized and left to rest at room temperature for 60 min. After, they were centrifuged at 15,000 rpm for 15 min, and the supernatant was collected. Subsequently, 5 mL of 50% acetone was added to the residue for extraction for 60 min at room temperature, followed by centrifugation. The methanol and acetone extracts were combined, completed with sterile water. After, stock solutions were made up in 1% DMSO. Working solutions were done by diluting the stock solution in cell culture medium. The concentration of DMSO in cell culture medium was never higher than 0.1%.

2.4 Preparation and characterization of lipid nanoparticle

LN-FUCO were prepared using high shear homogenization. Briefly, the lipid phase was composed of bacuri butter (5%), tucumã oil (4%), FUCO (0.05%) and sorbitan monooleate (2%). The aqueous phase was composed of polysorbate 80 (4%) and sterile water. The lipid phase and aqueous phase were simultaneously heated at 65 °C under constant magnetic stirring, until all components were melted. Then, the aqueous phase was poured over the lipid phase under agitation and with controlled temperature. The suspension was subjected to shaking using an Ultra-turrax® T10 Basic (Ika, Germany) mixer at 24,000 rpm during 20 min and, finally, the novel LN-FUCO were obtained after cooling. LN without FUCO was also prepared.

The particle size and zeta potential were determined by dynamic light scattering using a Zetasizer® Nano ZS, model ZEN 3600 (Malvern Instruments, UK). The measurements were made at 25 °C after appropriate dilution of the samples in Milli Q® water and 10 m*M* sodium chloride solution, respectively. The particle size distribution was given by the polydispersity index. The results reported are the average of three measurements.

2.5 Cell culture

The 3T3 cells were routinely cultured in 75 cm^2 flasks using Dulbecco's Modified Eagle's medium (DMEM) supplemented with 10% heat inactivated fetal bovine serum (FBS), 100 U/mL penicillin and 100 mg/mL streptomycin. Cells were maintained at 37 °C in a humidified 5% CO_2-95% air atmosphere. The cells were fed every 2-3 days, and subcultured once 70-80% confluence was reached.

2.6 Cytotoxicity assay

The cytotoxicity was evaluated through the MTT ((3-(4,5-dimethylthiazol-2-yl)-2,5-diphenyltetrazolium bromide) tetrazolium) reduction, neutral red (NR) uptake, and trypan blue exclusion assays. For MTT e NR assays, cells were seeded at a density of 3,000 cells per well in 96 well plates. For trypan blue exclusion assay, cells were seeded at a density of 30,000 cells per well in 48 well plates. Concentration–response curves were obtained incubating the cells with 10 to 100 µg/mL for 24 h at 37°C. Triton X-100 1% was used as a positive control.

2.6.1 MTT reduction assay

The MTT reduction assay was performed as previously described (Barbosa et al., 2014; Arbo et al., 2016). This assay is one of the most frequently used methods for measuring cell proliferation and cytotoxicity, measuring cellular dehydrogenases activity, an indicator of metabolically active mitochondria, and therefore of cell viability (Barbosa et al., 2014). After the 24 h incubation with the treatments, the cells were incubated at 37°C with fresh medium containing 0.5 mg/mL MTT. After 3 h incubation, the cell culture medium was removed, and the formed formazan crystals were dissolved in DMSO. The absorbance was measured at 550 nm in a multi-well plate reader (SpectraMax M2e, SoftMax® Pro 5, Molecular Devices, Sunnyvale, CA, USA). Results were presented as percentage of cell death related to control conditions. All samples were tested in three independent experiments with each concentration tested in six replicates within each experiment.

2.6.2 Neutral red uptake assay

To confirm the results obtained with the MTT reduction assay, we performed the NR uptake assay. The assay was performed as previously described by Romero and collaborators (2012) and Arbo and collaborators (2016). This assay is based on the ability of viable cells to incorporate and bind the weak cationic dye NR, which penetrates into the cells by non-ionic diffusion, accumulating in lysosomes by interaction with anionic sites in the lysosomal matrix (Labonne et al., 2009). At the end of 24 h incubations with the treatments, the medium was replaced by new medium containing 50 µg/mL NR. The cells were incubated at 37 °C in a humidified, 5%CO_2–95% air atmosphere for 3 h allowing the lysosomes of viable cells to take up

the dye. Thereafter, the cells were carefully washed with 200 µL of phosphate buffer saline (PBS) to eliminate extracellular dye and lysed with a 50% ethanol:1% glacial acid acetic solution (*v/v*). Triton X-100 1% was used as positive control. The absorbance was measured at 540 nm in a multi-well plate reader (SpectraMax M2e, SoftMax® Pro 5, Molecular Devices, Sunnyvale, CA, USA).The percentage of cell death relative to that of the control cells were used as the cytotoxicity measure. All samples were tested in three independent experiments with each concentration tested in six replicates within each experiment.

2.6.3 Trypan blue exclusion assay

The cell mortality was evaluated by trypan blue assay, which determines the number of dead (blue staining) and live (clear cytoplasm) cells (Strober, 2015). After 24 h incubation with the treatments, cells were harvested by trypsinization. Medium with FBS was added to inhibit trypsin activity, the cells were centrifuged at 1,600 rpm for 5 min and the pellet was diluted in 50 µL fresh media. A 10 µL aliquot of cell suspension was diluted in 10 µL trypan blue stain and counted in a Neubauer chamber. Trypsin/EDTA and stained with 0.2% (*w/v*) trypan blue solution. The percentage of viable cells was calculated by dividing the number of live cells by the total number of cells, multiplied by 100. At least three replicates were performed for each concentration, in three independent experiments.

2.7 Measurement of intracellular reactive oxygen and nitrogen species

The intracellular reactive oxygen (ROS) and nitrogen (RNS) species production was monitored by means of the 2',7'–dichlorofluorescindiacetate (DCFH-DA) assay as previously described (Dias da Silva et al., 2013; Arbo et. al., 2014). For this determination, cells were seeded at a density of 3,000 cells per well in 96 well plates and allowed to grow for 24 h. On the day of the experiment, the cells were pre-incubated with 10 m*M* DCFH-DA for 30 min at 37 °C in the dark. The cells were rinsed with PBS and incubated with samples at 10 to 100 µg/mL for 24 h. Fluorescence was recorded on a fluorescence microplate reader (SpectraMax M2e, SoftMax® Pro 5, Molecular Devices, Sunnyvale, CA, USA) set at 485 nm excitation and 530 nm emission. The data obtained were calculated as the percentage of

control conditions for each experiment from at least three independent experiments with each concentration tested in six replicates within each experiment.

2.8 Assessment of mitochondrial membrane potential (Δψm)

Evaluation of mitochondrial integrity was performed by measuring tetramethylrhodamine ethyl ester (TMRE) inclusion as previously described (Dias da Silva et al., 2013; Arbo et al., 2014). After 24 h of incubation at 37 °C, the medium was gently aspirated, and the cells were incubated with samples at 10 to 100 µg/mL. After 24 h, the medium was substituted by fresh medium containing 2 m*M* TMRE for 30 min at 37 °C in the dark. Afterward, the medium was gently aspirated and replaced by PBS. Fluorescence was measured on a fluorescence microplate reader set to 544 nm excitation and 590 nm emission. The data obtained were calculated as the percentage of control conditions for each experiment from at least three independent experiments with each concentration tested in six replicates within each experiment.

2.10 Statistical analysis

Statistical analyses were performed with GraphPad Prism software. Results are presented as mean ± standard error of the mean from at least three independent experiments. Normality of the data distribution was assessed by the Kolmogorov-Smirnov test. Significance was accepted at $p<0.05$. Statistical comparisons between groups were performed by one-way ANOVA followed by Bonferroni post-hoc. Details of the statistical analysis are provided in the text and legend of the figures.

3. Results and discussion

3.1 Fucoxanthin

FUCO is one of the major carotenoids in brown algae chloroplasts and possesses as unique chemical features as biological effects. Previously, we identified and characterized two raw materials of FUCO and, FUCO in oil was identified as all-*trans* FUCO and FUCO in powder was identified as 9'-*cis* FUCO (Cordenonsi et al., 2017). FUCO in oil, when compared with FUCO in powder, showed greater stability. Usually, cis isomers are thermodynamically less stable. In addition, the correct

identification of isomers is a fundamental point, because the biological effects of FUCO is dependent on its isomeric structure (Nakazawa et al., 2009).

To compare the two isomers, cytotoxicity of all-*trans* FUCO and 9'-*cis* FUCO in 3T3 cells were determined by means of MTT and NR uptake assays. As can be seen in Figure 2, the MTT and NR uptake results for all-*trans* FUCO were different. For all-*trans* FUCO, the concentrations of 60, 80, and 100 µg/mL presented a significant decrease of cell viability in MTT test (Figure 2A), however, no cell death was observed in NR uptake assay (Figure 2C). 9'-*cis* FUCO showed similar results for both cell viability tests, with significant loss of cell viability at 100 µg/mL in MTT assay (Figure 2B), and 80 and 100 µg/mL in NR uptake assay (Figure 2D). A previous study in B16-F10 melanoma cells observed that FUCO isolated from *S. japonica* presented a significant decrease in cell viability evaluated by MTT after 24 h incubation with 100 µM (~65 µg/mL) (Chung, 2013), agreeing with our findings.

For the same purpose, however, based on different mechanism, MTT reduction and NR uptake tests are complementary and, this comparative assay may serve as a reliable approach for predictive toxicity screening. Nogueira and collaborators (2011) reported a significant difference in the cytotoxicity of five anionic lysine-based surfactants by MTT reduction and NR uptake assays after 24 h incubations in tumor (HeLa, MCF-7) and non-tumor (3T3, 3T6, HaCaT, NCTC 2544) cell lines. These differences are attributed to differences in the sensitivity of the cell model to these compounds and the characteristics of the two cytotoxicity assays used. The main difference between these two assays is that MTT measures the activity of succinate dehydrogenase, which is present in the mitochondrial inner membrane (Putnam et al., 2002), while NR is based on the storage of the dye in the lysosomes and probably in the Golgi apparatus (Zwolak, 2013).

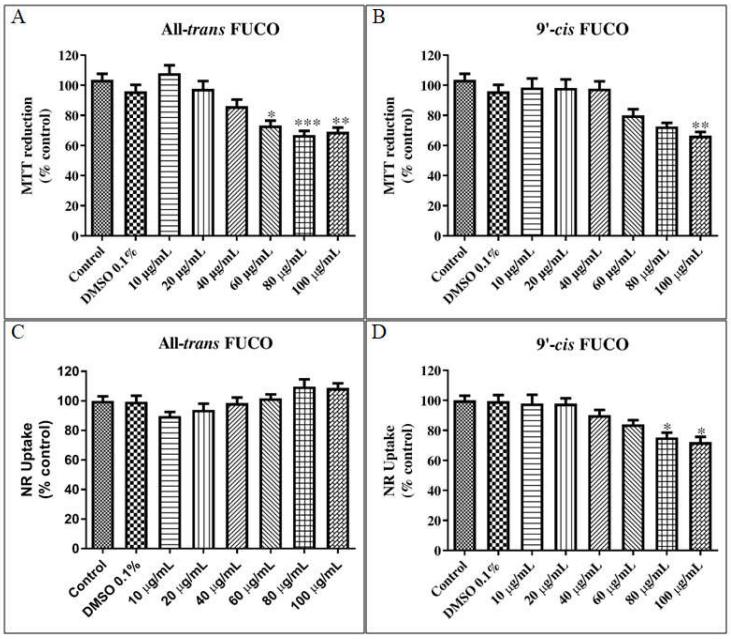


Figure 2. Evaluation of cytotoxicity of all-*trans* and 9'-*cis* FUCO in 3T3 cells lineage, by MTT reduction and NR uptake assays. The cells were incubated with concentrations from 10 to 100 µg/mL, for 24 h. Optical density of untreated cells was taken as 100% of cell viability. Statistical comparisons were made using one-way ANOVA/Bonferroni post-hoc test (*P<0.05; **P<0.01; ***P<0.0001 vs. control).

As shown in Figure 3, for *all*-trans FUCO, cellular measurement of reactive species showed significant increase in ROS and RNS production after the 24 h incubation, whereas for all tested concentrations (Figure 3A). 9'-*cis* FUCO presented a significant increase in reactive species at 80 and 100 µg/mL (Figure 3B). ROS function as second messengers that are necessary for ligand mediated regulation of protein kinase activation, gene expression, and/or proliferative responses (Arnold et al., 2001). Heo and collaborators (2009) isolate FUCO from *S. siliquastrum* and its protective effects against UV-B induced cell damage were evaluated via ROS, MTT, comet assay, and microscopic analysis. FUCO effectively reduced UV-B induced cell damage and apoptotic stimulation, presenting as an effective natural source to make cosmeceutical products. In another study, Kim and collaborators (2010) attributed the antitumor effect of FUCO by the induction of apoptosis through the increase in ROS production, the decrease of Bcl-xL levels, and activation of caspases 3 and 7. Interestingly, at higher concentrations FUCO might play a role of pro-oxidant instead

of antioxidant. This pro-oxidant activity may arise by 5,6-monoepoxide which has been shown to undergo ring opening reactions resulting from attacking nucleophiles (Geacintov et al., 1984). However, the mechanism needs further investigations to be elucidated.

Changes in the Δψm after FUCO exposure were analyzed using TMRE. ΔΨm is critical for maintaining the physiological function of the respiratory chain to generate ATP. TMRE is a lipophilic dye, which can be readily taken up by active mitochondria into the negatively charged mitochondrial matrix. All-*trans* FUCO exhibited a significant increase in Δψm after 24 h incubations of 3T3 cells in all tested concentrations (Figure 3C), unlike, 9'-*cis* FUCO that showed no alterations in Δψm (Figure 3D). In cells, the fluorescence intensity increases when TMRE accumulates in healthy mitochondria. This means that a healthy cell will contain more dye while an apoptotic cell will contain less (Ly, Grubb and Lawen, 2003).

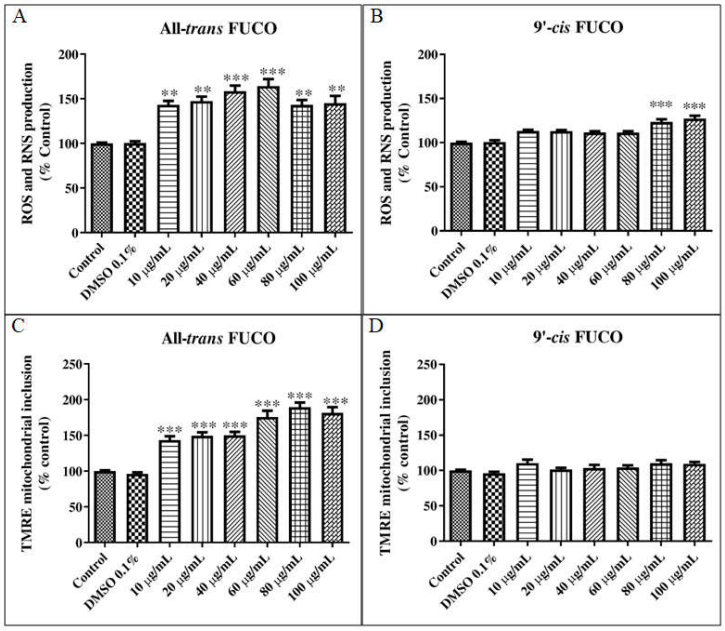


Figure 3. Results of intracellular reactive oxygen (ROS) and nitrogen (RNS) species and mitochondrial membrane potential (Δψm) measured as TMRE incorporation in mitochondria of 3T3 cells treated with all-*trans* and 9'-*cis* FUCO. The cells were incubated with concentrations from 10 to 100 µg/mL, for 24 h. Results are expressed as percentage (%) of control conditions. Statistical comparisons were made using one-way ANOVA/Bonferroni post-hoc test (**P<0.01; ***P<0.0001 vs. control).

3.2 Bacuri butter and tucumã oil

Figure 4 shows the results related to the effect of bacuri butter and tucumã oil on MTT test. It was observed that only the bacuri butter presented a significant decrease in cell viability at concentrations of 60, 80, and 100 µg/mL (Figure 4A). Costa Júnior and collaborators (2013) evaluated the toxicity of the dichloromethane and ethyl acetate fractions from bacuri seed ethanolic extract by MTT in mammalian V79 cells. The results revealed that both fractions do not induce significant cytotoxicity at concentrations up to 100 µg/mL.

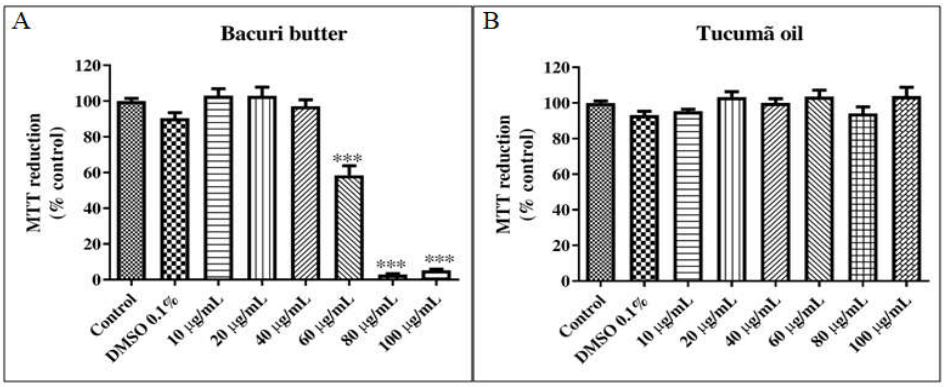


Figure 4. Evaluation of cytotoxicity of bacuri butter and tucumã oil in 3T3 cells lineage, by MTT test. The cells were incubated with concentrations from 10 to 100 µg/mL, for 24 h. Optical density of untreated cells (control) was taken as 100% of cell viability. Statistical comparisons were made using one-way ANOVA/Bonferroni post-hoc test (***P<0.0001 vs. control).

3.3 Lipid nanoparticle

Particle size, pdI, and zeta potential were measured for characterization of LN as shown in Table 1. Particle size showed that LN and LN-FUCO were smaller than 250 nm and the pdI were less than 0.3, which showed that LN had a homogeneous size distribution. As regarding the zeta potential, the LN had a negative surface charge. These results suggested that a good LN-FUCO could be formed by high shear homogenization. The chosen of this method for the preparation of LN-FUCO was because there is no need of organic solvents, minimizing the cytotoxicity.

Table 1. Summary of results from the characteristics of LN and LN-FUCO.

	LN	LN-FUCO
Particle size (nm)*	212.4 ± 0.7	243.0 ± 1.6
Polydispersity index*	0.18 ± 0.01	0.22 ± 0.01
Zeta-potential (mV)*	-24.2±0.2	-44.9 ± 2.3

The size and chemical composition of LN and, other physicochemical properties such as crystallinity, agglomeration, surface positive or negative and porosity have been attributed as critical determinants of toxicity and they are crucial for the activity as a nanocarrier (Grassian et al., 2007; Wang et al., 2008; Pan et al., 2009; Rabolli et al., 2010). This can modify the properties of the NL as well as create the opportunity for increased uptake and interaction with biological tissues (Nel et al., 2006).

Evaluating toxicity demands a testing strategy that includes a characterization of each particle type and, development of a suitable set of *in vitro* assays. Nowadays, standardized *in vitro* techniques to accurately assess toxicity of nanomaterials have not been already established because classical tests might not provide reliable data since nanomaterials can interfere with assay components and readout systems (Monteiro-Riviere et al., 2009). Kroll and collaborators (2012) evaluated four common *in vitro* assays for oxidative stress, cell viability, cell death and inflammatory cytokine production using 24 well characterized engineered nanoparticles. Results varied considerably depending on the assay system used and the authors suggest that each *in vitro* assay have to be evaluated for each single nanoparticle type. Therefore, for LN-FUCO the MTT assay and NR uptake assay were not conclusive due to the interaction of nanomaterials with the readout system (data not shown). Probably the color of FUCO (orange) and other components interfered in the tests.

The cell membrane integrity is a criterion for distinguishing dead from live cells. Then, dyes capable of selectively penetrate the cytoplasm of dead cells have been widely used as vital dyes. The trypan blue assay is based on the fact that living cells can actively exclude the dye, while dead cells accumulate the dye (Strober, 2015). Trypan blue test after 24 h incubation of 3T3 cells with LN-FUCO showed significant cytotoxicity at 80 and 100 µg/mL (Figure 5). Therefore, LN-FUCO

concentrations lower than 80 µg/mL could be considered biocompatible with 3T3 cells.

3T3 cells are murine embryonic fibroblasts and they are the most common *in vitro* model of connective tissue in mammals. This cell line is involved in two OECD *in vitro* toxicity testing guidelines (OECD 129 (2010) and OECD 432 (2004)), and has been used in biocompatibility assays. Furthermore, they are sensitive to the irritating components of pharmaceutical and cosmetic formulations (Dickson et al., 1993; Spielmann et al., 1996; Clothier et al., 1988). It is essential that the components of LN for drug delivery systems exert minimal cytotoxic effect towards cells. In order to minimize cytotoxicity caused, the choice of LN is important because the production is done without organic solvent. Increased cell death may be explained by the use of surfactants in the formulation of LN. Surfactants, as polysorbate 80, were evaluated for their effects on HeLa cells and the cell viability decreased in a concentration-dependent way. Physical properties are the main reason of the cytotoxicity of surfactants in cells, generally they are associated with reduction in surface tension of the cell, leading to cell death (Ernst and Arditti, 1980).

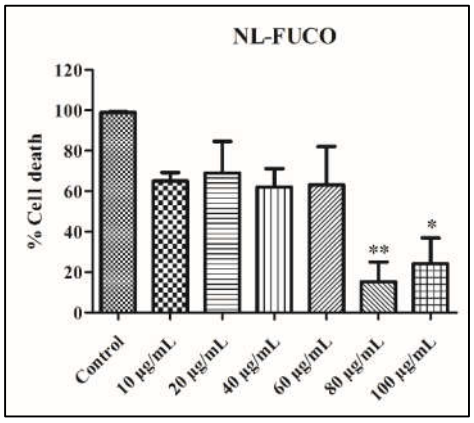


Figure 5. Trypan blue test employed 3T3 cells treated with LN-FUCO. The cells were incubated with concentrations from 10 to 100 µg/mL, for 24 h. Results are expressed as percentage (%) of control conditions. Statistical comparisons were made using one-way ANOVA/Bonferroni post-hoc test (*P<0.05; **P<0.01 vs. control).

For LN and LN-FUCO, cellular measurement of reactive species showed significant increase in ROS and RNS production after the 24 h incubation (Figure 6A

and B). Oxygen is essential for life, when the cells consume oxygen to generate energy, free radicals are created as a consequence of ATP production by the mitochondria. In spite of the deleterious effects of these subproducts, ROS and RNS are necessary for the maturation process of cellular structures and can act in the defense of the organism. Their role in intracellular and extracellular signaling processes has already been established. The mitochondrial ROS generation is regarded as a component of the TNF (tumor necrosis factor)-signal transduction pathway during apoptosis. ROS may also interfere with the expression of genes and influence protein phosphorylation. In some cases, ROS might be regarded as “protective” molecules having a positive impact on inflammation. Another beneficial activity of free radicals is the induction of a mitogenic response (Palmer et al., 1997; Halliwell, 2006; Storz, 2005; Genestra, 2007).

As shown in Figure 6D, LN-FUCO exhibited a significant increase in Δψm after 24 h incubations of 3T3 cells for all concentrations tested. Unlike, LN showed a significant increase in Δψm at 40, 60, 80, and 100 µg/mL (Figure 6C). These results are in agreement with those found in the research comparing all-*trans* and 9'-*cis* FUCO. LN-FUCO induced an increase in Δψm, which hyperpolarizes the mitochondrial membrane and drives ATP synthesis. In cells, oxidative phosphorylation is the main source of ATP under physiological condition, and inhibition of mitochondrial metabolism impaired homeostasis and leads to cell death (Baggaley, Elliottand Bruce, 2008).

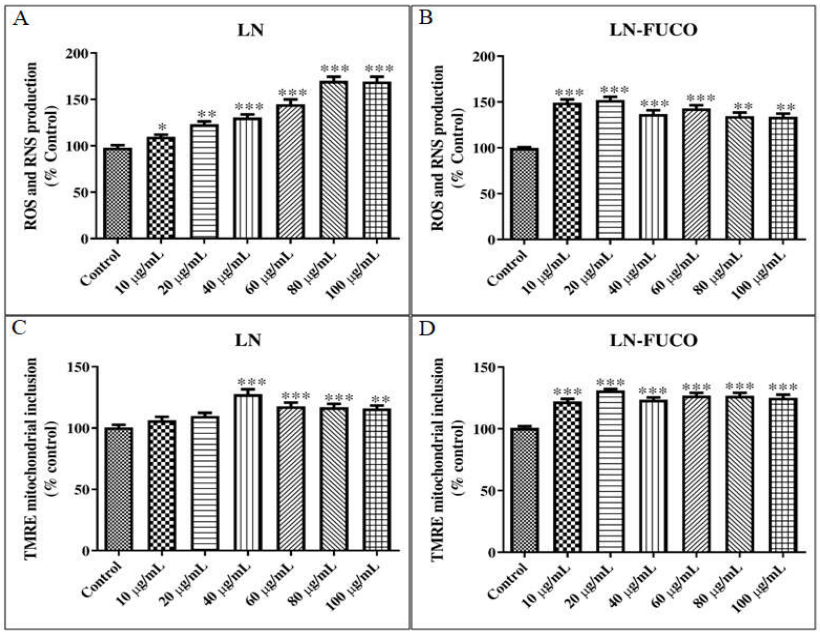


Figure 6. Results of intracellular reactive oxygen (ROS) and nitrogen (RNS) species and mitochondrial membrane potential (Δψm) measured as TMRE incorporation in mitochondria of 3T3 cells treated with LN and LN-FUCO. The cells were incubated with concentrations from 10 to 100 µg/mL, for 24 h. Results are expressed as percentage (%) of control conditions. Statistical comparisons were made using one-way ANOVA/Bonferroni post-hoc test (*P<0.05; **P<0.01; ***P<0.0001 vs. control).

Conclusion

LN-FUCO were prepared by high shear homogenization and the particle size, polydispersity index, and zeta potential are suitable for skin application. Safety studies are a critical part of nanoparticle development and the current study showed that LN-FUCO is biocompatible with 3T3 cells up to 80 µg/mL, suggesting its applicability in skin diseases. However, further studies are required to guarantee the safety of these LN-FUCO, in order to determine the toxic effects.

References

Arbo, M. D., Silva, R., Barbosa, D. J., Silva, D. D., Silva, S. P., Teixeira, J. P., Carmo, H., 2016. *In vitro* neurotoxicity evaluation of piperazine designer drugs in differentiated human neuroblastoma SH-SY5Y cells. J AppToxicol. 36, 121-130.

Arbo, M. D., Silva, R., Barbosa, D. J., da Silva, D. D., Rossato, L.G., de Lourdes Bastos, M., Carmo, H., 2014. Piperazine designer drugs induce toxicity in

cardiomyoblast h9c2 cells through mitochondrial impairment. Toxicologyletters. 229, 178-189.

Arnold, R. S, Shi, J., Murad, E., Whalen, A. M., Sun, C. Q., Polavarapu, R., 2001. Hydrogen peroxide mediates the cell growth and transformation caused by the mitogenic oxidase Nox1. Proc Natl Acad Sci. 98, 5550–5555.

Baggaley, EM., Elliott, A.C., Bruce, J.I., 2008. Oxidant-induced inhibition of the plasma membrane Ca2+-ATPase in pancreatic acinar cells: role of the mitochondria. Am J Physiol Cell Physiol. 295, 1247–1260.

Barbosa, D.J., Capela, J.P., Silva, R., Villas-Boas, V., Ferreira, L.M., Branco, P.S., Fernandes, E., Bastos, M.L., Carvalho, F., 2014. The mixture of "ecstasy" and its metabolites is toxic to human SH-SY5Y differentiated cells at in vivo relevant concentrations. Arch. Toxicol. 88, 455–4739.

Bora, P.S., Narain, N., Rocha, R.V.M., De Oliveira Monteiro, A.C., 2011. De Azevedo Moreira, R. Characterization of the oil and protein fractions of Tucuma (Astrocaryum Vulgare Mart.) fruit pulp and seed kernel. Ciencia y Technologia Alimentaria, v. 3, 111-116.

Chung, T.W., Choi, H.J., Lee, J.Y., Jeong, H.S., Kim, C.H., Joo, M., Ha, K.T., 2013. Marine algal fucoxanthin inhibits the metastatic potential of cancer cells. Biochem Biophys Res Commun. 439, 580-585.

Clothier, R.H., Hulme, L., Ahmed, A.B., Reeves, H.L., Smith, M. and Balls, M., 1988. *In vitro* cytotoxicity of 150 chemicals to 3T3-L1 Cells, assessed by the FRAME Kenacid Blue Method. ATLA. 16, 84-95.

Cordenonsi, L.M., Santer, A., Sponchiado, R.M., Steppe, M., Raffin, R.P., Scherman Schapoval, E.E., 2017. Characterization and Analysis of Fucoxanthin and its Isomers. J PharmSciBioscientific Res. 7, 322-334.

Costa Júnior, J.S., Ferraz, A.B., Sousa, T.O., Silva, R.A., Lima, S.G., Feitosa, C.M., Péres, V.F., 2013. Investigation of biological activities of dichloromethane and ethyl acetate fractions of Platonia insignis Mart. seed. Basic Clin Pharmacol Toxicol. 112, 34-41.

Crupi, P., Toci, A.T., Mangini, S., Wrubl, F., Rodolfi, L., Tredici, M.R.; Antonacci, D., 2013. Determination of fucoxanthin isomers in microalgae (Isochrysis sp.) by high-performance liquid chromatography coupled with diode-array detector multistage mass spectrometry coupled with positive electrospray ionization. Rapid Commun. Mass Spectrom. 27, 1027-1035.

De Rosso, V.V., Mercadante, A.Z., 2007. Identification and quantification of carotenoids, by HPLC-PDA-MS/MS, from Amazonian fruits**.** J Agric Food Chem, 55, 5062-5072.

DeLouise, L.A., 2012. Applications of nanotechnology in dermatology J Invest Dermatol. 132, 964-975.

Dias da Silva, D., Carmo, H., Lynch, A., Silva, E., 2013. An insight into hepatocellular death induced by amphetamines, individually and in combination: the involvement of necrosis and apoptosis. Arch Toxicol. 87, 2165–2185

Dickson, F.M., Lawrence, J.N. and Benford, D.J., 1993. Surfactant-induced cytotoxicity in cultures of human keratinocytes and a commercially available cell line (3T3). Toxicol In Vitro. l7, 381-384.

Doktorovova, S., Souto, E.B., Silva, A.M., 2014. Nanotoxicology applied to solid lipid nanoparticles and nanostructured lipid carriers – A systematic review of *in vitro* data. Eur J Pharm Biopharm. 87, 1–18.

Ernst, R., Arditti, J., 1980. Biological effects of surfactants, VI. Effects of non-ionics and amphoterics on HeLa cells. Toxicology. 15, 233–242.

Geacintov, N. E., Hibshoosh, H., Ibanez, V., Benjamin, M. J., Harvey, R. G., 1984. Mechanisms of reaction of benzo(a)pyrene-7,8-diol-9,10-epoxide with DNA in aqueous solutions. Biop Chem. 20, 121–133.

Genestra, M., 2007. Oxyl radicals, redox-sensitive signalling cascades and antioxidants. Review Cell Signal. 19, 1807-1819.

Grassian, V.H., O'Shaughnessy, P.T., Adamcakova-Dodd, A., Pettibone, J.M., Thorne, P.S., 2007. Inhalation exposure study of titanium dioxide nanoparticles with a primary particle size of 2 to 5 nm. Environ Health Perspect. 115, 397–402.

Halliwell, B., 2006. Phagocyte-derived reactive species: Salvation or suicide? Trends Biochem Sci. 31, 509–515.

Heo, S.J., Jeon, Y.J., 2009. Protective effect of fucoxanthin isolated from Sargassum siliquastrum on UV-B induced cell damage. J PhotochemPhotobiol B. 95, 101-107.

Hii, S.L., Choong, P.Y., Woo, K.K., Wong, C.L., 2010. Stability studies of fucoxanthin from Sargassum binderi. AJBAS*,* 4, 4580–4584.

How, C.W., Abdullah, R., Abbasalipourkabir R., 2013. Characterization and cytotoxicity of nanostructured lipid carriers formulated with olive oil, hydrogenated palm oil and Polysorbate 80, IEEE Trans. Nanobiosci. 12 , 72–78.

Kim KN, Heo SJ, Yoon WJ, Kang SM, Ahn G, Yi TH, et al. Fucoxanthin inhibits the inflammatory response by suppressing the activation of NF-kappaB and MAPKs in lipopolysaccharide-induced RAW 264.7 macrophages. Eur J Pharmacol 2010;649:369–75.

Kroll, A., Pillukat, M.H., Hahn, D., Schnekenburger, J., 2012. Interference of engineered nanoparticles with *in vitro* toxicity assays. Arch Toxicol. 86, 1123–1136.

Kumar, S.R., Masashi, H., Kazuo, M., 2013. Fucoxanthin: A marine carotenoid exerting anti-cancer effects by affecting multiple mechanisms. Marine drugs. 11, 5130–5147.

Labonne, B.E.F., Gutiérrez, M., Gómez-Quiroz, L.E., Fainstein, M.K., Bucio, L., Souza, V., Gutiérrez-Ruíz, M.C., 2009. Acetaldehyde-induced mitochondrial dysfunction sensitizes hepatocytes to oxidative damage. Cell biology and toxicology, 25, 599.

Larrauri, J.A., Rupérez, P., Saura-Calixto, F., 1997. Effect of drying temperature on the stabilitity of polyphenols and antioxidant activity of red grape pomace peels. J. Agric. Food Chem. 45, 1390–1393.

Lustosa, A.K.M., Arcanjo, D.D., Ribeiro, R.G., Rodrigues, K.A.F., Passos, F.F.B., Piauilino, C.A., Carvalho, F.A.A., 2016. Immunomodulatory and toxicological evaluation of the fruit seeds from Platonia insignis, a native species from Brazilian Amazon Rainforest. RevBrasFarmacog. 26, 77-82.

Ly, J.D., Grubb, D.R., Lawen, A., 2003. The mitochondrial membrane potential (deltapsi(m)) in apoptosis; an update. Apoptosis. 8, 115–128.

Miyashita, K., Nishikawa, S., Beppu, F., Tsukui, T., Abe, M., Hosokawa, M., 2011. The allenic carotenoid fucoxanthin, a novel marine nutraceutical from brown seaweeds. J Sci Food Agric.91, 1166-1174.

Monteiro-Riviere, N.A., Inman, A.O., Zhang, L.W., 2009. Limitations and relative utility of screening assays to assess engineered nanoparticle toxicity in a human cell line. ToxicolAppl Pharmacol, 234, 222–235.

Muller, R.H., Maéder, K., Gohla, S., 2000. Solid lipid nanoparticles (SLN) for controlled drug delivery–a review of the state of the art. Eur J Pharm Biopharm, 50, 161-177.

Nakazawa, Y., Sashima, T., Hosokawa, M., Miyashita, K., 2009. Comparative evaluation of growth inhibitory effect of stereoisomers of fucoxanthin in human cancer cell lines. J Funct Foods, 1, 88-97.

Nel, A., Xia, T., Mädler, L., Li, N., 2006. Toxic potential of materials at the nanolevel. Science, 311, 622-627.

Nogueira, D.R., Mitjans, M., Infante, M.R., Vinardell, M.P., 2011. Comparative sensitivity of tumor and non-tumor cell lines as a reliable approach for *in vitro* cytotoxicity screening of lysine-based surfactants with potential pharmaceutical applications. Int. J. Pharm. 1, 51-58.

OECD. No. 129. Guidance Document On Using Cytotoxicity Tests To Estimate Starting Doses For Acute Oral Systemic Toxicity Tests. 2010.

OECD. Test No. 432: *In Vitro* 3T3 NRU Phototoxicity Test 2004.

Palmer, H.J., Paulson, K.E., 1997. Reactive oxygen species and antioxidants in signal transduction andgene expression. Nutr Rev. 55, 353–361.

Pan, Z., Lee, W., Slutsky, L., Clark, R.A., Pernodet, N., Rafailovich, M.H., 2009. Adverse effects of titanium dioxide nanoparticles on human dermal fibroblasts and how to protect cells. Small. 5, 511– 520.

Papakostas, D., Rancan, F., Sterry W., 2011. Nanoparticles in dermatology Arch Dermatol Res. 303, 533-550.

Pardeike, J., Hommoss, A., Müller, R.H., 2009. Lipid nanoparticles (SLN, NLC) in cosmetic and pharmaceutical dermal products. Int J Pharm. 366, 170–84.

Putnam, K.P., Bombick, D.W., Doolittle, D.J., 2002. Evaluation of eight *in vitro* assays for assessing the cytotoxicity of cigarette smoke condensate. Toxicol in Vitro 16, 599–607.

Rabolli, V., Thomassen, L.C., Princen, C., Napierska, D., Gonzalez, L., Kirsch-Volders, M., Hoet, P.H., Huaux, F., Kirschhock, C.E., Martens, J.A., Lison, D., 2010. Influence of size, surface area and microporosity on the *in vitro* cytotoxic activity of amorphous silica nanoparticles in different cell types. Nanotoxicology, 4, 307–318.

Ridolfi, D.M., Marcato, P.D., Machado, D., Silva, R.A., Justo, G.Z., Duran N., 2011. *In vitro* cytotoxicity assays of solid lipid nanoparticles in epithelial and dermal cells. J PhysConf Ser. 304, 012-032.

Romero, A., Ramos, E., Castellano, V., Martínez, M.A., Ares, I., Martínez, M., Martínez-Larrañaga, M.R., Anadón, A., 2012. Cytotoxicity induced by deltamethrin and its metabolites in SH-SY5Y cells can be differentially prevented by selected antioxidants. ToxicolIn Vitro. 26, 823–830.

Spielmann, H., Liebsch, M., Kalweit, S., Moldenhauer, F., Wirnsberg, T., Holzhuntter, H.G., Schnider, B., Glaser, S., Gemer, I., Pape, W.J.W., Kreiling, R., Krauser, K., Spengler, J., Bertramneis, E., Siegmund, B. and Wiebel, F.J., 1996. Results of a validation study in Germany on two *in vitro* alternatives to the Draize eye irritation test, the HET-CAM test and the 3T3 NRU cytotoxicity test. ATLA. 24, 741-858.

Storz, P., 2005. Reactive oxygen species in tumor progression. Front. Biosci. 10, 1881–1896.

Strober, W., 2015. Trypan blue exclusion test of cell viability. Curr. Protoc. Immunol. 111, A3- B3.

Svilenov, H., Tzachev, C., 2014. Solid Lipid Nanoparticles–A Promising Drug Delivery System. In: Nanomedicine. One Central Press Manchester. 2014, 187-237.

Wang, J., Chen, C., Liu, Y., Jiao, F., Li, W., Lao, F., Li, Y., Li, B., Ge, C., Zhou, G., Gao, Y., Zhao, Y., Chai, Z., 2008. Potential neurological lesion after nasal instillation

of TiO(2) nanoparticles in the anatase and rutile crystal phases. Toxicol Lett, 183, 72–80.

Wang, M., Thanou, M., 2010. Targeting nanoparticles to cancer. Pharmacol Res. 62, 90–9.

Zwolak, I., 2013. Comparison of five different *in vitro* assays for assessment of sodium metavanadate cytotoxicity in Chinese hamster ovary cells (CHO-KI line). Toxicol. Ind. 1, 1–14.

8. CAPÍTULO V – O papel da quitosana como revestimento de nanopartículas lipídicas na liberação de fucoxantina na pele

8.1 Introdução

Os polímeros mucoadesivos são macromoléculas naturais ou sintéticas que são capazes de se aderirem às mucosas biológicas. Atualmente é uma estratégia para prolongar o tempo de permanência do fármaco no local de absorção e também é uma forma de direcionar especificamente o fármaco para diversas membranas (GRABOVAC, GUGGI e BERNKOP-SCHNÜRCH, 2005).

Os polímeros mais utilizados são os poliacrilatos e derivados, como a quitosana e derivados, o alginato de sódio e os derivados da celulose. A quitosana é o único polímero pseudonatural catiônico que apresenta propriedades como biocompatibilidade, biodegrabilidade, mucoadesividade e capacidade de regeneração dérmica ordenada durante a reconstrução da pele, regulando a deposição e disposição mais rápida de fibras de colágeno. Além disso, a quitosana tem efeito sobre a ativação de fibroblastos, apoiando a regeneração da matriz extracelular, facilitando a migração celular e estimulando a formação de tecido de granulação (RINAUDO, 2006; NAGPAL, SINGH e MISHRA, 2010; FRANCESKO e TZANOV, 2011).

Desta forma, uma estratégia é o revestimento de NL com quitosana para aumentar a absorção de fármacos nas mucosas. O revestimento ocorre através da solubilização da quitosana em uma solução de pH controlado, tornando o polímero ativo. De seguida, e fazendo com que este se concentre na superfície das NL. A associação de NL com quitosana tem como objetivo melhorar as propriedades biofarmacêuticas, mucoadesão e penetração de substância ativa em diversos epitélios (ROSSI et al., 2007; CARAMELLA et al., 2010; SANDRI et al., 2017). Sandri e colaboradores (2011) relatam que a quitosana aumenta a proliferação celular e a cicatrização de feridas.

Deste modo, o presente capítulo tem como objetivo unir as vantagens das NL-FUCO com as propriedades biológicas da quitosana para aumentar o tempo de contato com a pele. As características físico-químicas das NL-FUCO com quitosana foram avaliadas. Além disso, foi utilizado um método simples com membrana de casca de ovo como modelo substituto, para o estudo de bioadesão *in vitro*. O estudo de biocompatibilidade *in vitro* foi realizado utilizando fibroblastos dérmicos humanos.

O trabalho foi desenvolvido na *Università Degli Studi di Pavia* (Pavia/Itália) e está disposto na forma de artigo científico, de acordo com as normas da revista na qual foi aceito.

8.2 Artigo científico

The role of chitosan as lipid nanoparticle coating in skin delivery of fucoxanthin

Aceito para publicação no periódico *International Journal of Pharmaceutics*.

The role of chitosan as lipid nanoparticles coating in skin delivery of fucoxanthin

Leticia Malgarim Cordenonsi[a], Angela Faccendini[b], Maria Cristina Bonferoni[b], Silvia Rossi[b], Lorenzo Malavasi[b], Renata Platcheck Raffin[c], Elfrides Eva Scherman Schapoval[a], Giuseppina Sandri[b], Franca Ferrari[b]

[a] Programa de Pós-Graduação em Ciências Farmacêuticas, Faculdade de Farmácia, Universidade Federal do Rio Grande do Sul, 90610-000 Porto Alegre - RS, Brasil.
[b] Università degli Studi di Pavia, Dipartimento di Scienze del Farmaco, 27100, Pavia – Itália.
[c] Programa de Pós-Graduação em Nanociências, Centro Universitário Franciscano, 97010-032 Santa Maria – RS, Brasil.

Abstract

Fucoxanthin (FUCO) is a marine carotenoid characterized by antiproliferative properties against diseased cells. The aim of the present paper was to design and develop lipid nanoparticles (LN) based on bacuri butter and tucumã oil and loaded with FUCO, intended for skin application to prevent skin hyperproliferative diseases. The presence of FUCO should control skin diseased cells hyperproliferation and the lipids, rich in antioxidants and characterized by wound healing properties, should favor the restoring of skin integrity. LN were coated with chitosan (CS) to improve their biopharmaceutical properties (bio/mucoadhesion and wound healing) and to combine the advantages of LN with the biological properties of CS. The LN were prepared by means of high shear homogenization. The systems were characterized by means of particle size, zeta-potential, microscopic structure, FUCO loading, bioadhesion, and *in vitro* biocompatibility. The systems were characterized by dimensions ranging from about 253 to 416 nm and CS coating and FUCO loading determined an increase of LN size confirmed by TEM. Moreover, TEM and zeta-potential analysis confirmed the presence of CS coating on LN surface and evidenced difference in particle structure attributable to drug loading which could rearrange the lipid structure of nanoparticle core. Moreover, the presence of CS coating conferred to LN good bioadhesion. Fibroblast proliferation study evidenced

that FUCO loaded LN maintained proliferation properties of CS and lipid systems towards normal fibroblasts. Also, CLSM analysis evidenced LN internalization into fibroblasts. Considering the overall results topic application of CS coated and FUCO loaded LN seems a promising approach to preserve skin integrity.

Keywords: fucoxanthin, natural lipids, lipid nanoparticle, chitosan, skin, hyperproliferative diseases

1. Introduction

Fucoxanthin (FUCO) is a marine carotenoid found in numerous classes of microalgae (such as bacillariophytes, bolidophytes, chrysophytes, silicoflagellates, and pinguiophytes) and present in edible brown seaweeds (macroalgae such as phaeophytes). It is known that certain long-lived populations have a regular consumption of brown algae (major source of FUCO) and this seems related to carotenoids role in prevention and treatment of cell hyperproliferation typical of cancer. In particular, FUCO is a bioactive compound, which has several proven biological properties, including anticancer, antioxidant, anti-inflammatory, antimicrobial, and anti-angiogenic properties (Miyashita et al., 2011; Kumar, Masashi and Kazuo, 2013).

FUCO activity as cancer preventive and antiproliferative is mainly related to the activation of caspase pathway. Moreover FUCO presents a down-regulation of Bcl-2 proteins with a pro-apoptotic effect, it is able to interfere with MAPK and GADD45 proteins that regulate mitosis and cell proliferation, down-regulates DNA binding activities of NF-kB and pIkB, and upregulates IkB it is able to reduce expression of N-Myc oncogene and survivin with anti-angiogenic activity (Hosokawa et al., 2004; Liu et al., 2009; Chung et al., 2013; Martin, 2015).

According to previous researches, FUCO has been proved to be effective against many different kinds of cancer cell lines (liver cancer, bladder cancer, prostate cancer, breast cancer, leukemia, cervical cancer, osteosarcoma cancer and skin cancer) (Kumar, Masashi and Kazuo, 2013; Martin, 2015). In particular, considering skin, FUCO has been shown to dramatically decrease metastatic potential of melanoma (one of the major malignant cancer). It was evidenced that FUCO is able to inhibit the expression and secretion of matrix metalloproteinase-9 (MMP-9) linked to tumor migration and invasion and cancer cell capability of endothelial adhesion. Moreover, FUCO inhibits skin pigmentation with an anti tyrosinase activity also in melanoma, decreasing melanogenesis. This suggested also the possible use as anti-pigmentary ingredient in cosmetics. Moreover, no effect has been proved in normal cells (Moghadamtousi et al., 2014).

Lipids are key factors in stratum corneum layer and horny cells (dead keratinocytes) which are fundamental in maintain skin moisture and integrity. Lipid nanoparticle (LN) have been extensively studied starting from 90s, as carriers in skin

delivery and natural lipids have been considered as enabling excipients thanks to their unstoppable fractions rich in eutrophic factors such as vitamins and antioxidants (Mandawgade and Patravale, 2008; Hajj Ali et al., 2015).

Bacuri butter (*Platonia insignis* Mart., Clusiaceae) and tucumã oil (*Astrocaryum vulgare*, Arecaceae) are lipids from Amazonian region. Bacuri butter is rich of fatty acid that is mainly composed of 50-55% palmitic acid (C16:1), 10-20% oleic acid (C18:1). It has a high amount of unsaturated fatty acid and the ratio saturated / unsaturated is 3:1. The unsoapable fraction is up to 5% and represents a rich source of polyisoprenylated xanthones and benzophenones, which are responsible for biological activities and in particular antioxidant and wound healing properties (Kumar et al., 2013; Lustosa et al., 2016). Tucumã oil is composed of 30% palmitic acid (C16:0), 65% oleic acid (C18:1), 3.5% linoleic acid (C18:2) and 5% linolenic acid (C18:3). The ratio of saturated / unsaturated is 1:3. The unsoapable fraction is up to 1.5-2% and the oil contains high amount of vitamin B2 (riboflavin) and bioactive compounds. In particular, it is rich of polyphenols such as catechin and quercetin with antioxidant and wound healing properties (Bora et al., 2001; de Rosso and Mercadante, 2007).

LN were coated with chitosan (CS) to improve their biopharmaceutical properties. CS is an in vivo degradable and biocompatible cationic polysaccharide based on glucosamine and N-acetylglucosamine and it is obtained by partial deacetylation of chitin (Duan et al., 2010; Sailaja et al., 2010; Zhang and Kawakami, 2010). CS possesses crucial properties fundamental in skin diseases: it is able to enhance coagulation, by both hemagglutination and promoting platelet activation, it prolongs its retention to targeted substrates by means of bio/mucoadhesion, it is able to supports extracellular matrix regeneration by promoting physiologically ordered dermal regeneration during skin reconstruction and wound healing in the early phases of healing (Sandri et al., 2011; Jayakumar et al., 2010; Manivasagan et al., 2017). Moreover, it is able to enhance remodeling process increasing also angiogenesis.

LN loaded with FUCO and associated CS should combine the advantages of LN with the biological properties of CS in particular should enhance the residence time in the application area, via bioadhesive interaction. This should allow an intimate contact between skin lesions and carriers to allow system penetration into the skin

layers and promote FUCO activities in the hyperproliferative skin layers. The LN were prepared by means of high shear homogenization. The systems were characterized by means of particle size, zeta-potential, microscopic structure, FUCO loading, bioadhesion, and *in vitro* biocompatibility.

2. Materials and methods

2.1 Materials

A reference standard of FUCO (C42H58O6) with purity of >95%, was supplied by Cayman Chemical Company® (Ann Arbor, MI, USA). FUCO (2%) was kindly donated by Shaanxi Jiahe Phytochem Co., Ltd. (Xian, China). Bacuri butter and tucumã oil were kindly donated by Amazon Oil Industry. Chitosan (CS) (MW: 250000 Da, deacetylation degree 98%, Chitoclear®, Giusto Faravelli, Italy), polysorbate 80, sorbitan monooleate, nile red (NR) were purchased from Sigma-Aldrich®. All chemicals used were of pharmaceutical or special analytical grade. Ultrapure water was obtained from a Milli Q® apparatus (Millipore®, USA).

2.2 Preparation of lipid nanoparticles

LN were prepared by means of high shear homogenization. The lipid phase was composed of bacuri butter (5% *w/w*), tucumã oil (4% *w/w*), FUCO (0.05% *w/w*) and sorbitan monooleate (2% *w/w*), and was melted at 65 °C. The aqueous phase was based on polysorbate 80 (4% *w/w*) solution and heated to 65 °C. The aqueous phase was poured into the lipid phase under homogenization at 25,000 rpm for 20 min with UltraTurrax (T25, IKA-Werke GmbH Germany).

CS associated LN (LN-FUCO-CS), were prepared using the same procedure by adding 1% *w/w* CS in the aqueous solution. Both the systems (with and without CS) were prepared also as blanks without drug (LN-CS and LN) with the same components.

NR (0.25% *w/w*) was added in all the preparations in the lipid phases as hydrophobic fluorescent marker, to visualize the localization of the LN.

2.3 Chemico-physical lipid nanoparticles characterization

2.3.1 Particle size, zeta-potential, and microscopy

The mean particle size and the polydispersion index were determined at 25 °C by a photon correlation spectroscopy apparatus (N5 Beckman Coulter, Instrumentation Laboratory, Milan, Italy). Each sample was diluted with ultrapure water to obtain concentrations according to the operating procedure of the instrument. The zeta-potential were determined by electrophoretic mobility (Zetasizer®, ZEN 3600, Malvern Instruments) after 500 folds (*v/v*) sample dilution with 10 mM sodium chloride solution, at 25 °C.

The system examination of the samples was performed using a transmission electron microscopy (TEM) (Jeol JEM-1200 EX II, JP) equipped with TEM CCD camera Mega View III (Jeol, JP) (Mehnert e Mader, 2001). The samples were placed on copper grids with 2% of phosphotungstic acid (PTA) at pH 7.0 for TEM analysis.

2.3.2 Entrapment efficiency and drug loading

The drug loading in the different formulations was determined by HPLC method (as described in the paragraph “HPLC analysis”). The entrapment efficiency (EE%) was determined by ultrafiltration–centrifugation technique (Ultrafree-MC 10.000 MW, Merck, Millipore®) at 8,000 rpm for 10 min. FUCO EE% was calculated as percent ratio between the difference between the total concentration of FUCO in the formulation and the FUCO concentration in the aqueous phase after centrifugation and the total concentration. Drug loading was determined as the % ratio between the drug amount present in the LN (determined by EE%) and the total amount of nanoparticle weight.

2.4 High performance liquid chromatography (HPLC) analysis

HPLC was used to determine FUCO. A stability indicating method has been developed (Cordenonsi et al., 2017). The chromatographic analysis was performed on a HPLC Agilent® model 1200 system (Santa Clara, USA), using an Agilent® Eclipse Plus apparatus equipped with C18 analytical column (4.6 mm x 150 mm, 5 µm) as stationary phase and a mobile phase composed of acetonitrile and water, adjusted to pH 7.0 with sodium hydroxide 0.1 *M* (9.5:0.5 *v/v*) in isocratic mode with a flow rate of 1.0 ml/min. The injection volume was 50 µl. The column was

thermostated at 40 ºC. FUCO peak area was determined at 450 nm as reference wavelength. The method was linear in the range from 1 µg/ml to 40 µg/ml with R^2 of 0.9994. All analyses were performed under dark conditions. FUCO was extracted using acetonitrile, quantified and FUCO concentration in the LN-FUCO and LN-FUCO-CS was calculated.

2.5 Biopharmaceutical lipid nanoparticles characterizations

2.5.1 Bioadhesion measurements

Bioadhesion measurements were performed using a TA.XT plus texture analyzer (Stable Microsystem, Enco, Spinea, I) equipped with a 1 kg load cell, a cylinder probe having a diameter of 10 mm (P10) and the measuring system A/MUC (mucoadhesion test system) (Szucs et al., 2008; Sandri et al., 2012; Sandri et al., 2013). The measuring system A/MUC consists of a ring in which a biological support can be fixed. In this case, the biological support was eggshell membrane (Tao et al., 2009), chosen to mimic damaged skin. The eggshell membrane was wetted with 100 µl of isotonic saline (NaCl 0.9% *w/v*). 100 µl of each sample (n=6) were placed on filter paper disc having diameter of 10 mm, and were stuck with cyanoacrylate glue to the cylinder probe. The sample and the biological substrate were put in contact under a preload of 600 mN for 1 min. The cylinder probe was then moved upward at a prefixed speed of 2.50 mm/s up to the complete separation of the bioadhesive interface (eggshell membrane-sample). The force of detachment was recorded as a function of displacement and the parameter Work of adhesion (mN mm) (AUC) was calculated as area under the force versus displacement curve. Blank measurements were performed by using a filter paper disc wetted with 100 µl of isotonic saline solution (NaCl 0.9% *w/v*).

2.5.2 *In vitro* proliferation test

NHDF from juvenile foreskin (PromoCell GmbH, VWR, Milan, Italy) were grown in a polystyrene flask (Corning, Sigma–Aldrich, Italy) containing 13–15 ml of complete culture medium, consisting of Dulbecco's Modified Eagles Medium (DMEM, Sigma–Aldrich, Milan, Italy) supplemented with 1% (*v/v*) antibiotic-antimycotic solution (100x; stabilized with 10,000 units penicillin, 10.0 mg streptomycin and 25 µg amphotericin B, Sigma- Aldrich, Italy), and 10% (*v/v*) inactivated fetal bovine serum

(VWR, Milan, Italy). Cell cultures were kept at 37°C in 95% air and 5% CO_2 atmosphere. All the operations required for cell culture were carried out in a vertical laminar airflow hood (Ergosafe Space 2, VWR, Milan, Italy). Cell growth and morphology were evaluated by means of an optical inverse microscope (VWR, Milan, Italy). For biocompatibility test, fibroblasts (7^{th} passage) were seeded in 96-well plates (area 0.34 cm^2) at a density of 10^5 cells/cm^2 per well. After 24 h, to allow cell adhesion to well bottom, 100 µl of each LN suspension (dilution volume ratio from 1:1 to 1:8 in growth medium) were put in contact with the cell substrates at 37 °C in 95% air and 5% CO_2 atmosphere. As control, the cells were grown in standard condition (growth medium without samples). After 4 and 24 h of contact time MTT assay was performed: it is basically based on the evaluation of mitochondrial dehydrogenases activity of vital cells, which convert MTT to formazan.

Cell substrates were washed with 100 µl PBS and, then, 50 µl of MTT (3-(4,5-dimethylthiazol-2-yl)-2,5-diphenyltetrazolium bromide, Sigma-Aldrich, Milan, Italy) at the concentration of 2.5 mg/ml in DMEM without phenol red (Sigma-Aldrich, Milan, Italy) were added to each well and incubated for 3 h. Finally, 100 µl of dimethyl sulfoxide (DMSO, Sigma-Aldrich, Milan, Italy), used as solubilization agent, was added to each well, in order to promote the complete dissolution of formazan crystals, obtained from MTT dye reduction by mitochondrial dehydrogenases of alive cells. The absorbance of resulting solution was measured by means of an iMark® Microplate reader (Bio-Rad Laboratories, Milan, Italy) at a wavelength of 570 nm and 690 nm (reference wavelength) after 60 seconds of mild shaking. Viability was expressed as optical density (OD) and the performance of LN was compared to standard growth conditions (GM, growth medium).

2.5.3 Fibroblast uptake

Fibroblasts (8^{th} passage) were seeded in Culture-Inserts (Ibidi® Cell, Giardini, Milan, Italy) with growth area for well of 0.22 cm^2 at the same seeding density as for biocompatibility test. The Culture-Inserts were fixed on µ-Dish (diameter of 35 mm), consisting of a plastic with highest optical quality (Ibidi® Cell). After 24 h fibroblasts were then put in contact with NR labelled LN suspension at 1:8 volume ratio for 24 h.

Then, the cells grown were fixed using a 3% (w/v) glutaraldehyde solution in PBS (Sigma-Aldrich®) for 1 h at 5 °C. The substrates were than washed three times

with PBS. Cellular cytoskeleton was stained by incubating with 2.5% of phalloidin-FITC Atto 488 solution in PBS (Sigma-Aldrich, Milan, Italy) for 40 min, in the dark. Then each substrate was washed twice in PBS and cell nuclei were stained using Hoechst 33258 (Sigma-Aldrich) at 1:10,000 in PBS for 15 min in the dark.

LN taken up by fibroblast cell were observed using Confocal laser scanning microscopy (CLSM) (Leica TCS SP2, Leica Microsystems, Italy) with λex=480 nm and λem=570 nm for phalloidin-FITC Atto 488, λem=628 nm for the visualization of NR and λex=340 nm and λem =460 nm for the visualization of Hoechst 33258. The acquired images were processed with software associated with the microscope (Leica Microsystem, Italy).

2.6 Statistical analysis

Statistical analysis was performed using ANOVA one-way analysis of variance and Tukey's post-hoc comparison. Differences were considered significant at $p<0.05$.

3. Results and discussion

3.1 Chemico-physical lipid nanoparticles characterization

LN were successfully prepared using high shear homogenization method and the procedure was suitable to prepare CS associated nanocarriers using bacuri butter and tucumã oil as natural lipids. Previous studies (Sandri et al., 2010; Sandri et al, 2017) evidenced that the protocol used allowed to obtain a stronger CS coupling at LN surface with respect to coating by mixing. Table 1 reports the physicochemical properties of LN: blank LN (LN), FUCO loaded LN (LN-FUCO) and blank and FUCO loaded LN coated by CS (LN-CS and LN-FUCO-CS, respectively). Particle size, polydispersion index, zeta-potential, drug loading and EE% have been evaluated.

Table 1: Physicochemical properties of LN: blank LN (LN), FUCO loaded LN (LN-FUCO) and blank and FUCO loaded LN coated by CS (LN-CS and LN-FUCO-CS, respectively).

	LN	**LN-CS**	**LN-FUCO**	**LN-FUCO-CS**
Particle size (nm)	253.7± 5.6	301.5± 4.9*	297.1± 7.1	416.3± 4.2*
Polydispersion index	0.214± 0.08	0.346± 0.04	0.259± 0.09	0.314± 0.09
Zeta-potential (mV)	-25.87± 2.47	9.45± 1.58*	-44.97± 3.19	23.33± 1.36*
Drug loading	-	-	103.65 ± 0.66	101.34 ± 0.98
Entrapment efficiency	-	-	98.90 ± 0.32	95.13 ± 0.76

LN were characterized by a particle size close to 253 nm: the CS coating (LN-CS) significantly increased their size of about 19%. This behavior was evident also in the FUCO loaded systems: CS caused a significant increase in particle size of about 40% from 297 nm (LN-FUCO) to 416 nm (LN-FUCO-CS). The drug loading determined an increase in particle size independently of CS coating and this could be due to a disorder in the lipid core higher than that of unloaded systems: the presence of liquid lipids in the nanoparticle core conferred to the nanoparticles an extremely disordered structure and this allowed the host of drug molecules into the lipid phase preventing drug expulsion. This behavior was previously reported also by Viera et al. (2018). Moreover, a further increase in particles size due to CS coating is conceivable due to the interaction of lipids and surfactants, present in the nanoparticle core, and CS coating that could cause a different rearrangement of lipid matrix.

The polydispersion index was around 0.2 and 0.3 for all systems (no significant difference) suggesting a narrow particle size distribution (Luo and Wang, 2014).

Unloaded and loaded nanoparticles, LN and LN-FUCO, were characterized by negative zeta-potentials of −25.87 mV and –44.97 mV, respectively. In both the systems, potential values remained highly negative: however, the drug loading caused a dramatic decrease confirming the influence of FUCO on the rearrangement of lipid core, and consequently of surfactants. Furthermore, CS coating caused a reversal of zeta-potential changing surface charge from negative to positive and, in particular, LN-CS and LN-FUCO-CS were characterized by 9.45 mV and 23.33 mV,

respectively. This confirmed CS coating. Moreover, drug loading influenced the surface properties and the loaded systems showed a higher zeta-potential demonstrating also in this case the rearrangement of nanoparticle structure due to drug loading. Generally, the highly negative or positive zeta-potentials characterizing all the systems suggested a systems stability due to electrostatic repulsion. Drug loading and EE% were close to 100% in all cases and no statistically significant difference was obtained: this could be due to the high FUCO lipophilicity. Although CS coating probably changed core structure, this did not interfere with FUCO affinity for the lipid matrix.

Figure 1 reports TEM images of all the systems. The TEM images confirm in all cases the colloidal sizes of LN. All the LN showed spherical borders. As for uncoated systems (Figure 1a LN and 1b LN-FUCO), the borders appeared as a dark continuous line whereas the drug loading seemed to determine more electrodense borders conceivably due to different core structure. CS coating (Figure 1c LN-CS and 1b LN-FUCO-CS) completely change particle borders which appeared less uniform and characterized by an electrodense material aggregation onto particle surface: this was related to nanoparticle staining with PTA (negative staining) which is able to preferably interact with acidic mucopolysaccharide as CS is. This confirmed the CS localization onto the LN surface and moreover a different CS distribution onto LN surface related to composition: drug loading could determine a thicker CS layer supporting increase in particle size and in zeta-potential

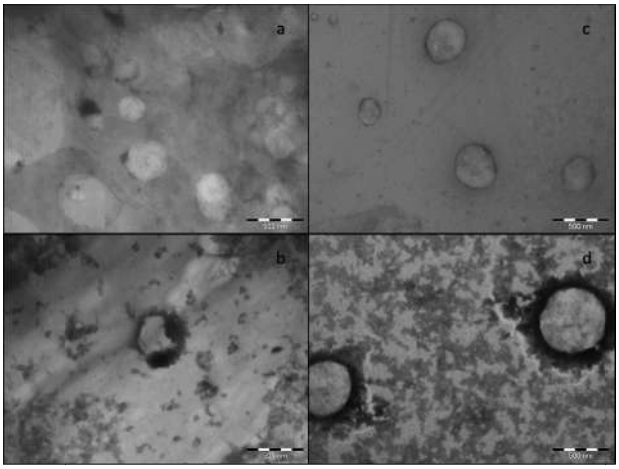


Figure 1: TEM images of all the systems: a) LN; b) LN-FUCO: c) LN-CS; d) LN-FUCO-CS.

3.2 Biopharmaceutical lipid nanoparticles properties

3.2.1 Bioadhesion properties

Figure 2 shows the results of bioadhesion properties of LN. Unloaded and FUCO loaded LN were considered and the performance of CS coated LN was compared to that of uncoated systems and to saline solution (NaCl 0.9% *w/v*). CS coating determined a significantly higher bioadhesive performance of LN-CS and LN-CS-FUCO with respect to uncoated systems, LN and LN-FUCO. The drug loading did not influence interfacial interaction between the nanoparticle surface and the biological substrate.

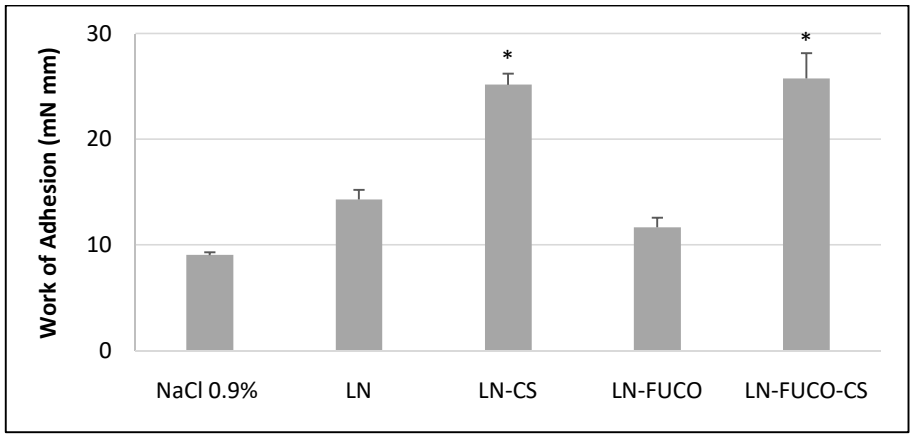


Figure 2: Bioadhesion properties (Work of Adhesion, mN.mm) of LN, LN-CS, LN-FUCO, and LN-FUCO-CS in comparison to saline solution (NaCl 0.9% *w/v*) as control (mean values±sd; n=6).

The positive surface charge of CS coated LN seemed responsible for the interaction with the biological substrate and consequently for the bioadhesive joint (Saporito et al., 2018). Eggshell membrane is mainly constituted by collagen and it is rich in aminoacids and in particular in proline, glutamic acid glycine along with uronic acid and sialic acid (Pillai et al., 2015) and it is widely used in literature to mimic skin wound bed. The interaction between eggshell membrane and CS could involve hydrogen bonds between chains and charge-charge interactions due to aminoacids and acidic groups of the membrane and CS amino groups (Sionkowska et al., 2004). Bioadhesion is a crucial property to allow an intimate contact between diseased area and formulation, to assure FUCO efficacy.

3.2.2 *In vitro* proliferation properties

Figure 3 shows % viability values of fibroblasts put in contact with unloaded and FUCO loaded LN with and without CS coating. After 4 h of contact LN impaired fibroblasts growth independently of their composition (CS association or drug loading). The higher system dilution was able to determine a lower effect with a viability close to 100%. This was probably due not to a real cytotoxic or cytostatic effect but mainly to the particle interference onto cell adhesion in the more concentrated samples. After 24 h of cell growth independently from LN composition there was a significant increase of cell proliferation. This could be due to the presence in the LN of unsaturated fatty acid that are widely reported in literature as enhancer of cell proliferation (Sandri et al., 2018). The presence of FUCO did not impair the positive effect of lipid composition, moreover it is reported that FUCO does not impair the proliferation of normal cells since it has a specific mechanism of action (Moghadamtousi et al., 2014). This could be useful in the treatment of hyperproliferative disease of the skin: the proliferative effect onto normal cells could enhance skin reparation while the antiproliferative effect of FUCO against the diseased cells could inhibit the replication of cells.

This was confirmed by means of CLSM in Figure 4. The fibroblasts maintained their fusiform shape, as demonstrated by cytoskeleton labelling (green staining), and normal nuclei (blue staining). LN stained in red could be localized close to the nuclei and entrapped between actin filaments of cell cytoskeleton. When CS coating was present cell substrates (independently of FUCO) formed subconfluent cell substrates while without CS cells appeared isolated without contact between each other.

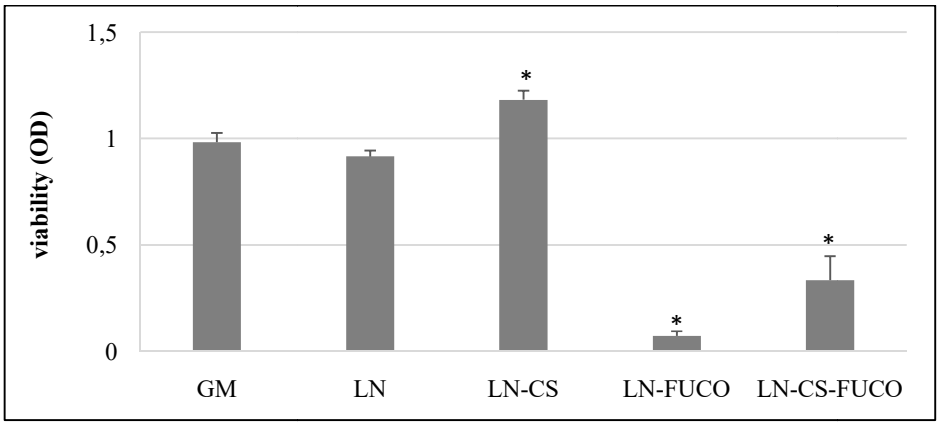


Figure 3: % viability values of fibroblasts after 4 or 24 h in contact with blank LN (LN), FUCO loaded LN (LN-FUCO) and blank and FUCO loaded LN coated by CS (LN-CS and LN-FUCO-CS, respectively) normalized against growth medium (mean values±sd; n=8).

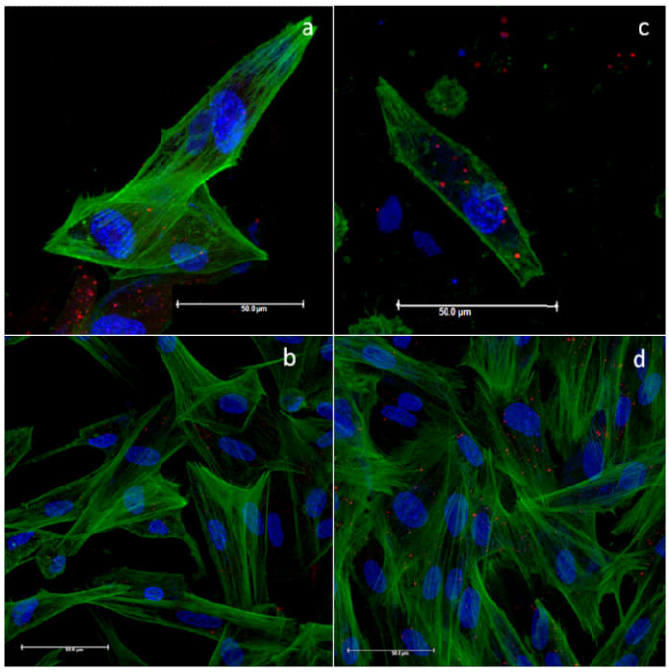


Figure 4: CLSM microphotographs of fibroblasts after 24 h in contact with blank LN (LN), FUCO loaded LN (LN-FUCO) and blank and FUCO loaded LN coated by CS (LN-CS and LN-FUCO-CS, respectively) all loaded with nile red (NR) (red dots: LN fibroblasts; green staining: cytoskeleton labelling; blue staining: nuclei).

4. Conclusions

High shear homogenization was proved as suitable method to prepare CS coated LN, loaded with FUCO. The systems were characterized by dimensions ranging from about 253 to 416 nm with a narrow distribution. CS coating and FUCO loading determined a LN size increase confirmed by TEM. Moreover, TEM and zeta-potential analysis confirmed the presence of CS coating on LN surface and evidenced difference in particle structure attributable to drug loading which could rearrange the lipid structure of nanoparticle core. Moreover, the presence of CS coating conferred to nanoparticle good bioadhesion. Fibroblast proliferation study evidenced the maintained properties of the systems on normal fibroblasts and the capability of CS to support cell viability while CLSM analysis evidenced LN internalization into fibroblasts. Considering the overall results topic application of CS coated LN-FUCO-CS seems a promising approach to control skin hyperproliferation and to preserve skin integrity.

Acknowledgements: The authors wish to thank Dr. P. Vaghi for CLSM, Dr. M. Boiocchi for TEM (Centro Grandi Strumenti, University of Pavia).

References

Bora, P.S., Narain, N., Rocha, R.V.M., De Oliveira Monteiro, A. C., De Azevedo Moreira, R., 2011. Characterization of the oil and protein fractions of Tucuma (Astrocaryum Vulgare Mart.) fruit pulp and seed kernel. CYTA-Journal of Food. 3, 111-116.

Chung, T.W., Choi, H.J., Lee, J.Y., Jeong, H.S., Kim, C.H., Joo, M., Ha, K.T., 2013. Marine algal fucoxanthin inhibits the metastatic potential of cancer cells. Biochem. Biophys. Res. Commun. 439, 580-585.

Cordenonsi, L.M., Santer, A., Sponchiado, R.M., Steppe, M., Raffin, R.P., Scherman Schapoval, E.E., 2017. Characterization and Analysis of Fucoxanthin and its Isomers. J Pharm Sci Bioscientific Res. 7, 322-334.

de Rosso, V.V., Mercadante, A.Z., 2007. Identification and quantification of carotenoids, by HPLC-PDA-MS/MS, from Amazonian fruits. J. Agric. Food Chem. 55, 5062-5072. doi: 10.1021/jf0705421

Duan, J., Zhang, Y., Han, S., Chen, Y., Li, B., Liao, M., Chen, W., Deng, X., Zhao, J., Huang, B., 2010. Synthesis and in vitro/in vivo anti-cancer evaluation of curcumin-

loaded chitosan/poly(butyl cyanoacrylate) nanoparticles. Int. J. Pharm. 400, 211-220. doi: 10.1016/j.ijpharm.2010.08.033.

Hajj Ali, H., Michaux, F., Ntsama, B., Sandrine, I., Durand, P., Jasniewski, J., Linder, M., 2015. Shea butter solid nanoparticles for curcumin encapsulation: Influence of nanoparticles size on drug loading. Eur. J. Lipid Sci. Technol. 118, 1168-1178. https://doi.org/10.1002/ejlt.201500348

Hosokawa, M., Kudo, M., Maeda, H., Kohno, H., Tanaka, T., Miyashita, K., 2004. Fucoxanthin induces apoptosis and enhances the antiproliferative effect of the PPARγ ligand, troglitazone, on colon cancer cells. Biochim. Biophys. Acta. 1675, 113-119. DOI: 10.1016/j.bbagen.2004.08.012

Jayakumar, R., Menon, D., Manzoor, K., Nair, S., Tamura, H., 2010. Biomedical applications of chitin and chitosan based nanomaterials: A short review", Carbohydr. Polym. 82, 227–232. https://doi.org/10.1016/j.carbpol.2010.04.074

Kumar, S., Sharma, S., Chattopadhyay, S.K., 2013. The potential health benefit of polyisoprenylated benzophenones from Garcinia and related genera: ethnobotanical and therapeutic importance. Fitoterapia. 89, 86–125. doi: 10.1016/j.fitote.2013.05.010.

Liu, C.L., Huang, Y.S., Hosokawa, M., Miyashita, K., Hu, M.L., 2009. Inhibition of proliferation of a hepatoma cell line by fucoxanthin in relation to cell cycle arrest and enhanced gap junctional intercellular communication. Chem. Biol. Interact. 182, 165–172. doi: 10.1016/j.cbi.2009.08.017.

Luo, Y., Wang, Q., 2014. Zein-based micro- and nano-particles for drug and nutrient delivery: A review. J. Appl. Polym. Sci. 131. https://doi.org/10.1002/app.40696

Lustosa, A.K.M., Arcanjo, D.D., Ribeiro, R.G., Rodrigues, K.A.F., Passos, F.F.B., Piauilino, C.A., Carvalho, F.A.A., 2016. Immunomodulatory and toxicological evaluation of the fruit seeds from Platonia insignis, a native species from Brazilian Amazon Rainforest. Rev. Bras. Farmacogn. 26, 77-82. http://dx.doi.org/10.1016/j.bjp.2015.05.014

Mandawgade, S.D., Patravale, V.B., 2008. Development of SLNs from natural lipids: application to topical delivery of tretinoin. Int. J. Pharm. 363, 132-138. doi: 10.1016/j.ijpharm.2008.06.028.

Manivasagan, P., Bharathiraja, S., Moorthy, M.S., Oh, Y.O., Seo, H., Oh, J., 2017. Marine biopolymer-based nanomaterials as a novel platform for theranostic applications. Polymer Reviews. 57, 631-667. https://doi.org/10.1080/15583724.2017.1311914

Martin, L.J., 2015. Fucoxanthin and its metabolite fucoxanthinol in cancer prevention and treatment. Mar. drugs. 13, 4784-4798. doi: 10.3390/md13084784

Mehnert, W., Mader, K., 2001. Solid lipid nanoparticles production, characterization and applications, Adv. Drug Deliv. Rev. 47, 165–196. https://doi.org/10.1016/S0169-409X(01)00105-3

Miyashita, K., Nishikawa, S., Beppu, F., Tsukui, T., Abe, M., Hosokawa, M., 2011. The allenic carotenoid fucoxanthin, a novel marine nutraceutical from brown seaweeds. J. Sci. Food Agric. 91, 1166-1174. doi: 10.1002/jsfa.4353.

Moghadamtousi, S. Z., Karimian, H., Khanabdali, R., Razavi, M., Firoozinia, M., Zandi, K., Kadir, H. A. 2014. Anticancer and Antitumor Potential of Fucoidan and Fucoxanthin, Two Main Metabolites Isolated from Brown Algae, The Scientific World Journal,2014, Article ID 768323 http://dx.doi.org/10.1155/2014/768323

Pillai, M.M., Akshaya, T.R., Elakkiya, V., Gopinathan, J., Sahanand, K.S., Rai, B.D., Selvakumar, R., 2015. Egg shell membrane–a potential natural scaffold for human meniscal tissue engineering: an in vitro study. RSC Advances. 5, 76019-76025. DOI: 10.1039/C5RA09959E

Ridolfi, D.M., Marcato, P.D., Justo, G.Z., Cordi, L., Machado, D., Durán, N., 2012. Chitosan-solid lipid nanoparticles as carriers for topical delivery of tretinoin. Colloids and Surfaces B: Biointerfaces. 93, 36– 40. doi: 10.1016/j.colsurfb.2011.11.051.

Sailaja, A.K., Amareshwar, P., Chakravarty, P., 2010. Chitosan nanoparticles as a drug delivery system. Res. J. Pharm. Biol. Chem. Sci. 1, 474-484. doi: 10.1016/j.colsurfb.2011.11.051.

Sandri, G., Bonferoni, M.C., Rossi, S., Ferrari, F., Mori, M., Del Fante, C., Caramella, C., 2011. Platelet lysate formulations based on mucoadhesive polymers for the treatment of corneal lesions. J. Pharm. Pharmacol. 63, 189-198. doi: 10.1111/j.2042-7158.2010.01208.x.

Sandri, G., Bonferoni, M.C., D'Autilia, F., Rossi, S., Ferrari, F., Grisoli, P., 2013. Wound dressings based on silver sulfadiazine SLN for tissue repairing. Eur. J. Pharm. Biopharm. 84, 84–90. doi: 10.1016/j.ejpb.2012.11.022.

Sandri, G., Motta, S., Bonferoni, M. C., Brocca, P., Rossi, S., Ferrari, F., Del Favero, E., 2017. Chitosan-coupled solid lipid nanoparticles: tuning nanostructure and mucoadhesion. Eur. J. Pharm. Biopharm. 110, 13-18. https://doi.org/10.1016/j.ejpb.2016.10.010

Sandri, G., Rossi, S., Bonferoni, M.C., Ferrari, F., Mori, M., Caramella, C., 2012. The role of chitosan as a mucoadhesive agent in mucosal drug delivery. J. Drug Deliv. Sci. Technol. 21, 275–284. https://doi.org/10.1016/S1773-2247(12)50046-8

Saporito, F., Sandri, G., Rossi, S., Bonferoni, M.C., Riva, F., Malavasi, L., Ferrari, F., 2017. Freeze dried chitosan acetate dressings with glycosaminoglycans and traxenamic acid. Carbohydrate Polymers. 184, 408–417. doi: 10.1016/j.carbpol.2017.12.066.

Sionkowska, A., Wisniewski, M., Skopinska, J., Kennedy, C.J., Wess, T.J., 2004. Molecular interactions in collagen and chitosan blends. Biomaterials. 25, 795-801. https://doi.org/10.1016/S0142-9612(03)00595-7

Szucs, M., Sandri, G., Bonferoni, M.C., Caramella, C.M., Vaghi, P., Szabó-Révész, P., Erős, I. Mucoadhesive behaviour of emulsion containing polymeric emulsifier. Eur. J. Pharm. Sci. 34, 226–235. https://doi.org/10.1016/j.ejps.2008.03.005

Tao, Y., Lu, Y., Sun, Y., Gu, B., Lu, W., Pan, J., 2009. Development of mucoadhesive microspheres of acyclovir with enhanced bioavailability, Int. J. Pharm. 378, 30–36. doi: 10.1016/j.ijpharm.2009.05.025.

Viera, A.C.C., Chaves, L.L., Pinheiro, S., Pinto, S., Pinheiro, M., Costa Lima, S., Ferreira, D., Sarmento, B., Reis, S.,2018. Mucoadhesive chitosan-coated solid lipid nanoparticles for better managenet of tuberculosis, Int. J. Pharm. 536, 478-485. doi: 10.1016/j.ijpharm.2017.11.071.

Zhang, S., Kawakami, K., 2010. One-step preparation of chitosan solid nanoparticles by electrospray deposition. Int. J. Pharm. 397, 211–217. doi: 10.1016/j.ijpharm.2010.07.007

9. DISCUSSÃO GERAL

Face aos resultados descritos na literatura sobre a relevância e o interesse na funcionalidade de produtos marinhos, devido ao fato de haver evidências epidemiológicas entre o consumo de alimentos marinhos e a redução do risco de doenças crônicas, tais como o câncer. Neste contexto, o isolamento e a investigação de novos bioativos, como o carotenoide marinho FUCO estão em evidência (FOTUHI, MOHASSEL e YAFFE, 2009; GAMMONE e D'ORAZIO, 2015).

Para tanto, o presente trabalho visou o desenvolvimento de uma formulação de NL inovadoras com matérias-primas da Amazônia brasileira, a manteiga de bacuri e o óleo de tucumã, contendo FUCO incorporada em um veículo semissólido para aplicação cutânea. Além disso, a validação de metodologia analítica indicativa de estabilidade por CLAE para o controle de qualidade e estudo de estabilidade da mesma foram realizados. Até o presente momento, não há relatos na literatura de uma formulação de nanopartículas contendo a combinação de manteiga de bacuri e de óleo de tucumã pela técnica de homogeneização de alto cisalhamento.

Na literatura, foi descrito o desenvolvimento de sistemas de liberação de fármacos, como as nanoemulsões (SALVIA-TRUJILLO et al., 2015), o nanogel (RAVI e BASKARAN, 2015) e as microesferas (QUAN et al., 2013) para a encapsulação da FUCO. Em um destes estudos, a FUCO foi incorporada em nanogéis híbridos de quitosana-glicolípidica, preparados pelo método de geleificação iônica, para melhorar a estabilidade e a biodisponibilidade (RAVI e BASKARAN, 2015). Da mesma forma, Salvia-Trujillo e colaboradores (2015) estudaram o impacto de 3 tipos de carreadores lipídicos sobre a biodisponibilidade da FUCO em nanoemulsões para uso em modelo gastrointestinal *in vitro*. Porém, diferentemente da descrição na literatura, o presente trabalho teve como objetivo desenvolver uma metodologia de preparo de NL simples, de fácil escalonamento e que não necessitasse o uso de solventes orgânicos para uso tópico. Ressalta-se que a manteiga de bacuri e o óleo de tucumã, além de serem utilizados como matéria-prima para a preparação das NL, possuem efeitos farmacológicos.

Inicialmente, a FUCO matéria-prima foi adquirida em duas apresentações, incorporada em um óleo e na forma de pó. Deste modo, no **Capítulo I**, foi realizada a caracterização das duas matérias-primas visando seu uso em estudos futuros por EM e RMN ^{1}H. A EM é uma técnica analítica que permite que substâncias químicas possam ser detectadas de acordo com suas razões massa-carga (*m/z*), fornecendo

o valor do seu íon molecular e/ou seus fragmentos moleculares (HOFFMANN e STROOBANT, 2007). A FUCO possui massa molecular de 658,92 g/mol e os resultados demonstram que as duas matérias-primas da FUCO possuem a mesma fórmula molecular, $C_{42}H_{58}O_6$, com íon molecular principal *m/z* 659 $[M+H]^+$ idênticos, porém com diferentes fragmentações. Com a interpretação dos espectros de RMN ^1H e COSY, foi possível fazer uma comparação detalhada focando na identificação dos prótons olefínicos. Conclui-se que a FUCO em óleo e em pó foram identificadas como a forma total-*trans* FUCO e 9'-*cis* FUCO, respectivamente.

Em continuidade, foi desenvolvido e validado um método analítico por CLAE indicativo de estabilidade para quantificação da total-*trans* e 9'-*cis* FUCO. A capacidade do método de separar a FUCO e seus produtos de degradação, formados em condições de estresse, garantem a validação de um método cromatográfico indicativo de estabilidade, extremamente útil para o controle de qualidade (MAGGIO, VIGNADUZZO e KAUFMAN, 2013). Na análise e quantificação de carotenoides, o principal problema é devido a sua instabilidade, sendo assim, devem ser tomadas precauções para evitar perdas de teor e formação de produtos de degradação (RODRIGUEZ-AMAYA, 2001). Para o desenvolvimento do método foi realizado um estudo da molécula da FUCO, levando em consideração sua polaridade, solubilidade e pKa. Da mesma forma, várias condições experimentais foram testadas e otimizadas, modificando a temperatura da coluna, a vazão, a proporção de acetonitrila na fase móvel e, por fim, foram testados diferentes valores de pH.

De acordo com os requisitos da Farmacopeia Americana (USP) (2017) e ICH (2005), testes de adequabilidade do sistema são parte integrante de métodos, sendo uma etapa inicial a ser estabelecida para que todo o sistema selecionado para o desenvolvimento do processo de análise esteja apto a fornecer resultados com precisão e exatidão aceitáveis e confiáveis. Portanto, os parâmetros de adequabilidade do sistema investigados foram: eficiência da coluna, tempo de retenção, fator de cauda, fator de retenção e resolução. Foi realizada a comparação de diferentes valores de pH, 3,0; 5,0; 7,0 e 9,0; com o pH 7,0 a eficiência da coluna produziu resultados mais satisfatórios. A resolução e fator de cauda não foram afetados com a mudança de pH. Com base em estudos anteriores desenvolvidos por Muthuirulappan e Francis (2013) e Yip e colaboradores (2014), a FUCO

mostrou-se mais estável em pHs de 5,0-7,0.

Deste modo, foi desenvolvido e validado um método indicativo de estabilidade por CLAE com a utilização de coluna cromatográfica C18, com detector de arranjo de diodos (DAD) no comprimento de onda de 450 nm e fase móvel composta por acetonitrila e água pH 7,0 (9.5:0,5 *v/v*). A determinação qualitativa e quantitativa da FUCO e seu isômero procederam-se de forma rápida, com 8 minutos de análise, eficiente e com resolução adequada. O método foi validado segundo os Guias Oficiais (BRASIL, 2003; ICH, 2005), avaliando os parâmetros especificidade, linearidade, precisão, exatidão, limite de detecção, limite de quantificação e robustez.

Para a avaliação da especificidade, foram realizados estudos de degradação forçada. A total-*trans* FUCO foi exposta a condições fotolíticas, oxidativa, térmica, ácida e básica. Os meios oxidativo e sob irradiação com raios ultravioletas C (UVC) foram os principais aceleradores de degradação. Houve surgimento de produtos de degradação durante o estudo, porém esses picos foram detectados com boa resolução utilizando as condições cromatográficas otimizadas. Como outros carotenoides, a FUCO pode ser degradada quando exposta ao calor, luz, oxigênio e outras moléculas pró-oxidantes (MÍNGUEZ-MOSQUERA et al., 2002). A formação de alguns isômeros *cis* pode ocorrer devido às condições de estresse as quais a molécula é submetida. Geralmente, a FUCO resulta em um pico principal composto de sua forma total-*trans*, juntamente com os seus isômeros que são gerados através da quebra de várias ligações duplas carbono-carbono na cadeia de polieno (SUGIMURA et al., 2012; ZHANG et al., 2015).

A linearidade do método foi comprovada através do método dos mínimos quadrados e da ANOVA, em que o método proposto apresentou regressão linear significativa ($p<0,05$) na faixa de concentração estudada, de 1,0-40,0 µg/mL, com $r=0,9994$ e o desvio da linearidade mostrou-se não significativo ($p>0,05$). A precisão do método foi comprovada por meio da repetibilidade e da precisão intermediária, apresentando valores de desvio padrão relativo (DPR) inferiores a 0,7%. A exatidão apresentou valor de 103,25%, que está dentro do recomendado. A robustez do método foi avaliada por desenho experimental Box-Behnken através da modificação da temperatura da coluna, pH e comprimento de onda. De acordo com os resultados obtidos, as modificações nos fatores estudados não interferiram na quantificação da

FUCO, demonstrando que o método analítico é robusto. Em conclusão, demonstrou-se que o método proposto cumpre os requisitos de validação, estando de acordo com os parâmetros de qualidade preconizados.

O isômero 9'-*cis* da FUCO foi analisado com as condições cromatográficas anteriormente descritas e exposto sob as mesmas condições de degradação forçada. Os resultados demonstraram que o isômero 9'-*cis* apresenta um tempo de retenção em 6,1 minutos, diferindo do padrão e da forma total-*trans* que apresenta o tempo de retenção em 3,0 minutos. No estudo de degradação forçada, o isômero 9'-*cis* mostrou-se menos estável que a forma total-*trans* e não houve a formação de nenhum pico de degradação.

Posteriormente, no **Capítulo II** visou-se o desenvolvimento de uma formulação de NL inovadoras contendo uma combinação de manteiga de bacuri e óleo de tucumã pelo método de homogeneização de alto cisalhamento. Sistemas de liberação modificados, como os lipossomas e nanopartículas, são métodos utilizados para melhorar a penetração cutânea de fármacos e aumentar o efeito farmacológico, minimizar efeitos colaterais, bem como proteger a substância ativa (WELSS, BASKETTER e SCHRÖDER, 2004; MOSER et al., 2001). Visando o uso tópico, optou-se pela preparação de NL, pois em outras estratégias como as ciclodextrinas, há o uso de solventes orgânicos que interferem na permeabilidade da pele. Do mesmo modo, as NL apresentam cerca de 10 a 100 vezes menos toxicidade do que as partículas poliméricas (MARCATO, 2009). Como relatado por Almeida Borges e colaboradores (2013), em formulações para uso tópico, a fase aquosa afeta a permeabilidade da pele, porque a hidratação do estrato córneo é alterada e existe quebra da matriz de lipoproteína, resultando numa diminuição da resistência da substância ativa à difusão, promovendo um aumento da permeação.

As técnicas para preparação de NL incluem principalmente homogeneização a alta pressão, microemulsificação, evaporação de solvente e inversão de fase. A seleção do método mais adequado depende das propriedades dos componentes da formulação, avaliando sua estabilidade a temperaturas elevadas e solubilidade (SVILENOV e TZACHEV, 2014). Para objetivar a preparação das NL inovadoras por um método simples e rápido, que não utilize solvente orgânico, optou-se pelo método de homogeneização de alto cisalhamento. Primeiramente, foram produzidas NL sem a incorporação da FUCO, apenas com a combinação de manteiga de bacuri

e de óleo de tucumã, visto que essas duas matérias-primas oriundas da Amazônia possuem atividades farmacológicas. Foram realizados diversos ensaios pilotos para a produção das NL e, por fim, houve a produção de formulações variando a proporção de manteiga de bacuri e do óleo de tucumã. As concentrações dos tensoativos na fase oleosa e aquosa se mantiveram constantes. Sabe-se que a combinação de tensoativos, com caráter hidrofílico e lipofílico, geralmente tende a produzir partículas de tamanhos menores e mais estáveis (OLBRICH e MULLER, 1999).

O tamanho de partícula das NL pode ser afetado por vários parâmetros, como a composição da formulação, o método de produção e as condições estabelecidas para produção, como tempo de preparo e temperatura. Tensoativos ou lipídeos em altas concentrações favorecem a formação de partículas menores, porém, a diminuição destes significa aumento do tamanho das partículas, principalmente durante o período de estocagem. Do mesmo modo, a temperatura escolhida durante o processo de obtenção de NL interfere diretamente no tamanho das partículas. Baixas temperaturas tendem à formação de partículas maiores (LIPPACHER, MULLER e MADER, 2002; UNER, 2006).

Como passo inicial para a caracterização das NL inovadoras produzidas, o aspecto visual foi analisado, a fim de confirmar a presença de um sistema homogêneo. Todas as formulações apresentaram aspecto macroscópico homogêneo, com coloração amarela a alaranjada. A medida do diâmetro das partículas foi realizada por espalhamento de luz dinâmico (DLS) e difração de laser. A difração de laser, apesar de ser utilizada para a caracterização de tamanho de partícula, tem seu uso voltado do para verificar a presença de partículas de tamanho maiores além de partículas menores, visto que existem outros métodos mais adequados para caracterizar partículas pequenas isoladas como, por exemplo, o DLS (KECK e MULLER, 2008). Por DLS, o diâmetro médio de partícula foi menor que 255 nm. O pdI foi menor que 0,3, indicando homogeneidade na distribuição das partículas. O fator SPAN foi calculado e expressa a distribuição em relação ao diâmetro médio, isto é, a homogeneidade da população. Valores de SPAN próximos de 1,0 indicam uma estreita distribuição de tamanhos. O fator SPAN das formulações variou entre 0,3 e 0,7. Estes resultados demonstram que o método de homogeneização de alto cisalhamento foi adequado para o preparo das NL com

manteiga de bacuri e óleo de tucumã, produzindo partículas com tamanho desejado para aplicação cutânea. A distribuição de tamanho das partículas é uma característica relevante, pois pode influenciar na farmacocinética, na biodistribuição e na segurança de um produto (DESAI, PATLOLLA e SINGH 2010).

Os valores de potencial zeta são adequados para manter o sistema sem agregação e precipitação, devido à repulsão eletrostática que as mesmas apresentam, resultante da densidade de carga da superfície. Portanto, é um parâmetro fundamental que afeta diretamente a estabilidade das NL e a interação das partículas com a superfície das células *in vivo* (QI et al, 2004). As NL inovadoras apresentaram uma carga negativa superficial, e os valores de potencial zeta ficaram entre -11 mV e -24 mV. Os valores negativos estão relacionados à natureza química dos componentes da formulação na interface partícula/água. Em adição, a presença de monooleato de sorbitano e o revestimento com polissorbato 80 determinaram um valor negativo (MOSQUEIRA et al., 2000). As médias das medidas do pH foram entre 5,44 e 5,64. Todas as formulações foram ácidas, mas os valores de pH, ainda assim, foram apropriados para uma aplicação no estrato córneo, que não apresenta alteração fisiológica quando submetido a um pH na faixa de 3,50 a 8,50 (SZNITOWSKA, JANICKI e BACZEK, 2001).

Um dos maiores problemas encontrados no desenvolvimento das NL é a sua instabilidade por longos períodos de tempo. Isto se da porque podem ocorrer transições polimórficas, uma vez que os lipídeos sólidos possuem estrutura cristalina, levando à formação de cristais perfeitos e expulsão da substância ativa. A preservação do arranjo de lipídeos durante a estocagem até a administração das NL leva a uma liberação controlada da substância ativa encapsulada, pois no geral, esta situa-se no espaço entre as cadeias dos lipídeos (SOUTO e MULLER, 2008; HELGASON et al., 2009; SWATHI et al., 2010). A combinação de tensoativos provavelmente permitirá a formação de um filme interfacial coeso ao redor das partículas, constituindo uma camada estabilizante altamente resistente, permitindo que as formulações permaneçam estáveis ao longo do tempo de armazenamento (KRUGLYAKOV, 2000). A fim de investigar a estabilidade, as seis formulações produzidas foram deixadas em temperatura ambiente por dois meses e avaliou-se quanto ao tamanho de partícula, potencial zeta, pH, MET e DSC. Os resultados estabeleceram a adequada compatibilidade de compostos, pois todas as

formulações se mantiveram estáveis durante o período.

A partir dos resultados obtidos na caracterização da FUCO, a total-*trans* FUCO apresentou maior estabilidade que a 9'-*cis* FUCO. Geralmente, os isômeros *cis* são termodinamicamente menos estáveis. Além disso, a correta identificação dos isômeros é um ponto fundamental, uma vez que os isômeros diferem substancialmente em sua atividade.

Para o desenvolvimento das NL inovadoras contendo manteiga de bacuri e óleo de tucumã, a FUCO foi incorporada na formulação que apresentou os melhores resultados no estudo de estabilidade. A composição selecionada foi com 5% de manteiga de bacuri e 4% de óleo de tucumã. Os sistemas nanoestruturados, baseados em lipídeos, estão entre as tecnologias de encapsulação mais promissoras e têm se mostrado adequados para a encapsulação de compostos lipofílicos, como a FUCO (MOZAFARI et al., 2006).

Nesse contexto, no **Capítulo III** estão descritos os resultados da incorporação da FUCO nas NL inovadoras. Ao analisar macroscopicamente, a formulação de NL-FUCO apresentou-se homogênea com coloração laranja. A distribuição do tamanho mostrou-se na escala manométrica, com valor de 243 nm, com distribuição monomodal e pdI de 0,22. Com a adição da FUCO, o tamanho de partícula aumentou de 212,3 nm para 243 nm; os valores de pdI aumentaram de 0,18 a 0,22. Os valores de pdI foram inferiores a 0,3, sugerindo que o método de preparação produziu NL com distribuição de tamanho controlado. Valores similares de tamanho médio das partículas foram obtidos por Khoee e Yaghoobian (2009) em pesquisas para obtenção de nanopartículas para uso tópico, em que o tamanho variou entre 137 e 296 nm. Do mesmo modo, Taveira e colaboradores (2009) desenvolveram nanopartículas contendo doxorrubicina com diâmetro médio de 175 e 278 nm, apresentando tamanho adequado para o tratamento tópico do câncer de pele.

A formulação de NL-FUCO foi carregada negativamente, e o potencial zeta encontrado foi de -44,9 mV. Com a adição da FUCO, o potencial zeta aumentou e, consequentemente, valores de potenciais zeta elevados contribuem para a estabilidade físico-química da formulação.

Visando confiabilidade na quantificação de FUCO encapsulada nas NL inovadoras, o método analítico foi validado. Os métodos foram validados segundo os Guias Oficiais (BRASIL, 2003; ICH, 2005) e os resultados demonstraram que o

método utilizado foi linear, preciso, exato, específico e reprodutível para a faixa de análise utilizada (1,0 a 40,0 µg/mL).

A taxa de encapsulação foi determinada pela técnica de ultrafiltração-centrifugação, na qual uma membrana de 100 kDa é utilizada, as NL inovadoras com FUCO encapsulada permanecem na parte superior do tubo, enquanto a fase aquosa com a FUCO na sua forma livre move-se para a parte inferior (PUGLIA et al., 2008). A taxa de encapsulação encontrada foi alta, de 98,9%, esse resultado era esperado em razão da natureza lipofílica da FUCO. Ali e colaboradores (2010) encontraram valores de 99,9% em nanopartículas lipídicas sólidas de sinvastatina, outro fármaco lipofílico. A concentração de FUCO nas suspensões ficou próxima da teórica, pois o teor encontrado foi de 103%.

Visando o uso tópico, as suspensões de NL necessitam ser incorporadas em formulações semissólidas a fim de se obter consistência adequada para a aplicação. Então, na etapa seguinte as NL-FUCO foram incorporadas em um hidrogel de Carbopol 940®. Esta preparação é usualmente utilizada em bases para uso tópico, devido a sua habilidade de proporcionar alta viscosidade em baixas concentrações, sua compatibilidade com diversas substâncias, sendo de fácil aquisição e apresenta fácil transposição para a escala industrial. Adicionalmente, estudos comprovam a boa estabilidade física de formulações de hidrogel contendo NL (SHAHGALDIAN et al., 2003; SOUTO et al., 2004). Uma vez que o uso de parabenos é mal aceita pelos consumidores, o Sharomix CPP® foi utilizado como conservante na formulação. Sharomix CPP® é um composto de caprililglicol e fenilpropanol, criando assim, uma mistura de amplo espectro altamente eficiente.

A formulação apresentou-se homogênea em relação a cor e aspecto, mantendo as características específicas de um gel. O valor de pH obtido, de 5,95, é compatível com a aplicação cutânea e similar aos valores relatados na literatura para estes sistemas. O diâmetro médio encontrado na formulação das NL-FUCO incorporadas ao hidrogel foi de 220,1 nm e pdI de 0,22. Após a incorporação, o diâmetro médio das partículas diminuiu e o pdI manteve-se estável, demonstrado a viabilidade da incorporação das nanoestruturas no hidrogel. Da mesma forma, o diâmetro mostrou-se adequado para aplicação tópica, pois segundo Verma e colaboradores (2003) partículas com diâmetro médio em torno de 300 nm são capazes de liberar seu conteúdo nas camadas da pele.

Para assegurar a qualidade da preparação semissólida produzida contendo FUCO, além das propriedades físico-químicas, é necessário quantificá-la. Foi utilizado o método anteriormente desenvolvido por CLAE, e o teor apresentou-se adequado, em torno de 100%.

O estudo de fotoestabilidade, realizado em raios ultravioletas A (UVA), demonstrou que as NL inovadoras protegeram a FUCO, em 240 minutos as NL-FUCO e as NL-FUCO incorporadas em gel degradaram cerca de 11%, enquanto a FUCO na sua forma livre degradou 27%. Puglia e colaboradores (2008) relatam que as nanopartículas obtidas a partir de lipídios são capazes de melhorar a estabilidade química de compostos sensíveis à luz, oxidação e hidrólise.

Previamente ao ensaio de permeação cutânea *in vitro*, o estudo de dissolução das NL-FUCO foi realizado. Este método é uma forma para avaliar a liberação do fármaco em sistemas nanoestruturados e prever como esses sistemas se comportarão frente a meios biológicos, como a pele (BABY et al., 2009). Após 10 minutos, a concentração da FUCO livre foi de 98,76%. Entretanto, após 4 horas, observa-se que a NL-FUCO liberou 81,50%. Estes resultados demonstraram a capacidade das NL em controlar a liberação da FUCO. Estudos de permeação cutânea *in vitro* são empregados para a avaliação da segurança, eficácia e para a otimização dos processos de desenvolvimento de produtos para uso tópico. Do mesmo modo, possibilita também prever e correlacionar dados obtidos a partir de experimentos *in vitro* (BETTONI, 2009). Para a realização do estudo de permeação cutânea foram utilizadas células de difusão de Franz. Estas células são constituídas por um compartimento receptor e um doador o qual é separado por uma membrana, que pode ser uma membrana sintética, de origem humana ou animal. Entretanto, a disponibilidade da pele humana, é limitada e a utilização de pele animal é uma alternativa para a realização do estudo. Entre os animais, a pele de orelha de porco é a mais semelhante à pele humana, em características como o arranjo das fibras de colágeno na derme, o índice de lipídios e a espessura do estrato córneo (SARVEIYA et al., 2004; GODIN et al., 2007). Com base nos resultados, a FUCO não foi encontrada no compartimento receptor após 8 horas de estudo, evitando assim, possíveis efeitos sistêmicos. O hidrogel contendo NL-FUCO reteve uma maior quantidade de FUCO na epiderme e na derme, quando comparado à FUCO na sua forma livre. Junyaprasert e colaboradores (2009) desenvolveram NL com coenzima

Q10 pelo método de homogeneização a alta pressão. Os autores evidenciaram um aumento significativo do efeito oclusivo e da permeação da quantidade de fármaco com o uso do NL, em comparação com a nanoemulsão.

As NL tem se tornado muito atraentes para aplicações sobre a pele, inclusive peles danificadas ou inflamadas, principalmente por sua composição baseada em lipídios biocompatíveis (WISSING e MULLER, 2003). Em muitas condições clínicas, como o câncer, a integridade do estrato córneo é comprometida e sua remoção faz parte de alguns protocolos *in vitro* (SAIJA et al., 1998). Quando o estrato córneo foi removido, a penetração das NL-FUCO na epiderme e na derme aumentou, após 8 horas de experimento. Jain e colaboradores (2014) ressaltam que um sistema carreador efetivo para o tratamento tópico deve ser capaz de transportar o fármaco até as camadas mais externas da pele, apresentando localização transdérmica mínima e ausência de absorção sistêmica. Os resultados encontrados no estudo de permeação cutânea *in vitro* demonstram que a formulação desenvolvida apresenta-se como um sistema carreador promissor para a FUCO.

A carência de informações e regulamentações a respeito da avaliação toxicológica de nanopartículas expõe a necessidade de pesquisa nesta área. Centros internacionais de pesquisa e validação como a *Organisation for Economic Co-operationand Development* (OECD, 2010) recomendam a utilização de métodos alternativos a animais para avaliação toxicológica. O **Capítulo IV** apresenta os resultados da avaliação toxicológica *in vitro* da FUCO e das NL-FUCO realizados com células 3T3 através dos ensaios de citotoxicidade por MTT, vermelho neutro e o método de exclusão com azul de Tripan. Concomitantemente, foram avaliadas as espécies reativas de oxigênio e nitrogênio e o potencial de membrana mitocondrial.

As células 3T3 têm origem de culturas de embrião inteiras, são capazes de dividir-se indefinidamente e são altamente sensíveis à inibição após a confluência da divisão celular (SAKAI, 2007). Huang e colaboradores (2017) realizaram um estudo com o objetivo de verificar se as células 3T3 são capazes de predizer a toxicidade. Para isto, investigaram 120 resultados de citotoxicidade e compararam com estudos de toxicidade aguda realizados em camundongos. O resultado demonstrou que as células 3T3 são capazes de prever com relativa certeza a toxicidade em camundongos, permitindo a redução do uso de roedores.

A citotoxicidade do total-*trans* e 9'-*cis* FUCO em células 3T3 foi determinada por meio de ensaio MTT e NR. Nas concentrações estudadas, os dois testes apresentaram resultados diferentes. Com o mesmo propósito, no entanto, utilizando mecanismos diferentes, o MTT e o NR são complementares e, estes ensaios podem servir como uma abordagem confiável para a triagem de estudos de toxicidade. Resultados semelhantes foram encontrados por Nogueira e colaboradores (2011), que relataram uma diferença significativa na citotoxicidade de cinco surfactantes à base de lisina por MTT e NR. A medição celular de espécies reativas mostrou um aumento significativo na produção de ROS e RNS na total-*trans* FUCO*,* após as 24 h de incubação. A 9'-*cis* FUCO apresentou um aumento significativo nas espécies reativas nas concentrações de 80 e 100 µg/mL. Apesar dos efeitos deletérios de ROS e RNS, estes subprodutos, são necessários para o processo de maturação das estruturas celulares e podem atuar na defesa do organismo (STORZ, 2005; GENESTRA, 2007). Na avaliação do potencial de membrana, a total-*trans* FUCO exibiu um aumento significativo após 24 h de incubação. Ao contrário, a 9'-*cis* FUCO não apresentou aumento no potencial de membrana. Quando ocorre perda significativa no potencial de membrana, há comprometimento na fosforilação oxidativa que restringe a energia celular com posterior liberação de fatores apoptóticos ocasionando a morte celular (SILVA et al., 2013).

Na literatura, a maior parte dos estudos toxicológicos com nanopartículas disponíveis estão baseados em ensaios *in vitro*. Isso ocorre por serem testes mais rápidos, com custo mais baixo e pela facilidade de serem executados (MARQUIS et al., 2009). Outro fator é que permitem elucidar o mecanismo de interação das nanopartículas com as células (HUANG, WU e ARONSTAM, 2010). Existe, ainda, um controle maior nas culturas celulares humanas e de animais e, com isso, gerar resultados mais reprodutíveis que estudos *in vivo*, entretanto é necessária uma padronização rígida desses ensaios para maximizar a reprodutibilidade (ARORA, RAJWADE e PAKNIKAR, 2012). Deste modo, Kroll e colaboradores (2012) avaliaram quatro ensaios *in vitro* para estresse oxidativo, viabilidade celular, morte celular e produção de citocinas inflamatórias utilizando 24 nanopartículas já caracterizadas. Os resultados variaram dependendo do ensaio utilizado e os autores ainda sugerem que cada ensaio *in vitro* deve ser avaliado para cada tipo de nanopartículas.

Para as NL-FUCO, os ensaios de MTT e NR não foram conclusivos. Para avaliar a citotoxicidade, foi utilizado o método de exclusão com azul de Tripan. Este método é utilizado para avaliar a integridade da membrana celular, pois quando ocorre morte celular ocorrem mudanças da permeabilidade da membrana. Na célula morta, não viável, este corante se difunde rapidamente para dentro do citoplasma (STROBER, 2015). Após 24 h, NL-FUCO mostrou citotoxicidade significativa nas concentrações de 80 e 100 µg/mL. Portanto, concentrações de NL-FUCO menores que 80 µg/mL podem ser consideradas biocompatíveis com células 3T3. Na avaliação celular de espécies reativas, os resultados foram similares à total-*trans* FUCO, pois as NL e as NL-FUCO apresentaram um aumento significativo na produção de ROS e RNS, demonstrando assim uma capacidade pró-oxidante significativa. Na avaliação do potencial de membrana, as NL-FUCO apresentaram um aumento significativo, ocasionando a hiperpolarização da membrana mitocondrial e impulsionando a síntese de adenosina trifosfato (ATP) (BAGGALEY, ELLIOTT e BRUCE, 2008). Estudos de segurança são uma parte crítica do desenvolvimento de nanopartículas e o atual estudo mostrou que as NL-FUCO são biocompatíveis com células 3T3 até a concentração de 80 µg/mL. No entanto, estudos são necessários para elucidar a toxicidade *in vivo* destas NL.

No **Capítulo V** estão apresentados os resultados obtidos na *Università Degli Studi di Pavia* (Pavia/Itália). A quitosana é um polissacarídeo natural formado de copolímeros de *N*-acetil-*D*-glicosamina e *D*-glicosamina em proporções variáveis, obtida pela desacetilação da quitina. A quitina é o segundo polissacarídeo mais abundante na natureza e é encontrada na carapaça de crustáceos, insetos, moluscos e parede celular de alguns fungos. Além de ser um polímero biocompatível, biodegradável e atóxico, a quitosana apresenta características antimicrobianas, biodegradáveis, biocompatíveis e mucoadesivas. A propriedade mucoadesiva é devido às cargas positivas em pH fisiológico, assim a quitosana tem a capacidade de aderir a superfícies carregadas negativamente como pele e as mucosas, aumentando a retenção do fármaco no local de aplicação, melhorando desta forma a biodisponibilidade. Além disso, a quitosana tem a capacidade de induzir uma abertura temporária das junções epiteliais (BERGER et al., 2004; RINAUDO, 2006; NAGPAL, SINGH e MISHRA, 2010).

Nanopartículas têm sido recobertas com quitosana para associar as

vantagens destes sistemas e as propriedades biológicas da quitosana. Sandri e colaboradores (2010) desenvolveram NL contendo ciclosporina A associada com quitosana, para aplicação ocular. As NL associadas com quitosana foram biocompatíveis, aumentaram a permeação/penetração de ciclosporina A juntamente com um possível mecanismo de internalização/captação das nanopartículas *in vitro* (cultura de células) e *ex vivo* (córnea de porco). Do mesmo modo, Viera e colaboradores (2018) desenvolveram NL carregadas com rifampicina e revestidas de quitosana. O revestimento com quitosana aumentou as propriedades de mucoadesão, promovendo uma absorção mais eficaz após a administração pulmonar.

As NL-FUCO e as NL-FUCO revestidas com quitosana foram preparadas por meio de homogeneização de alto cisalhamento, como anteriormente descrito, e logo após foram caracterizadas. O revestimento com quitosana aumentou significativamente o tamanho das NL, o que pode ser explicado pela interação de lipídios e tensoativos e também pelo revestimento, que pode ter causado um rearranjo diferente nas NL (VIEIRA et al., 2018). Além disso, a variação no potencial zeta era esperada, pois o revestimento de quitosana modifica a carga superficial devido às interações eletrostáticas (HU, SUN e WU, 2013). A MET confirmou a presença do revestimento de quitosana na superfície das NL e evidenciou as diferenças na estrutura. O teor e a eficiência de encapsulação não foram alterados com o revestimento de quitosana, corroborando com estudos anteriores (LIU et al., 2016; SANDRI et al., 2010).

Para o estudo de bioadesão *in vitro* foi empregado um método simples com membrana de casca de ovo. A membrana da casca do ovo é constituída por colágeno, ácido glutâmico, ácido urônico, ácido siálico e é rica em aminoácidos, em particular prolina e glicina (PILLAI et al., 2015). Parodi e colaboradores (1999) avaliaram a mucoadesão de comprimidos bucoaderentes utilizando membrana de casca de ovo e compararam com uma membrana sintética de polipropileno. Os resultados demonstraram uma boa correlação e ainda, a membrana de casca de ovo forneceu valores mais confiáveis nos parâmetros de mucoadesão. Quando as NL e NL-FUCO foram avaliadas, o revestimento de quitosana aumentou significativamente a bioadesão. A carga superficial positiva das nanopartículas revestidas com quitosana é a responsável pela interação com o substrato biológico

e, consequentemente, pela articulação bioadesiva (SAPORITO et al., 2018).

O estudo de proliferação *in vitro* com fibroblastos dérmicos humanos evidenciou que as NL-FUCO mantiveram as propriedades de proliferação da quitosana e das NL em relação aos fibroblastos. Além disso, no microscópio confocal de varredura a laser (CLMS) evidenciou a internalização das NL em fibroblastos. Considerando a aplicação tópica, os resultados evidenciam que as NL-FUCO revestidas com quitosana são uma abordagem promissora para preservar a integridade da pele.

10. CONCLUSÕES

- A fim de identificar as duas apresentações da FUCO, estas foram caracterizadas por EM, RMN ^{1}H e COSY. Estes testes foram realizados de forma satisfatória, permitindo adequada caracterização. A FUCO em óleo e em pó foram identificadas como total-*trans* FUCO e 9'-*cis* FUCO, respectivamente;
- O método indicativo de estabilidade desenvolvido e validado por CLAE mostrou-se rápido, específico, linear, preciso, exato e robusto na faixa de concentração proposta. Assim, sendo adequado para a determinação quantitativa da FUCO e seu isômero;
- A robustez, quando avaliada através do planejamento fatorial Box-Behnken, permitiu uma análise mais ampla da influência dos parâmetros analíticos na quantificação da FUCO;
- Na avaliação da estabilidade, a total-*trans* FUCO demonstrou maior estabilidade que seu isômero, 9'-*cis*;
- As NL inovadoras contendo uma combinação de manteiga de bacuri e de óleo de tucumã, utilizando homogeneização de alto cisalhamento, mostraram-se alternativa promissora, especialmente por suas propriedades benéficas para aplicação tópica;
- A caracterização físico-química das NL inovadoras mostrou resultados satisfatórios quando preparadas com diferentes concentrações da manteiga de bacuri e do óleo de tucumã;
- No estudo de estabilidade, as NL inovadoras contendo diferentes proporções de manteiga de bacuri e óleo de tucumã mantiveram-se homogêneas e estáveis quando armazenadas em temperatura ambiente, durante dois meses;
- A formulação de NL inovadora que apresentou os melhores resultados foi a composta com 5% de manteiga de bacuri e 4% de óleo de tucumã;
- A incorporação da FUCO nas NL inovadoras apresentou valores de diâmetro de partícula, pdI, potencial zeta e pH de acordo com as características de um sistema nanométrico e com características próprias para uso tópico;
- O método por CLAE demonstrou ser linear, preciso e exato, ou seja, adequado para o controle de qualidade e quantificação da FUCO nas NL inovadoras;
- A incorporação da FUCO nas NL conferiu maior fotoestabilidade frente à luz UVA, quando comparadas com a forma livre;

- A estrutura das NL-FUCO foi mantida após a incorporação em hidrogel, mostrando-se homogênea em relação à cor e aspecto, com tamanho nanométrico e valores de pH compatível com a aplicação cutânea;
- As NL-FUCO mostraram-se estáveis durante 45 dias nas temperaturas de armazenagem em 6 ºC, 25 ºC e 40 ºC, de acordo com os valores de tamanho de partícula, potencial zeta e teor;
- No estudo de dissolução, as NL-FUCO apresentaram um fluxo de liberação sustentada, o que demonstra a capacidade das NL em controlar a liberação da FUCO;
- Através dos estudos de permeação cutânea *in vitro* foi possível quantificar a FUCO nas diferentes camadas da pele e demonstrou a capacidade das NL em modificar a permeação da FUCO encapsulada;
- Quando o estrato córneo foi removido, as concentrações da FUCO aumentoram na epiderme e na derme;
- Na avaliação toxicológica *in vitro,* as concentrações de NL-FUCO menores que 80 µg/mL podem ser consideradas biocompatíveis em células 3T3;
- Na avaliação celular de espécies reativas, houve aumento significativo na produção de ROS e RNS, sugerindo que a FUCO possui capacidade pró-oxidante significativa;
- Na avaliação do potencial de membrana, a FUCO induziu um aumento, o que hiperpolariza a membrana mitocondrial e impulsiona a síntese de ATP;
- O revestimento com quitosana aumentou o tamanho das NL, entretanto os valores se mostraram adequados para sistemas nanométricos. Com a análise do potencial zeta e a da MET pode-se confirmar a presença da quitosana;
- No estudo de bioadesão *in vitro*, o revestimento de quitosana aumentou significativamente a bioadesão das NL;
- O estudo de proliferação *in vitro* com fibroblastos evidenciou que as NL-FUCO mantiveram as propriedades de proliferação da quitosana.

11. REFERÊNCIAS

ACUNA, U.M.; JANCOVSKI, N.; KENNELLY, E.J. Polyisoprenylated benzophenones from clusiaceae: potential drugs and lead compounds. *Current topics in medicinal chemistry*, v. 9, n. 16, p. 1560-1580, 2009.

ALI, H.; SHIRODE, A.B.; SYLVESTER, P.W.; NAZZAL, S. Preparation, characterrization and anticancer effects of simvastatin-tocotrienol lipid nanoparticles. *International Journal of Pharmaceutics,* v. 389, n. 1, p. 223-231, 2010.

ALMEIDA BORGES, V.R.; SIMON, A.; SENA, A.R.C.; CABRAL, L.M.; SOUSA, V.P. Nanoemulsion containing dapsone for topical administration: a study of in vitro release and epidermal permeation*. International Journal of Nanomedicine,* v. 8, p. 535-544, 2013.

ALMEIDA, A.J.; SOUTO, E. Solid lipid nanoparticles as a drug delivery system for peptides and proteins. *Advanced drug delivery reviews,* v. 59, n. 6, p. 478-490, 2007.

ALVAREZ-ROMÁN, R.; NAIK, A.; KALIA, Y.N.; FESSI, H. Skin penetration and distribution of polymeric nanoparticles. *Journal of Controlled Release,* v. 99, p. 53-62, 2004.

ALVES, R.E.; DE BRITO, E.S.; RUFINO, M.S.M.; SAMPAIO, C.G. Antioxidant activity measurement in tropical fruits: A case study with acerola. *Acta Horticulturae,* 2008.

AMAN, R.; SCHIEBER, A.; CARLE, R. Effects of heating and illumination on trans−cis isomerization and degradation of carotene and lutein in isolated spinach Chloroplasts. *Journal of Agricultural and Food Chemistry,* v. 53, n. 24, p. 9512–9518, 2005.

ARORA, S.; RAJWADE, J.M.; PAKNIKAR, K.M. Nanotoxicology and in vitro studies: the need of the hour. *Toxicology and Applied Pharmacology,* v. 258, n. 2, p. 151-65, 2012.

ASAI, A.; YONEKURA, L.; NAGÃO, A. Low bioavailability of dietary epoxyxanthophylls in humans. *British journal of nutrition*, v. 100, n. 02, p. 273-277,

2008.

BABY, A. R.; HAROUTIOUNIAN, C.A.; SARRUF, F.D.; PINTO, C.A.; KANEKO, T.M.; VELASCO, M.V. Influence of urea, isopropanol, and propylene glycol on rutin in vitro release from cosmetic semisolid systems estimated by factorial design. *Drug Development and Industrial Pharmacy,* v. 35, p. 272-282, 2009.

BAGGALEY, E.M.; ELLIOTT, A.C.; BRUCE, J.I. Oxidant-induced inhibition of the plasma membrane Ca2+-ATPase in pancreatic acinar cells: role of the mitochondria. *American Journal of Physiology-Cell Physiology*, v. 295, n. 5, p. C1247-C1260, 2008.

BARRATT, G. Colloidal drug carriers: achievements and perspectives. Cellular and Molecular. *Life Sciences,* v. 60, n. 1, p. 21-37, 2003.

BENSON, H.A.E.; WATKINSON, A.H. *Transdermal and Topical Drug Delivery: Principles and Practice.* New Delhi, India: John Wiley & Sons, 2012.

BEPPU, F.; NIWANO, Y.; SATO, E.; KOHNO, M.; HOSOKAWA, M.; MIYASHITA, K. *In vitro* and *in vivo* evaluation of mutagenicity of fucoxanthin and its metabolite fucoxanthinol. *The Journal of toxicological sciences,* v. 34, n. 6, p. 693-698, 2009b.

BEPPU, F.; NIWANO, Y.; TSUKUI, T.; HOSOKAWA, M.; MIYASHITA, K. Single and repeated oral dose toxicity study of fucoxanthin (FX), a marine carotenoid, in mice. *The Journal Toxicological Sciences,* v. 34, n. 5, p. 501-510, 2009a.

BERGER, J.; REIST, M.; MAYER, J.M.; FELT. O.; PEPPAS, N.A.; GURNY, R. Structure and interactions in covalently and ionically crosslinked chitosan hydrogels for biomedical applications. *European Journal of Pharmaceutics and Biopharmaceutics,* v. 57, n. 1, p. 19-34, 2004.

BERTRAM, J.S.; VINE, A.L. Cancer prevention by retinoids and carotenoids: independent action on a common target. *Biochimica et Biophysica Acta (BBA)-Molecular Basis of Disease,* v. 1740, n. 2, p. 170-178, 2005.

BETTONI, C.C.; FELIPPI, C.C.; ANDRADE, C. RAFFIN, R.P.; JAGER, A.; GUTERRES, S.S.; COSTA, T.D. Isotretinoin-Loaded Nanocapsules: Stability and Cutaneous Penetration by Tape Stripping in Human and Pig Skin. *Journal of Biomedical Nanotechnology,* v. 8, n. 2, p. 258-271, 2012.

BOLZINGER, M.A; BRIANÇON, S.; PELLETIER, J.; CHEVALIER, Y. Penetration of drugs through the skin, a complex rate-controlling membrane. *Current Opinion in Colloid & Interface Science,* v. 17, n. 3, p. 156-165, 2012.

BONIFÁCIO, B.V.; SILVA, P.B.; RAMOS, M.A.S.; NEGRI, K.M.S.; BAUAB, T.M.; CHORILLI, M. Nanotechnology-based drug delivery systems and herbal medicines: a review. *International Journal of Nanomedicine,* v. 9, p. 1-15, 2014.

BOON, C.S.; MCCLEMENTS, D.J.; WEISS, J.; DECKER, E.A. Factors influencing the chemical stability of carotenoids in foods. *Critical reviews in food science and nutrition,* v. 50, n. 6, p. 515-532, 2010.

BORA, P.S.; NARAIN, N.; ROCHA, R.V.M.; DE OLIVEIRA MONTEIRO, A.C.; DE AZEVEDO MOREIRA, R. Characterization of the oil and protein fractions of Tucumã (*Astrocaryum Vulgare* Mart.) fruit pulp and seed kernel. *Ciencia y Technologia Alimentaria,* v. 3, n. 2, p. 111-116, 2001.

BOUABIDI, A.; ROZET, E.; FILLET, M.; ZIEMONS, E.; CHAPUZET, E.; MERTENS, B.; KLINKENBERG, R.; CECCATO, A.; TALBI, M.; STREEL, B.; BOUKLOUSE, A.; BOULANGER, B.; HUBERT, P. Critical analysis of several analytical method validation strategies in the framework of the fit for purpose concept. *Journal of Chromatography A,* v. 1217, n. 19, p. 3180-3192, 2010.

BRASIL. Agência Nacional de Vigilância Sanitária. Resolução n° 899, de 29 de maio de 2003. Determina a publicação do guia para validação de métodos analíticos e bioanalíticos. *Diário Oficial da República Federativa do Brasil,* Brasília/DF, 2003.

BRASIL. Ministério da Saúde. Instituto Nacional de Câncer José Alencar Gomes da Silva (INCA). *Estimativa 2018: Incidência de Câncer no Brasil.* Rio de Janeiro/RJ,

2017. https://www.inca.gov.br/publicacoes/livros/estimativa-2018-incidencia-de-cancer-no-brasil. Acesso em: 10.10.2018

BUTLER, M.S. The role of natural product chemistry in drug discovery. *Journal of natural products,* v. 67, n. 12, p. 2141-2153, 2004.

CARAMELLA, C.; FERRARI, F.; BONFERONI, M.C.; ROSSI, S.; SANDRI, G. Chitosan and its derivatives as drug penetration enhancers. *Journal of Drug Delivery Science and Technology*, v. 20, n. 1, p. 5-13, 2010

CHINEMBIRI, T.N.; DU PLESSIS, L.H.; GERBER, M.; HAMMAN, J. H.; DU PLESSIS, J. Review of Natural Compounds for Potential Skin Cancer Treatment. *Molecules,* v. 19, n. 8, p. 11679-11721, 2014.

CHUNG, T.W.; CHOI, H.J.; LEE, J.Y.; JEONG, H.S.; KIM, C.H.; JOO, M.H. Marine algal fucoxanthin inhibits the metastatic potential of cancer cells. *Biochemical and biophysical research communications*, v. 439, n. 4, p. 580-585, 2013.

CRUPI, P.; TOCI, A.T.; MANGINI, S.; WRUBL, F.; RODOLFI, L.; TREDICI, M.R.; ANTONACCI, D. Determination of fucoxanthin isomers in microalgae (Isochrysis sp.) by high□performance liquid chromatography coupled with diode□array detector multistage mass spectrometry coupled with positive electrospray ionization. *Rapid Communications in Mass Spectrometry*, v. 27, n. 9, p. 1027-1035, 2013.

D'ORAZIO, N.; GEMELLO, E.; GAMMONE, M.A.; DE GIROLAMO, M.; FICONERI, C.; RICCIONI, G. Fucoxanthin: A treasure from the sea. *Marine Drugs,* v. 10, n. 3, p. 604–616, 2012.

DAS, S.K.; HASHIMOTO, T.; SHIMIZU, K.; YOSHIDA, T.; SAKAI, T.; SOWA, Y.; KOMOTO, A.; KANAZAWA, K. Fucoxanthin induces cell cycle arrest at G0/G1 phase in human colon carcinoma cells through up-regulation of p21 WAF1/Cip1. *Biochimica et Biophysica Acta (BBA)-General Subjects,* v. 1726, n. 3, p. 328-335, 2005.

DEGIM, T.I. New tools and approaches for predicting skin permeability. *Drug Discovery Today,* v. 11, n. 11, p. 11-12, 2006.

DE ROSSO, V.V.; MERCADANTE, A.Z. Identification and quantification of carotenoids, by HPLC-PDA-MS/MS, from Amazonian fruits**.** *Journal of agricultural and food chemistry,* v. 55, n. 13, p. 5062-5072, 2007.

DESAI, P.; PATLOLLA, R.R.; SINGH, M. Interaction of nanoparticles and cell penetrating peptides with skin for transdermal drug delivery. *Molecular Membrane Biology,* v. 27, n. 7, p. 247-259, 2010.

DIDEROT, N.T.; SILVERE, N.; ETIENNE, T. Xanthones as therapeutic agents: chemistry and pharmacology. *Advances in Phytomedicine,* v. 2, p. 273-298, 2006.

DOKTOROVOVA, S.; SOUTO, E.B.; SILVA, A.M. Nanotoxicology applied to solid lipid nanoparticles and nanostructured lipid carriers–a systematic review of in vitro data. *European Journal of Pharmaceutics and Biopharmaceutics,* v. 87, n. 1, p. 1-18, 2014.

ENGLERT, G.; BJØRNLAND, T.; LIAAEN-JENSEN, S. 1D and 2D NMR study of some allenic carotenoids of the fucoxanthin series. *Magnetic Resonance in Chemistry,* v. 28, n. 6, p. 519-528, 1990.

ERB, P.; JI, J.; WERNLI, M.; KUMP, E.; BÜCHNER, S. A. Role of apoptosis in basal cell and squamous cell carcinoma formation. *Immunology letters,* v. 100, n. 1, p. 68-72, 2005.

FOTUHI, M.; MOHASSEL, P.; YAFFE, K. Fish consumption, long-chain omega-3 fatty acids and risk of cognitive decline or Alzheimer disease: a complex association. *Nature Clinical Practice Neurology,* v. 5, n. 3, p. 140-152, 2009.

FRANCESKO, A.; TZANOV, T. Chitin, chitosan and derivatives for wound healing and tissue engineering. In: *Biofunctionalization of Polymers and their Applications*. Springer, Berlin, Heidelberg, 2010. p. 1-27.

GAGEZ, A.L.; THIERY, V.; PASQUET, V.; CADORET, J.P.; PICOT, L. Epoxycarotenoids and cancer. *Current Bioactive compounds,* v. 8, n. 2, p. 109-141, 2012.

GAMMONE, M. A.; RICCIONI, G.; D'ORAZIO, N. Carotenoids: potential allies of cardiovascular health? *Food & nutrition research,* v. 59, 2015.

GAMMONE, M.A.; D'ORAZIO, N. Anti-Obesity Activity of the Marine Carotenoid Fucoxanthin. *Marine drugs,* v. 13, n. 4, p. 2196-2214, 2015.

GANDHI, R.; PILLAI, O.; THILAGAVATHI, R.; GOPALAKRISHNAN, B.; LAL KAUL, C.; PANCHAGNULA, R. Characterization of azithromycin hydrates. *European Journal of Pharmaceutical Sciences,* v. 16, n. 3, p. 175-184, 2002.

GENESTRA, M. Oxyl radicals, redox-sensitive signalling cascades and antioxidants. *Review Cell Signal,* v. 19, p. 1807-1819, 2007.

GIL, E.S. *Controle Físico-Químico de Qualidade de Medicamentos*. São Paulo: Pharmabooks, 2010. p. 48.

GODIN, B.; TOUITOU, E. Transdermal skin delivery: predictions for humans from in vivo, ex vivo and animal models. *Advanced Drug Delivery Reviews*, v. 59, p. 1152–1161, 2007.

GRABOVAC, V.; GUGGI, D.; BERNKOP-SCHNÜRCH, A. Comparison of the mucoadhesive properties of various polymers. *Advanced Drug Delivery Reviews,* v. 57, n. 11**,** p. 1713-1723, 2005.

HAJJ ALI, H.; MICHAUX, F.; NTSAMA, B.; SANDRINE, I.; DURAND, P.; JASNIEWSKI, J.; LINDER, M. Shea butter solid nanoparticles for curcumin encapsulation: Influence of nanoparticles size on drug loading. *European Journal of Lipid Science and Technology,* 2015.

HELGASON, T.; AWAD, T.S.; KRISTBERGSSON, K.; MCCLEMENTS, D.J.; WEISS, J. Effect of surfactant surface coverage on formation of solid lipid nanoparticles (SLN). *Journal of Colloid and Interface Science,* v. 334, n. 1, p. 75-81, 2009.

HEO, S.J.; JEON, Y.J. Protective effect of fucoxanthin isolated from Sargassum siliquastrum on UV-B induced cell damage. *Journal of Photochemistry and Photobiology B: Biology,* v. 95, n. 2, p. 101-107, 2009.

HII, S.L.; CHOONG, P.Y.; WOO, K.K.; WONG, C.L. Stability studies of fucoxanthin from Sargassum binderi. *Australian Journal of Basic and Applied Sciences,* v. 4, n. 10, p. 4580–4584, 2010.

HOFFMANN, E.; STROOBANT, V. *Mass Spectrometry: Principles and Applications*. England: John Wiley & Sons Ltd, 2007.

HU, L.; SUN, Y.; WU, Y. Advances in chitosan-based drug delivery vehicles. *Nanoscale*, v. 5, n. 8, p. 3103-3111, 2013.

HUANG, T.; YAN, L.; ZHENG, S.; WANG, Y.; WANG, X.; FAN, L.; LI, C.; ZHAO, Y.; MARTYNIUK, C.J. Discriminating modes of toxic action in mice using toxicity in BALB/c mouse fibroblast (3T3) cells. *Chemosphere,* v. 188, p. 73-80, 2017.

HUANG, Y.W.; WU, C.; ARONSTAM, R.S. Toxicity of Transition Metal Oxide Nanoparticles: Recent Insights from in vitro Studies. *Materials*, v. 3, p. 4842-4859, 2010.

ICH. *Harmonised Tripartite Guideline. Validation of analytical methods text and methodology Q2 (R1).* In: International Conference on Harmonization of Technical Requirements for Registration of Pharmaceuticals for Human Use, 2005.

ISHIKAWA, C.; TAFUKU, S.; KADEKARU, T.; SAWADA, S.; TOMITA, M.; OKUDAIRA, T.; NAKAZATO, T.; TODA, T.; UCHIHARA, J.N.; TAIRA, N. Antiadult T-cell leukemia effects of brown algae fucoxanthin and its deacetylated product, fucoxanthinol. *International journal of cancer,* v. 123, n. 11, p. 2702-2712, 2008.

JAIN, A.K.; JAIN, A.; NEERAJ, K.G.; AGARWALA, A.; JAIN, A.; JAIN, S.A.; TYAGIC, R.K.; JAIN, R.K.; AGRAWALE, H.; AGRAWALA,G.P. Adapalene loaded solid lipid nanoparticles gel: An effective approach for acne treatment. *Colloids and Surfaces B: Biointerfaces,* v. 121, p. 222–229, 2014.

JOHNSON, G.L.; LAPADAT, R. Mitogen-activated protein kinase pathways mediated by ERK, JNK, and p38 protein kinases. *Science,* v. 298, n. 5600, p. 1911-1912, 2002.

JUNQUEIRA, L.C.; CARNEIRO, J. *Histologia Básica.* Rio de Janeiro: Guanabara, 2004.

JUNYAPRASERT, V.B.; TEERANACHAIDEEKUL, V.; SOUTO, E.B.; BOONME, P.; MULLER, R. H. Q10-loaded NLC versus nanoemulsions: Stability, rheology and in vitro skin permeation. *International Journal of Pharmaceutics***,** v. 377, n. 1–2, p. 207-214, 2009.

KANAZAWA, K.; OZAKI, Y.; HASHIMOTO, T.; MATSUSHITA, S.; HIRANO, M.; OKADA, T.; NAKATSUKA, M. Commercial-scale preparation of biofunctional fucoxanthin from waste parts of brown sea algae *Laminalia japonica*. *Food science and technology research,* v. 14, n. 6, p. 573-573, 2008.

KECK, C.M.; MULLER, R.H. Size analysis of submicron particles by laser diffractometry—90% of the published measurements are false. *International Journal of Pharmaceutics,* v. 355, p. 150–163, 2008.

KHOEE, S.; YAGHOOBIAN, M. An investigation into the role of surfactants in controlling particle size of polymeric nanocapsules containing penicillin-G in double emulsion. *Europen Journal Medicine Chemistry*, v. 44, n. 6, p. 2392-2399, 2009.

KIM, K.N.; AHN, G.; HEO, S.J.; KANG, S.M.; KANG, M.C.; YANG, H.M.; KIM, D.; ROH, S.W.; KIM, S.K.; JEON, B.T. Inhibition of tumor growth *in vitro* and *in vivo* by fucoxanthin against melanoma B16F10 cells. *Environmental toxicology and pharmacology,* v. 35, n. 1, p. 39-46, 2013.

KIM, K.N.; HEO, S.J.; KANG, S.M.; AHN, G.; JEON, Y.J. Fucoxanthin induces apoptosis in human leukemia HL-60 cells through a ROS-mediated Bcl-xL pathway. *Toxicology in vitro,* v. 24, n. 6, p. 1648-1654, 2010.

KIM, S.M.; JUNG, Y.J.; KWON, O.N.; CHA, K.H.; UM, B.H.; CHUNG, D.; PAN, C.H. A potential commercial source of fucoxanthin extracted from the microalga Phaeodactylum tricornutum. *Applied Biochemistry and Biotechnology,* v. 166, n. 7, p. 1843–1855, 2012.

KODAMA, D.H.; GONÇALVES, A.E.D.S.S.; LAJOLO, F.M.; GENOVESE, M.I. Flavonoids, total phenolics and antioxidant capacity: comparison between commercial green tea preparations. *Food Science and Technology (Campinas),* v. 30, n. 4, p. 1077-1082, 2010.

KOTAKE-NARA, E.; KUSHIRO, M.; ZHANG, H.; SUGAWARA, T.; MIYASHITA, K.; NAGAO, A. Carotenoids affect proliferation of human prostate cancer cells. *The Journal of nutrition,* v. 131, n. 12, p. 3303-3306, 2001.

KROLL, A.; PILLUKAT, M.H.; HAHN, D.; SCHNEKENBURGER, J. Interference of engineered nanoparticles with in vitro toxicity assays. *Archives of toxicology,* v. 86, n. 7, p. 1123-1136, 2012.

KRUGLYAKOV, P.M. *Hydrophile-lipophile balance of surfactants and solid particles: physicochemical aspects and applications.* Amsterdam: Elsevier, 2000. p. 102-110.

KULKARNI, V.S. *Handbook of Non-invasive Drug delivery Systems***.** Elsevier Inc., 2010.

KUMAR, S.; SHARMA, S.; CHATTOPADHYAY, S.K. The potential health benefit of polyisoprenylated benzophenones from Garcinia and related genera: ethnobotanical and therapeutic importance. *Fitoterapia,* v. 89, p. 86-125, 2013.

KUMAR, S.R.; MASASHI, H.; KAZUO, M. Fucoxanthin: A marine carotenoid exerting anti-cancer effects by affecting multiple mechanisms. *Marine drugs,* v. 11, n. 12, p. 5130–5147, 2013.

LACHMAN, L.; LIEBERMAN, H. A.; LINKKANIG, J. L. *Teoria e prática na indústria farmacêutica*. Lisboa: Fundação Calouste Gulbenkian, 2010.

LADEMANN, J.; SCHANZER, S.; MEINKE, M.; STERRY, W.; DARVIN, M.E. Interaction between carotenoids and free radicals in human skin. *Skin pharmacology and physiology,* v. 24, n. 5, p. 238-244, 2011.

LANE, M.E. Skin penetration enhancers. *International journal of pharmaceutics,* v. 447, n. 1, p. 12-21, 2013.

LIEBERMANN, D.; TRONT, J.S.; SHA, X.; MUKHERJEE, K.; MOHAMED-HADLEY, A.; HOFFMAN, B. Gadd45 stress sensors in malignancy and leukemia. *Critical Reviews in Oncogenesis,* v. 16, n. 1-2, 2011.

LIPPACHER, A.; MULLER, R.H.; MADER, K. Semisolid SLN dispersions for topical application: influence of formulation and production parameters on viscoelastic properties. *European Journal of Pharmaceutics and Biopharmaceutics,* v. 53, n. 2, p. 155-160, 2002.

LIU, C.L.; HUANG, Y.S.; HOSOKAWA, M.; MIYASHITA, K.; HU, M.L. Inhibition of proliferation of a hepatoma cell line by fucoxanthin in relation to cell cycle arrest and enhanced gap junctional intercellular communication. *Chemico-biological interactions,* v. 182, n. 2, p. 165-172, 2009.

LIU, D.; LI, J.; PAN, H.; HE, F.; LIU, Z.; WU, Q. Potential advantages of a novel chitosanN-acetylcysteine surface modified nanostructured lipid carrier on the performance of ophthalmic delivery of curcumin. *Scientific reports,* v. 6, p. 28796, 2016.

LUSTOSA, A.K.M.; ARCANJO, D.D.; RIBEIRO, R.G.; RODRIGUES, K.A.F.; PASSOS, F.F.B.; PIAUILINO, C.A.; CARVALHO, F.A.A. Immunomodulatory and toxicological evaluation of the fruit seeds from *Platonia insignis*, a native species from Brazilian Amazon Rainforest*. Revista Brasileira de Farmacognosia,* v. 26, n. 1, p. 77-82, 2016.

MAEDA, H.; HOSOKAWA, M.; SASHIMA, T.; MIYASHITA, K. Dietary combination of fucoxanthin and fish oil attenuates the weight gain of white adipose tissue and decreases blood glucose in obese/diabetic KK-Ay mice. *Journal of Agricultural and Food Chemistry,* v. 55, n. 19, p. 7701-7706, 2007.

MAEDA, H.; HOSOKAWA, M.; SASHIMA, T.; MIYASHITA, K. Anti-obesity and anti-diabetic effects of fucoxanthin on diet-induced obesity conditions in a murine model. *Molecular medicine reports,* v. 2, n. 6, p. 897-902, 2009.

MAGGIO, R.M.; VIGNADUZZO, S.E.; KAUFMAN, T.S. Practical and regulatory

considerations for stability-indicating methods for the assay of bulk drugs and drug formulations. *TrAC Trends in Analytical Chemistry,* v. 49, p. 57-70, 2013.

MANDAWGADE, S.D.; PATRAVALE, V.B. Development of SLNs from natural lipids: application to topical delivery of tretinoin. *International Journal of Pharmaceutics,* v. 363, n. 1, p. 132-138, 2008.

MARCATO, P.D. Preparação, caracterização e aplicações em fármacos e cosméticos de nanopartículas lipídicas sólidas. *Revista Eletrônica de Farmácia,* v. 6, p. 01-37, 2009.

MARQUIS, B.J.; LOVE, S.A.; BRAUN, K.L.; HAYNES, L.C. Analytical methods to assess nanoparticle toxicity. *Analyst,* v. 134, n. 3, p. 425-39, 2009.

MARTIN, L.J. Fucoxanthin and Its Metabolite Fucoxanthinol in Cancer Prevention and Treatment. *Marine drugs,* v. 13, n. 8, p. 4784-4798, 2015.

MCNULTY, H.; JACOB, R.F.; MASON, R.P. Biologic activity of carotenoids related to distinct membrane physicochemical interactions. *American Journal of Cardiology,* v. 101, n. 10, p. 20D–29D, 2008.

MEHNERT, W.; MÄDER, K. Solid lipid nanoparticles: production, characterization and applications. *Advanced drug delivery reviews, v*. 47, n. 2, p. 165-196, 2001.

MÍNGUEZ-MOSQUERA, M.I.; HORNERO-MÉNDEZ, D.; PÉREZ-GÁLVEZ, A.; Carotenoids and provitamin A in functional foods, in: HURST, W.J. *Methods of analysis for functional foods and nutraceuticals.* Boca Raton, FL: CRC Press: 2002. p. 101-157.

MIYASHITA, K.; NISHIKAWA, S.; BEPPU, F.; TSUKUI, T.; ABE, M.; HOSOKAWA, M. The allenic carotenoid fucoxanthin, a novel marine nutraceutical from brown seaweeds. *Journal of the Science of Food and Agriculture,* v. 91, n. 7, p. 1166-1174, 2011.

MOLASSIOTIS, A.; FERNADEZ-ORTEGA, P.; PUD, D.; OZDEN, G.; SCOTT, J. A.; PANTELI, V.; MARGULIES, A.; BROWALL, M.; MAGRI, M.; SELVEKEROVA, S. Use

of complementary and alternative medicine in cancer patients: a European survey. *Annals of oncology,* v. 16, n. 4, p. 655-663, 2005.

MORAIS, L.R.B.; GUTJAHR, E. *Química de oleaginosas: Valorização da biodiversidade amazônica.* Brasília: Agência de Cooperação Técnica Alemã (GTZ), 2009. 83 p.

MOSER, K.; KRIWET, K.; FROEHLICH, C.; NAIK, A.; KALIA, Y.N.; GUY, R.H. Permeation enhancement of a highly lipophilic drug using supersaturated systems. *Journal of pharmaceutical sciences,* v. 90, n. 5, p. 607-616, 2001.

MOSQUEIRA, V.C.F.; LEGRAND, P.; PINTO□ALPHANDARY, H.; PUISIEUX, F.; BARRATT, G. Poly (D, L□lactide) nanocapsules prepared by a solvent displacement process: Influence of the composition on physicochemical and structural properties. *Journal of pharmaceutical sciences*, v. 89, n. 5, p. 614-626, 2000.

MOZAFARI, M.R.; FLANAGAN, J.; MATIA-MERINO, L.; AWATI, A.; OMRI, A.; SUNTRES, Z.E.; SINGH, H.J. Recent trends in the lipid based nanoencapsulation of antioxidants and their role in foods. *Journal of the Science Food and Agriculture,* v. 86, n. 13, p. 2038-2045, 2006.

MULLER, R.H.; MAÉDER, K.; GOHLA, S. Solid lipid nanoparticles (SLN) for controlled drug delivery–a review of the state of the art**.** *European journal of pharmaceutics and Biopharmaceutics,* v. 50, n. 1, p. 161-177, 2000.

MULLER, R.H.; PARDEIKE, J. Coenzyme Q10-loaded NLCs: preparation, occlusive properties and penetration enhancement. *Pharmaceutical Technology Europe,* v. 19, p. 46-49, 2007.

MULLER, R.H.; RADTKE, M.; WISSING, S.A. Solid lipid nanoparticles (SLN) and nanostructured lipid carriers (NLC) in cosmetic and dermatological preparations. *Advanced drug delivery reviews*, v. 54, p. S131-S155, 2002.

MURAKAMI, C.; TAKEMURA, M.; SUGIYAMA, Y.; KAMISUKI, S.; ASAHARA, H.; KAWASAKI, M.; ISHIDOH, T.; LINN, S.; YOSHIDA, S.; SUGAWARA, F. Vitamin A-

related compounds, all-*trans* retinal and retinoic acids, selectively inhibit activities of mammalian replicative DNA polymerases. *Biochimica et Biophysica Acta (BBA)-Gene Structure and Expression,* v. 1574, n. 1, p. 85-92, 2002.

MUTHUIRULAPPAN, S.; FRANCIS, S.P. Anti-cancer mechanism and possibility of nano-suspension formulation for a marine algae product fucoxanthin*. Asian Pacifi Journal of Cancer Prevention,* v. 14, n. 4, p. 2213-2216, 2013.

NAGPAL, K.; SINGH, S.K.; MISHRA, D.N. Chitosan nanoparticles: A promising system in novel drug delivery. *Chemical & Pharmaceutical Bulletin,* v. 58, n. 11, p. 1423-1430, 2010.

NAKAZAWA, Y.; SASHIMA, T.; HOSOKAWA, M.; MIYASHITA, K. Comparative evaluation of growth inhibitory effect of stereoisomers of fucoxanthin in human cancer cell lines. *Journal of Functional Foods,* v. 1, n. 1, p. 88-97, 2009.

NEL, A.; XIA, T.; MÄDLER, L.; LI, N. Toxic potential of materials at the nanolevel. *Science,* v. 311, n. 5761, p. 622-627, 2006.

NISHINO, H. Cancer chemoprevention by natural carotenoids and their related compounds*. Journal of Cellular Biochemistry,* v. 59, n. S22, p. 231-235, 1995.

NOGUEIRA, D.R.; MITJANS, M.; INFANTE, M.R.; VINARDELL, M.P. Comparative sensitivity of tumor and non-tumor cell lines as a reliable approach for in vitro cytotoxicity screening of lysine-based surfactants with potential pharmaceutical applications. *International journal of pharmaceutics,* v. 420, n. 1, p. 51-58, 2011.

OECD. *Organisation for Economic Co-operationand Development.* N. 129. Guidance Document On Using Cytotoxicity Tests To Estimate Starting Doses For Acute Oral Systemic Toxicity Tests. 2010.

OKADA, H.; MAK, T.W. Pathways of apoptotic and nonapoptotic death in tumour cells. *Nature Reviews Cancer,* v. 4, n. 8, p. 592-603, 2004.

OLBRICH, C.; MULLER, R.H. Enzymatic degradation of SLN—effect of surfactant and surfactant mixtures. *International journal of pharmaceutics,* v. 180, n. 1, p. 31-39, 1999.

OLIVEIRA, A.N.; do AMARAL, I.L. Florística e fitossociologia de uma floresta de vertente na Amazônia Central, Amazonas, Brasil1. *Acta Amazonica,* v. 34, n. 1, p. 21-34, 2004.

OSTROWSKI, A. D.; MARTIN, T. L.; CONTI, J.; HURT, B.; HARTHORN, H. Nanotoxicology: characterizing the scientific literature, 2000–2007. *Journal of Nanoparticle Research.* v. 11, n.2, p. 251–257, 2009.

PARODI, B.; RUSSO, E.; GATTI, P.; BIGNARDI, G. Development and *in vitro* evaluation of buccoadhesive tablets using a newmodel substrate for bioadhesion measures: the eggshell membrane. *Drug development and industrial pharmacy*, v. 25, n. 3, p. 289-295, 1999.

PILLAI, M.M.; AKSHAYA, T.R.; ELAKKIYA, V.; GOPINATHAN, J.; SAHANAND, K.S.; RAI, B.D.; SELVAKUMAR, R. Egg shell membrane–a potential natural scaffold for human meniscal tissue engineering: an in vitro study. *RSC Advances*, v. 5, n. 93, p. 76019-76025, 2015.

PIMENTEL, V.P.; VIEIRA, V.A.M.; MITIDIERI, T.L.; OLIVEIRA, F.F.S.; PIERONI, J.P. *Biodiversidade brasileira como fonte da inovação farmacêutica: uma nova esperança?* Revista do BNDES, Rio de Janeiro, n. 43, p. 41-89, 2015.

PUGLIA, C.; BLASI, P.; RIZZA, L.; SCHOUBBEN, A.; BONINA, F.; ROSSI, C.; RICCI, M. Lipid Nanoparticles for prolonged topical delivery: An in vitro and in vivo investigation. *International Journal of Pharmaceutics,* v. 357, n. 1, p. 295-304, 2008.

QI, L.; XU, Z.; JIANG, X.; HU, C.; ZOU, X. Preparation and antibacterial activity of chitosan nanoparticles. Carbohydrate Research, v.339, n. 16, p. 2693–2700, 2004.

QUAN, J.; KIM, S.M.; PAN, C.H.; CHUNG, D. Characterization of fucoxanthin-loaded microspheres composed of cetyl palmitate-based solid lipid core and fish

gelatin–gum arabic coacervate shell. *Food research international,* v. 50, n. 1, p. 31-37, 2013.

RAVI, H.; BASKARAN, V. Biodegradable chitosan-glycolipid hybrid nanogels: A novel approach to encapsulate fucoxanthin for improved stability and bioavailability. *Food Hydrocolloids,* v. 43, p. 717-725, 2015.

RINAUDO, M. Chitin and chitosan: Properties and applications. *Progress in Polymer Science,* v. 31, n. 7, p. 603–632, 2006.

RODRIGUEZ-AMAYA, D.B. *A guide to carotenoid analysis in foods*. Washington, DC: ILSI press, 2001.

ROSSI, S.; MARCIELLO, M.; SANDRI, G.; FERRARI, F.; BONFERONI, M.C.; PAPETTI, A.; GRISOLI, P. Wound-dressings based on Chitosans and hyaluronic acid for the release of chlorhexidine diacetate in skin ulcer therapy. *Pharmaceutical development and technology,* v. 12, n. 4, p. 415-422, 2007.

RUFINO, M.S.; ALVES, R E.; DE BRITO, E.S.; PÉREZ-JIMÉNEZ, J.; SAURA-CALIXTO, F.; MANCINI-FILHO, J. Bioactive compounds and antioxidant capacities of 18 non-traditional tropical fruits from Brazil. *Food chemistry,* v. 121, n. 4, p. 996-1002, 2010.

SAIJA, A.; TOMAINO, A.; TROMBETTA, D.; GIACCHI, M.; DE PASQUAL, A.; BONINA, F. Influence of different penetration enhancers on *in vitro* skin permeation and in vivo photoprotective effect of flavonoids. *International Journal of Pharmaceutics*, v. 175, n. 1, p. 85-94, 1998.

SAKAI, A. BALB/c 3T3 cell transformation assays for the assessment of chemical carcinogenicity. *Alternatives to Animal Testing and Experimentation,* v. 14, p. 367-373, 2007.

SALVIA-TRUJILLO, L.; SUN, Q.; UM, B.H.; PARK, Y.; MCCLEMENTS, D.J. In vitro and in vivo study of fucoxanthin bioavailability from nanoemulsion-based delivery

systems: Impact of lipid carrier type. *Journal of Functional Foods,* v. 17, p. 293-304, 2015.

SANDRI, G.; BONFERONI, M.; GOKCE, E.H; FERRARI, F.; ROSSI, S.; PATRINI, M.; CARAMELLA, C. Chitosan-associated SLN: in vitro and ex vivo characterization of cyclosporine A loaded ophthalmic systems. *Journal of Microencapsulation,* v. 27: p. 735-746, 2010.

SANDRI, G.; BONFERONI, M.C.; ROSSI, S.; FERRARI, F.; MORI, M.; DEL FANTE, C.; CARAMELLA, C. Platelet lysate formulations based on mucoadhesive polymers for the treatment of corneal lesions. *Journal of Pharmacy and Pharmacology,* v. 63, n. 2, p. 189-198, 2011.

SANDRI, G.; MOTTA, S.; BONFERONI, M.C.; BROCCA, P.; ROSSI, S.; FERRARI, F.; DEL FAVERO, E. Chitosan-coupled solid lipid nanoparticles: tuning nanostructure and mucoadhesion. *European Journal of Pharmaceutics and Biopharmaceutics,* v. 110, p. 13-18, 2017.

SANGEETHA, R.K.; BHASKAR, N.; BASKARAN, V. Comparative effects of beta-carotene and fucoxanthin on retinol deficiency induced oxidative stress in rats. *Molecular and Cellular Biochemistry,* v. 331, n. 1-2, p. 59–67, 2009.

SAPORITO, F.; SANDRI, G.; ROSSI, S.; BONFERONI, M.C.; RIVA, F.; MALAVASI, L.; FERRARI, F. Freeze dried chitosan acetate dressings with glycosaminoglycans and traxenamic acid. *Carbohydrate Polymers,* v. 184, p. 408–417, 2017.

SARVEIYA, V.; RISK, S.; BENSON, H.A.E. Liquid chromatographic assay for common sunscreen agents: application to in vivo assessment of skin penetration and systemic absorption in human volunteers. *Journal of Chromatography B,* v. 803, p. 225-231, 2004.

SATOMI, Y.; NISHINO, H. Fucoxanthin, a natural carotenoid, induces G1 arrest and GADD45 gene expression in human cancer cells. *In vivo,* v. 21, n. 2, p. 305-309, 2007.

SATOMI, Y.; NISHINO, H. Implication of mitogen-activated protein kinase in the induction of G1 cell cycle arrest and *gadd45* expression by the carotenoid fucoxanthin in human cancer cells. *Biochimica et Biophysica Acta-General Subjects*, v. 1790, n. 4, p. 260-266, 2009.

SHAH, K.A.; DATE, A.A.; JOSHI, M.D.; PATRAVALE, V.B. Solid lipid nanoparticles (SLN) of tretinoin: potential in topical delivery. *International journal of pharmaceutics,* v. 345, n. 1, p. 163-171, 2007.

SHAHGALDIAN, P.; QUATTROCCHI, L.; GUALBERT, J.; COLEMAN, A.W.; GORELOFF, P. AFM imaging of calixarene based solid lipid nanoparticles in gel matrices. *European journal of pharmaceutics and biopharmaceutics,* v. 55, n. 1, p. 107-113, 2003.

SHIMODA, H.; TANAKA, J.; SHAN, S. J.; MAOKA, T. Anti-pigmentary activity of fucoxanthin and its influence on skin mRNA expression of melanogenic molecules. *Journal of Pharmacy and Pharmacology,* v. 62, n. 9, p. 1137-1145, 2010.

SHO, H. History and characteristics of Okinawan longevity food*. Asia Pacific journal of clinical nutrition,* v. 10, n. 2, p. 159-164, 2001.

SIEKMANN, B.; WESTESEN, K. Melt-homogenized solid lipid nanoparticles stabilized by the nonionic surfactant tyloxapol. I. Preparation and particle size determination. *Pharmaceutical Science Pharmacology,* v. 3, p. 194-197, 1994.

SILVA, A.P.; FILHO, J.C.C.; DA COSTA JÚNIOR, J.S.; PELÁEZ, W.J.; FAILLACE, M.S.; FERRAZ, A.D.B.F.; FREITAS, R.M. Toxicological Study Employing Repeated Doses of Garcinielliptone FC, a Polyisoprenylated-Benzophenone Isolated from Seed of Platonia Insignis Mart. *Journal of Pharmacy and Pharmacology,* v. 3, p. 316-330, 2015.

SILVA, D.D.; CARMO, H.; LYNCH, A.; SILVA, E. An insight into the hepatocellular death induced by amphetamines, individuallu and in combinatio: the involvement of necrosis and apoptosis. *Archives Toxicology,* v. 87, p. 2165-2185, 2013.

SOUTO, E.B.; ALMEIDA, A.J.; MULLER, R.H. Lipid nanoparticles (SLN®, NLC®) for cutaneous drug delivery: structure, protection and skin effects. *Journal of Biomedical Nanotechnology*, v. 3, n. 4, p. 317-331, 2007.

SOUTO, E.B.; MULLER, R.H. Cosmetic features and applications of lipid nanoparticles (SLN, NLC). *International Journal of Cosmetic Science,* v. 30, n. 3, p. 157-165, 2008.

SOUTO, E.B.; WISSING, S.A.; BARBOSA, C.M.; MULLER, R.H. Evaluation of the physical stability of SLN and NLC before and after incorporation into hydrogel formulations. *European journal of pharmaceutics and biopharmaceutics,* v. 58, n. 1, p. 83-90, 2004.

STORZ, P. Reactive oxygen species in tumor progression. *Front Biosci,* v. 10, n. 1-3, p. 1881-1896, 2005.

STROBER, W. Trypan blue exclusion test of cell viability. *Current protocols in immunology,* v. 111, n. 1, p. A3. B. 1-A3. B. 3, 2015.

SUGIMURA, R.; SUDA, M.; SHO, A.; TAKAHASHI, T.; SASHIMA, T.; ABE, M.; MIYASHITA, K. Stability of fucoxanthin in dried Undaria pinnatifida (Wakame) and baked products (scones) containing wakame powder. *Food Science and Technology Research,* v. 18, n. 5, p. 687-693, 2012.

SVILENOV, H.; TZACHEV, C. Solid Lipid Nanoparticles – A Promising Drug Delivery System. In: SVILENOV, H.; TZACHEV, C.; SEIFEALIAN, A.; DE MEL, A.; KALASKAR, D.M. *Nanomedicine*. Manchester: One Central Press (OCP*)*,2014. p. 187-237.

SWATHI, G.; PRASANTHI, N.L.; MANIKIRAN, S.S.; RAMARAO, N. Solid lipid nanoparticles: Colloidal carrier systems for drug delivery. *International Journal of Pharmaceutical Sciences and Research,* n. 12, v. 1, p. 01-16, 2010.

SZNITOWSKA, M.; JANICKI, S.; BACZEK, A. Studies on the effect of pH on the lipoidal route of penetration across stratum corneum. *Journal of controlled release,* v. 76, n. 3, p. 327-335, 2001.

TAVEIRA, S.F.; DE SANTANA, D.C.; ARAÚJO, L.M.; NOMIZO, A.; LOPEZ, R.F. Effect of iontophoresis on topical delivery of doxorubicin-loaded solid lipid nanoparticles. *Journal of biomedical nanotechnology,* v. 10, n. 7, p. 1382-1390, 2014.

TROMMER, H.; NEUBERT, R.H.H. Overcoming the stratum corneum: the modulation of skin penetration. *Skin pharmacology and physiology,* v. 19, n. 2, p. 106-121, 2006.

UEKANE, T.M.; NICOLOTTI, L.; GRIGLIONE, A.; BIZZO, H.R.; RUBIOLO, P.; BICCHI, C.; REZENDE, C.M. Studies on the volatile fraction composition of three native Amazonian-Brazilian fruits: Murici, bacuri, and sapodilla. *Food Chemistry,* v. 219, p. 13-22, 2017.

UENOJO, M.; MAROSTICA, M.R.; PASTORE, G.M. Carotenoides: propriedades, aplicações e biotransformação para formação de compostos de aroma. *Química Nova,* v. 30, n. 3, p. 616-622, 2007.

UNER, M. Preparation, characterization and physico-chemical properties of solid lipid nanoparticles (SLN) and nanostructured lipid carriers (NLC): their benefits as colloidal drug carrier systems. *Pharmazie,* v. 61, n. 5, p. 375-386, 2006.

URIKURA, I.; SUGAWARA, T.; HIRATA, T. Protective effect of fucoxanthin against UVB-induced skin photoaging in hairless mice. *Bioscience, biotechnology, and biochemistry,* v. 75, n. 4, p. 757-760, 2011.

USP 40. *The United States Pharmacopeia.* Rockville: United States Pharmacopeial Convention, 2017. 37 ed.

VERMA, D.D.; VERMA, S.; BLUME, G.; FAHR, A. Particle size of liposomes influences dermal delivery of substances into skin*. International Journal of Pharmaceutics,* v. 258, n. 1-2, p. 141-151, 2003.

VIERA, A.C.C.; CHAVES, L.L.; PINHEIRO, S.; PINTO, S.; PINHEIRO, M.; COSTA LIMA, S.; FERREIRA, D.; SARMENTO, B.; REIS, S. Mucoadhesive chitosan-coated solid lipid nanoparticles for better managenet of tuberculosis. *International journal of pharmaceutics*, v. 536, n. 1, p. 478-485, 2018.

WANG, J.; CHEN, S.; XU, S.; YU, X.; MA, D.; HU, X.; CAO, X. In vivoinduction of apoptosis by fucoxanthin, a marine carotenoid, associated with down-regulating STAT3/EGFR signaling in sarcoma 180 (S180) xenografts-bearing mice. *Marine drugs*, v. 10, n. 9, p. 2055-2068, 2012.

WELSS, T.; BASKETTER, D.A.; SCHRÖDER, K.R. In vitro skin irritation: facts and future. State of the art review of mechanisms and models. *Toxicology in vitro,* v. 18, n. 3, p. 231-243, 2004.

WHO. World Health Organization. International Agency for Research on Cancer. *GLOBOCAN 2012: Estimated cancer incidence, mortality and prevalence worldwide in 2012.* Available at: http://globocan.iarc.fr/Pages/fact_sheets_population.aspx. Published 2012. Accessed January 2018.

WISSING, S.A.; MULLER, R.H. The influence of solid lipid nanoparticles on skin hydration and viscoelasticity – in vivo study. *European Journal of Pharmaceutics and Biopharmaceutics*, v. 56, n. 1, p. 67-72, 2003.

WOO, M.N.; JEON, S.M.; KIM, H.J.; LEE, M.K.; SHIN, S.K.; SHIN, Y.C.; CHOI, M.S. Fucoxanthin supplementation improves plasma and hepatic lipid metabolism and blood glucose concentration in high-fat fed C57BL/6N mice. *Chemico-biological interactions,* v. 186, n. 3, p. 316-322, 2010.

YAHIA, E.M.; ORNELAS-PAZ, J.D.J. Chemistry, stability and biological actions of carotenoids. In: LAURA, A.; ALVAREZ-PARRILLA, E.; GONZALEZ-AGUILAR, G. A. *Fruit and vegetable phytochemicals: Chemistry, nutritional value and stability.* New Delhi, India: John Wiley & Sons, 2010. p. 177-222.

YAMAMOTO, K.; ISHIKAWA, C.; KATANO, H.; YASUMOTO, T.; MORI, N. Fucoxanthin and its deacetylated product, fucoxanthinol, induce apoptosis of primary effusion lymphomas. *Cancer letters,* v. 300, n. 2, p. 225-234, 2011.

YIP, W.H.; JOE, L.S.; MUSTAPHA, W.A.W.; MASKAT, M.Y.; SAID, M. Characterization and Stability of Pigments Extracted from Sargassum binderi Obtained from Semporna, Sabah. *Sains Malaysiana,* v. 43, n. 9, p. 1345-1354, 2014.

YU, R.; HU, X.; XU, S.; JIANG, Z.; YANG, W. Effects of fucoxanthin on proliferation and apoptosis in human gastric adenocarcinoma MGC-803 cells via JAK/STAT signal pathway. *European journal of pharmacology,* v. 657, n. 1, p. 10-19, 2011.

ZHANG, H.; TANG, Y.; ZHANG, Y.; ZHANG, S.; QU, J.; WANG, X.; KONG, R.; HAN, C.; LIU, Z. Fucoxanthin: A Promising Medicinal and Nutritional Ingredient**.** *Evidence-Based Complementary and Alternative Medicine,* v. 2015, 2015.

ZHAO, D.; KIM, S.M.; PAN, C.H.; CHUNG, D. Effects of heating, aerial exposure and illumination on stability of fucoxanthin in canola oil. *Food chemistry,* v. 145, p. 505-513, 2014.